REPORT DOCUMENTATION PAGE

Form Approved
OMB No. 0704-0188

1. AGENCY USE ONLY (Leave Blank)	2. REPORT DATE	3. REPORT TYPE AND DATES COVERED
	November 1997	Final Technical Report, June 1996 - November 1997

4. TITLE AND SUBTITLE
Accelerated Methods for the Determination of Long Term Fatigue Properties of Glass Reinforced Plastics for RotoroCraft Applications

5. FUNDING NUMBERS
N68171-96-C

6. AUTHOR(S)
Roderick H Martin

7. PERFORMING ORGANIZATION NAME(S) AND ADDRESS(ES)
Materials Engineering Research Laboratory Ltd
Tamworth Road, Hertford, SG13 7DG, England

8. PERFORMING ORGANIZATION REPORT NUMBER
ERO/1

9. SPONSORING/MONITORING AGENCY NAME(S) AND ADDRESS(ES)
USARDSG (UK)

10. SPONSORING /MONITORING AGENCY REPORT NUMBER

11. SUPPLEMENTARY NOTES

12a. DISTRIBUTION/AVAILABILITY STATEMENT

12b. DISTRIBUTION CODE

13. ABSTRACT (Maximum 200 words)

The aim of this work was to develop an accelerated and cost effective method of generating long term fracture data for use in life prediction analysis of structures. Two materials were used in this project. These were S2/8552 and S2/F584, both glass epoxy systems. Delamination onset was monitored at both 5Hz and 20Hz and no difference in cycles to delamination onset was identified. It was concluded that longer term tests could be run at between 15 and 20Hz to represent structural tests at 5Hz. A multi-station fatigue machine was modified to allow up to six composite DCB test pieces to be tested at the same time. Each station had its own instrumentation to monitor individual specimens for compliance changes. The machine operated electro-mechanically. The multi-station machine was used to generate delamination onset data up to 10^8 cycles at 17Hz for both materials. For both materials a consistent decrease in the values of G between 10^0 and 10^8 cycles was observed. It was estimated that the increase in frequency and the use of an electro-mechanical multi-station fatigue machine, reduces the cost of generating long term fatigue data to under 5% of that using conventional testing approaches.

14. SUBJECT ITEMS	15. NUMBER OF PAGES
Accelerated test; delamination onset; double cantilever beam; fatigue; frequency effect; interlaminar fracture; mode I delamination; multi-station	**83**
	16. PRICE CODE

17. SECURITY CLASSIFICATION OF REPORT	18. SECURITY CLASSIFICATION OF THIS PAGE	19. SECURITY CLASSIFICATION OF ABSTRACT	20. LIMITATION OF ABSTRACT
Unclassified	Unclassified	Unclassified	

Accelerated Methods for the Determination of Long Term Fatigue Properties of Glass Reinforced Plastics for Rotor Craft Applications

Final Technical Report

by

Roderick H. Martin

November 1997

United States Army
EUROPEAN RESEARCH OFFICE OF THE U.S. ARMY
London, England

Contract Number: N68171-96-C-9061

ABSTRACT

The U.S. Army Vehicle Technology Centre (VTC) at NASA Langley, has successfully used interlaminar fracture mechanics analysis on rotor craft structures to predict delamination initiation. The structure was analysed to determine the values of strain energy release rate (*G*) at critical locations in the structure. These predictions were compared with structural test data running out to 10^7 cycles. However, in reality these structures may experience between 10^8 and 10^9 cycles in service at a frequency of 5Hz. Hence, the aim of this work was to develop an accelerated and cost effective method of generating these long term fracture data for the analysis. Two materials were used in this project. These were S2/8552 and S2/F584, both glass epoxy systems. Delamination onset was monitored at both 5Hz and 20Hz and no difference in cycles to delamination onset was identified. It was concluded that longer term tests could be run at between 15 and 20Hz to represent structural tests at 5Hz. A multi-station fatigue machine was modified to allow up to six composite DCB test pieces to be tested. Each station had its own instrumentation to monitor individual specimens for compliance changes. This machine operates electro-mechanically and hence is less expensive to run than the conventional servo-hydraulic fatigue machines. The multi-station machine was used to generate delamination onset data up to 10^8 cycles at 17Hz for both materials. For both materials a consistent decrease in the values of *G* between 10^8 and 10^0 cycles was observed. It is estimated that the increase in frequency and the use of an electro-mechanical multi-station fatigue machine, reduces the cost of generating long term fatigue data to under 5% of that using conventional testing approaches. This allows additional data to be generated giving greater confidence.

KEY WORDS

accelerated test, delamination onset, double cantilever beam, fatigue, frequency effect, interlaminar fracture, mode I delamination, multi-station.

CONTENTS

FIGURE AND TABLE TITLES

NOMENCLATURE

a	delamination length
a_0	initial delamination length
b	specimen width
C	compliance, δ/P
G	strain energy release rate
G_{Ic}	interlaminar fracture toughness
G_{Ic}^{NL}	interlaminar fracture toughness using deviation from linearity values of P and δ
G_{Imax}	maximum cyclic strain energy release rate
m	constant in compliance calibration
N	fatigue cycles
P_c	critical load for delamination initiation
P_{max}	maximum cyclic load during fatigue test
δ_c	critical displacement for delamination initiation
δ_{max}	maximum cyclic displacement during fatigue test
Δ	correction to delamination length in compliance calibration

1.0 SYNOPSIS

Composite material bearing less rotor hubs are subject to high cycle tensile, bending and torsion loads. These structures are designed with increased thickness at the ends for mast and blade attachment and reduced thickness between these attachment points to increase the bending flexibility. The change in thickness is obtained by terminating internal plies. Stress concentrations arise where the plies terminate that may act as sites for delaminations to initiate. The U.S. Army Vehicle Technology Centre (VTC) at NASA Langley, has successfully used interlaminar fracture mechanics analysis on such structures to predict delamination initiation. The structure was analysed to determine the values of strain energy release rate (*G*) at critical locations in the structure. These values of *G* were compared with generic materials fracture data to predict if a delamination will initiate. These predictions were compared with structural test data running out to 10^7 cycles. However, in reality these structures may experience between 10^8 and 10^9 cycles in service at a frequency of 5Hz. It is not feasible to test the structures out to these number of cycles. Hence, it is proposed to generate the materials fracture data out to this number of cycles and extend the current analysis to allow longer term delamination initiation predictions to be made. Hence, the aim of this work was to develop an accelerated method of obtaining these long term fracture data. To achieve this, an acceptable increase in frequency for mode I double cantilever beam (DCB) testing must be found that does not influence the results. Further a multi-sample testing approach should be used with multiple replicate tests, to address the scatter inherent in fatigue behaviour.

Two materials were used in this project with a third being removed early on. These were S2/8552 and S2/F584, both glass epoxy systems. Fatigue tests were conducted on the S2/8552 at different frequencies to identify if any heat arose at the delamination front with high frequency testing. The tests were run up to 30Hz and no heat rise was detected. Further, delamination onset was monitored for shorter term fatigue tests ($<10^6$ cycles) at both 5Hz and 20Hz and no difference in cycles to delamination onset was identified. It was concluded that longer term tests could be run at between 15 and 20Hz to represent structural tests at 5Hz. A multi-station fatigue machine existed at MERL for testing four elastomer test pieces, each with its own instrumentation for stiffness measurement. This design was modified to allow up to six composite DCB test pieces to be tested. Each station had its own instrumentation to monitor individual specimens for compliance changes. This machine operates electro-mechanically and hence is less expensive to run than the conventional servo-hydraulic fatigue machines.

The multi-station machine was used to generate delamination onset data up to 10^8 cycles at 17Hz for both materials. The data, when plotted on a log-log plot gave no obvious indication of reaching a fatigue limit and a linear fit to the data was given. This result highlights the importance of generating the long term data rather than assuming a threshold or no growth limit based on data generated out only to 10^6 cycles. For both materials a consistent decrease in the values of *G* between 10^8 and 10^0 cycles was observed.

It is estimated that the increase in frequency and the use of an electro-mechanical multi-station fatigue machine, reduces the cost of generating long term fatigue data to under 5% of that using conventional testing approaches. This allows additional data to be generated giving greater confidence.

2.0 INTRODUCTION

For laminated polymeric matrix composites, the first damage event is often a single matrix crack resulting as a fibre matrix interface failure or a failure in the polymeric resin. The crack may appear across a lamina as a translaminar crack or between the laminae as an interlaminar crack or delamination. The latter is a far more critical damage mode. A delamination may occur from interlaminar stresses arising from an impact event or from geometric or material discontinuities resulting from design features, such as an edge, a hole, a dropped ply, etc. The delamination will go through an initiation and growth phase. During these phases damage may initiate in another part of the structure leading directly to failure of the part.

One composite material structure that may experience delamination type damage is a bearing less rotor hub. These structures have internally dropped plies to reduce the thickness for bending flexibility and increase the thickness at the ends for mast and blade attachment. The hubs typically rotate at 5 cycles per second (Hz) and may experience a combination of tension, bending and torsion loads.

The Vehicle Technology Centre (VTC) within the Army Research Laboratory (ARL) at NASA Langley, has (at the time of this work) two Co-operative Research and Development Agreements (CRDAs) on composite material rotor systems. One is with McDonnell Douglas Helicopter Systems (MDHS) (now Boeing Helicopters) and the other with Bell Helicopters Textron, Inc. (BHTI). The CRDA with MDHS is investigating delamination in flat laminates that are subjected to tension/torsion loads using S2/F584 glass epoxy. The CRDA with BHTI is investigating delamination in tapered flex beams that represent a critical section of the hub. These laminates are subjected to axial tension and bending loads and are fabricated from S2/E7T1 or S2/8552 glass toughened epoxies.

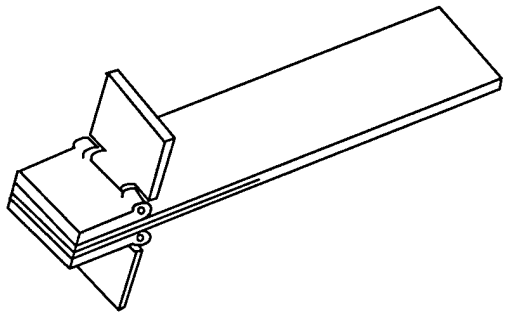

Figure 2.1 Double cantilever beam

The methodology for predicting durability and damage tolerance in both these CRDAs is based on interlaminar fracture mechanics. The relevant laminate or structure is analysed to determine the values of strain energy release rate (G) with different delamination lengths at critical locations. These values of G are compared with generic materials fracture data to predict when and to what extent a delamination will initiate and grow [1-3]. To determine if the composite rotor hubs will delaminate in fatigue, flex beams (the tapered region of a hub) have been tested at VTC for up to 10,000,000 (10^7) cycles. However, because of stroke and frequency limitations on typical hydraulic load frames and the cost of operation, it is not feasible to fatigue test the flex beam laminate beyond 10^7 cycles even though rotor hubs may easily experience between 10^8 and 10^9 cycles in service. Furthermore, should the design change, the fatigue tests would have to be repeated. Hence, it is proposed to use analysis and long term materials fracture data as a design evaluation tool to predict delamination onset in structures such as the flex beam after long term fatigue.

The generic material fracture data required for such analysis includes fracture initiation data from tension or peel forces, mode I and from shear forces, mode II and mode III (perpendicular shear forces acting in the interlaminar plane). In reality the peel and shear forces may be present together causing a mixed mode, e.g. modes I and II fracture. The specimens to characterise these delamination modes are the double cantilever beam (DCB) specimen for mode I, Figure 2.1; the end-notched flexure (ENF) specimen or the newly developed four point bend end-notched flexure (4ENF) for mode II; the edge cracked torsion specimen (ECT) or the modified split cantilever beam (SCB) for mode III; and the mixed mode bending (MMB) specimen from mode I/II. A review of these test methods is given in Reference 4. To provide a comparison for many different structural applications, the material's delamination onset criteria must be generated both under quasi-static conditions and in fatigue for a range of fracture modes. An example of the data to be generated is shown in Figure 2.2. On the traditional x-axis is the number of cycles to delamination onset. On the traditional y-axis is G_t, the total cyclic strain energy release rate. On the z-axis is the mode ratio. When G_I/G_t is zero, this is an all mode II test, or an ENF specimen. When G_I/G_t is 1, it is a pure mode I test or a DCB specimen. The data shown terminates at 10^6 cycles. However, for rotor systems the data must be extended beyond 10^8 cycles.

The data shown in Figure 2.2 is for the initiation or onset of delamination. There are different methods for handling delamination growth. The same specimens described above may be used to measure the rate of fatigue crack growth (da/dN) with the strain energy release rate. In many works [e.g. 4], it has been shown that once the fatigue crack has begun to grow that it grows very rapidly. For structures where the values of G increase with delamination growth, then the delamination growth phase is short and can be neglected. Hence, the design and the prediction approach taken at the VTC is that the delamination should not be allowed to initiate. Hence, no delamination growth work is included in this study.

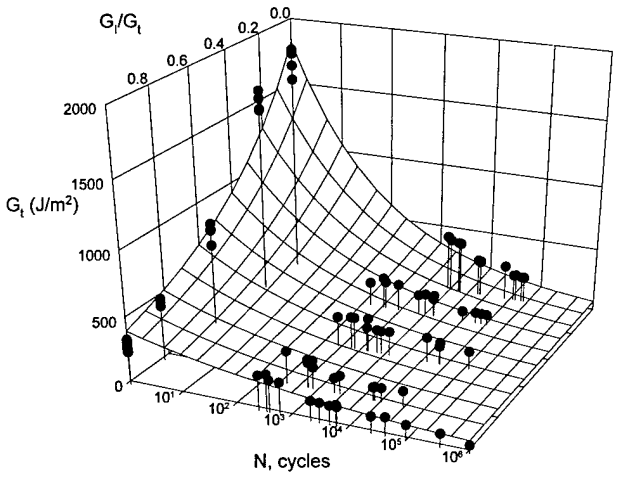

Figure 2.2 Mixed mode fatigue fracture data

To generate data out to 10^8 cycles requires long term tests and dedicated equipment. The cost and time to generate such data is largely proportional to the frequency used. Therefore, if the frequency can be increased there is a linearly proportional decrease in test time. However, increasing the frequency to accelerate the test may have an effect on the physics of the fatigue tests effecting the results. The information on what frequency is acceptable for testing is vital to the reduction of cost to generate these long term data. Further, because of the inherent scatter with fatigue data, it is necessary to test several specimens at the same load level to determine the scatter and allow a statistically accurate fit of the data to be performed. Hence, running several specimens for long duration becomes an even costlier exercise. At MERL, a unique multi-

station fatigue machine has been designed and built. Each station on the test machine has its own instrumentation allowing individual stiffnesses to be monitored during the test. The machine was developed for large displacement elastomer testing. Composite specimens undergo smaller displacements in fatigue, hence modification to the design would need to be made to allow composites to be tested with the result of greatly reduces the cost and time for long term data generation. Hence, the aim of this work is to identify the optimum frequency and employing the multi-station testing approach for mode I DCB testing This approach would then be used to generate the mode I delamination initiation criteria for two rotor craft composite materials out to 10^8 cycles. Because mode I is the critical delamination mode, the use of a mode I delamination criteria allows conservative predictions to be made when other loading modes are present in the structure. Identification of the frequency effects for the other delamination modes is an area for further work.

Initially, the two materials intended for the project were S2/E7T1 (of interest to BHTI) and S2/F584 (of interest to MDHS). A panel of S2/E7T1 was supplied to MERL. However on testing it was identified as containing a woven glass ply on the delamination plane. As no more of this material was readily available, this material was changed to S2/8552 (also of interest to BHTI) part way through the project. However, initial results on the woven panel were generated and are presented.

3.0 LITERATURE SURVEY ON FREQUENCY EFFECTS

The underlying theme to this work is the development of a method for accelerated testing to generate long term delamination characterisation data. One method is the utilisation of the multi-station testing approach already utilised by MERL. The other is the increase of test frequency. However, to identify what work had been done in this area before, a literature review was undertaken.

Most of the references found described frequency effects on laminate failure rather than delamination initiation. Also, many references investigated the effect of lowering frequencies to include time dependent effects rather than increasing the frequency to accelerate the test. However, a few references addressed delamination issues. Subramanian and Chan [5] conducted delamination onset tests on IM6/3501-6 $[(30/-30)_2/30/90]_s$ laminates at frequencies of 0.1, 1 and 10Hz. As the frequency was increased, the cycles to onset of delamination and the delamination growth rate increased. Adams *et al* [6] also investigated the frequency effect on edge delamination in carbon/epoxy laminates. They found no effect between frequencies of 5 and 10Hz, within the ranges of frequencies of interest in this work. Saff [7] found an effect of laminate failure between frequencies of 0.1 and 10Hz and surmised that the sensitivity to load frequency is a function of the stress state of the matrix. Other papers have investigated the effect of frequency and dynamic heating on fatigue life of laminates. Sun and Chan [8] looked at the effect of frequency on notched ±45 laminates and found that an increase in temperature around the hole was responsible for the decrease in fatigue life with increase in frequency (1 to 10Hz). However, if the frequency range being studied is less than 1Hz, such as down to 0.01, then fatigue life is lessened at the lower frequencies because of time dependent damage initiation and growth [9,10].

Hojo *et al* [11] investigated the effect of low frequencies of delamination growth rates in DCB specimens. As the frequency rate was lowered below 5Hz, the crack growth rate was accelerated. This arises from a fatigue/creep interaction. In the work under this contract, the frequency will be raised above 5Hz and so the effect may not be clear. In conclusion, no relevant work was found on the influence of raising frequency on the initiation of delamination in DCB samples.

4.0 TEST MACHINE DEVELOPMENT

The original MERL multi-station fatigue machine, in its present design, presents a low cost option (when compared with servo-hydraulic test equipment) for the performance of low load,

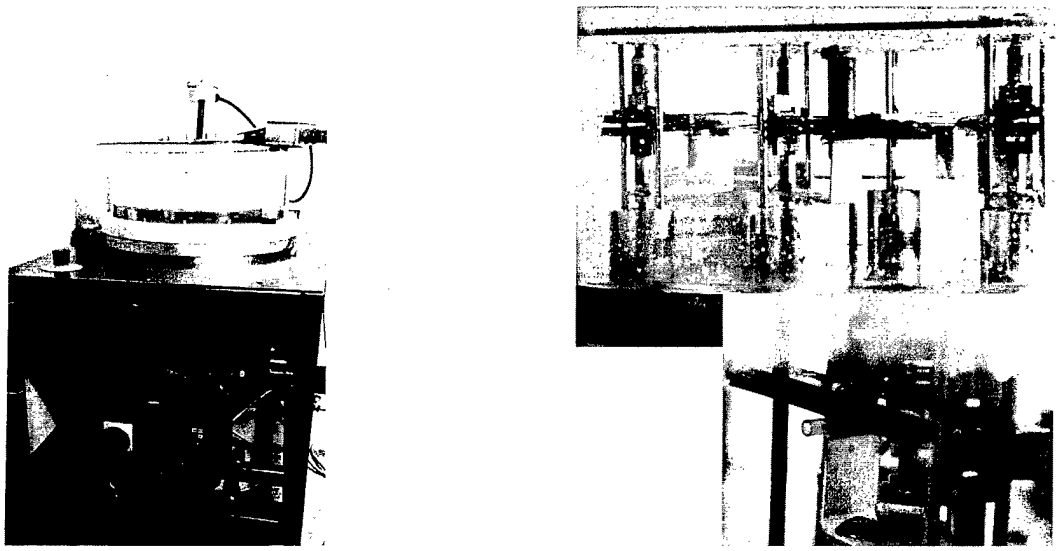

Figure 4.1 The re-designed multi-station machine

displacement controlled, long term fatigue tests. This machine provides a range of operation, in terms of amplitude, from 2.5 to 20mm. Below 2.5mm amplitude levels the accuracy and control of displacement applied to test pieces becomes unreliable. Double Cantilever Beam (DCB) test piece geometry can require cyclic displacements in the order of 1.0mm for long term fatigue tests, much smaller than that available from the present machine.

A design review phase was carried out to establish the necessary operational requirements for a modified machine to be able to test composite DCB specimens. Following preliminary design requirement discussions, two design (modification) concepts were developed. These were further refined with respect to the test requirements of the project and one concept further developed to a working design.

The chosen concept provided six instrumented test stations operating over a number of, discreet, amplitude ranges. This allowed three specimens of each material to be run together for the 10^8 cycle test. The resulting machine is illustrated in Figure 4.1. Each station allowed different amplitudes (within certain conditions) to be applied at different stations. Each load cell had a 1kN dynamic load cell. For each station, the data acquisition consisted of digitally recording the load and displacement data. Periodically, the slope of the loading and unloading curve was calculated to determine the specimen compliance. To improve accuracy of this measurement, the frequency of the test was reduced to 1Hz for a short period while the slope was being measured. The frequency was then returned to its original level until the next measurement. The periodicity of the measurements was a user input. The values of

compliance are plotted versus cycles on the screen and stored to disc with other test information. A typical screen output is illustrated in Figure 4.2.

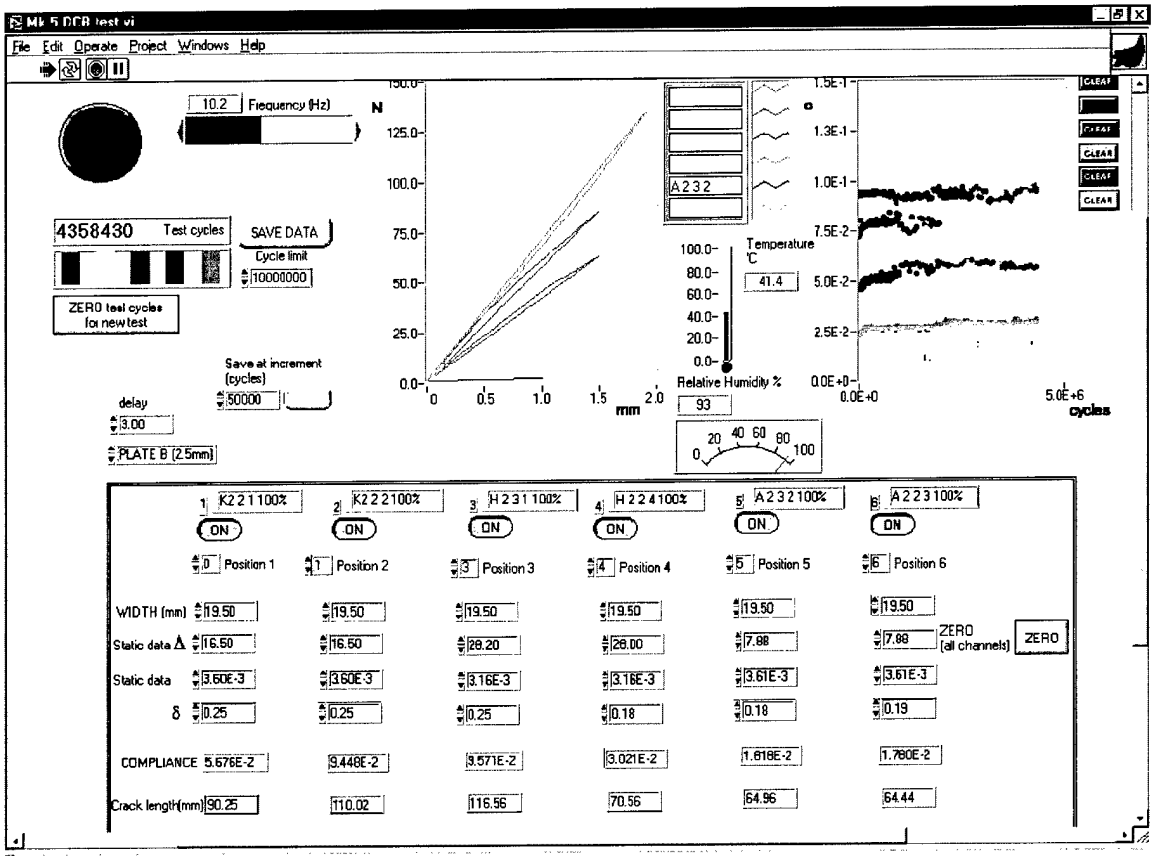

Figure 4.2 Typical screen from data acquisition

5.0 TEST METHODS

5.1 Quasi-static interlaminar fracture toughness tests

These tests were performed on a screw driven test machine at a constant displacement rate according to ASTM D5528. All tests were conducted with delamination from the insert. No unloading cycle was performed after delamination growth from the insert. Four test pieces were selected at random from each batch of material. The S2/8552 specimens for both static and fatigue tests were delivered with MS20001-6 extruded aluminium alloy hinges already attached. The adhesive was not known. For the S2/E7T1 and the S2/F584 specimens, MS20001-6 hinges were bonded on at MERL using Redux 420A/B. The adhesive was cured at 70°C for 2 hours. The thickness and width of each test specimen was measured at three points along the length and the average value determined and used for the calculations of G_{Ic}. The edge of each test specimen was then coated in water-based typewriter correction fluid and a grid marked starting with the first line at a_0 (the end of the insert). Lines were then marked at 1mm intervals for the first 10mm and subsequently at 5mm intervals to a crack length of at least 90mm.

For all specimens, the hinge was clamped firmly in the test grips and the specimen aligned. Load was then applied at a rate of 0.5mm/min. As the load increased the delamination length, a, was measured on one side of the test specimen using a microscope at approximately X25 magnification. At relevant intervals of delamination length, the load and the deflection were noted. Throughout the test, the load/deflection trace was stored in the computer.

The results of all the static tests were calculated using the different methods given in ASTM 5528. However, the tables and plots within this report are all calculated using the modified beam theory, where the compliance is determined from Equation 5.1 and the interlaminar fracture toughness from Equation 5.2.

$$C = m(a + \Delta)^3 \tag{5.1}$$

$$G_{Ic} = \frac{3P_c\delta_c}{2b(a + \Delta)} \tag{5.2}$$

The values of m and Δ are determined from a linear fit of the cube root of the compliance, $C^{1/3}$, plotted against the delamination length, a.

5.2 Effect of frequency on temperature in the DCB

As identified in the literature survey, laminates that undergo high degrees of strain during a fatigue tests may experience a rise in temperature that effects the fatigue life. To determine if this was so with the DCB fatigue tests, a study was conducted to determine the effects of frequency on the heat build up with the S2/8552 specimens. A thermal camera was used that

could determine the local heat in a region 2-3mm in diameter (larger areas were also possible). The thermal camera was capable of detecting a ±0.2°C change in temperature. The heat built up during fatigue should be a function of frequency, amplitude, R-ratio, damping properties of the material, and time. Hence, a specimen was fatigue tested at different frequencies and at different amplitudes for different durations as shown in Table 5.1 (the results are discussed in a later section). The camera was placed approximately 3mm from the crack tip on one specimen located in an MTS servo-hydraulic machine.

δ_{max}	Frequency (Hz)	Cycles (000s)	Time Elapsed (mins)	Specimen Temperature (°C)
1.75	5	12	40	25.2-25.3
2.5	5	20	67	25.6-26.2
3.5	5	60	200	25.6-25.9
3.5	10	50	83	25.0-25.6
3.5	20	250	50	25.4-25.6
3.5	30	59	140	25.1-25.2

Table 5.1 Summary of heat build up tests

5.3 Fatigue delamination initiation

The longer term fatigue tests (>10^6 cycles) were conducted on the new multi-station fatigue machine. Shorter term (<10^6 cycles) tests were performed on a servo-hydraulic MTS test system. These tests utilised a specialist fixture that allows four DCB test specimens to be cycled together with load monitoring on each station. A typical set-up is shown in Figure 5.1. This fixture allows accurate alignment of the test specimen with the load. Each station is monitored using a load cell giving accurate measurements of the load applied to each specimen. The outputs from each load cell are monitored using the same software as for the multi-station machine described above.

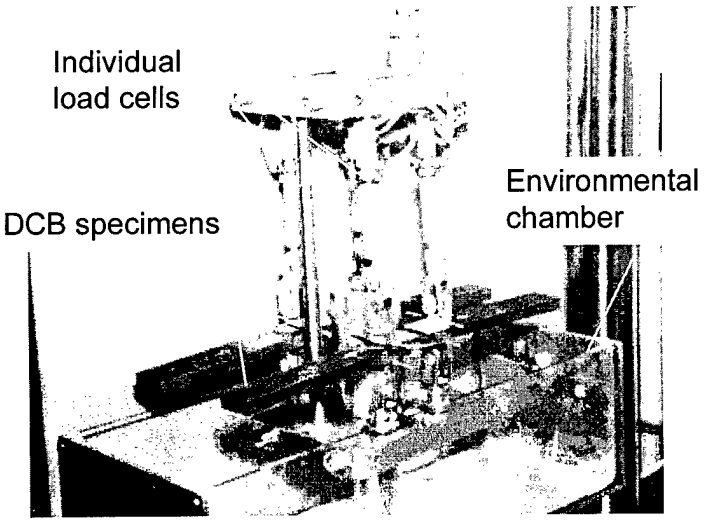

Figure 5.1 Four station multi-station fixture for attachment to servo-hydraulic test stand

The fatigue tests were conducted according to the procedures in ASTM D6115. DCB specimens were cycled between a minimum and maximum displacement, δ_{min}, and δ_{max}. For linear elasticity and small deflections ($\delta/a<0.4$) the displacement ratio, $\delta_{min}/\delta_{max}$, is identical to the R-ratio. A displacement ratio, $\delta_{min}/\delta_{max}$, of 0.1 was specified for this series of tests. The frequency used on the multi-station machine was 17 Hz for the long term tests On the

MTS machine a frequency of 5 and 20Hz was used. The two frequencies were used to make a comparison. Either three or four specimens were tested at four different cyclic displacements to allow a *G-N* curve to be generated as in ASTM D6115. The tests were run until a 5% (or more) change in compliance was obtained or until a test was stopped as a run-out.

The maximum mode I cyclic strain energy release rate, G_{Imax}, was calculated using the modified beam theory as above and in Equation 5.3. To run the test, an average value of Δ from all four static tests was used to identify the applied level of G_{Imax}. Once the fatigue test was complete, a compliance calibration for the individual specimen was conducted to determine the actual values of m and Δ for that specimen, this is an extra procedure not yet included in ASTM D6115. The post fatigue test compliance calibrations were not conducted on the S2/E7T1 specimens.

$$G_{\mathrm{Im}ax} = \frac{3P_{\max}\delta_{\max}}{2b(a+\Delta)} \tag{5.3}$$

6.0 TEST RESULTS

The static and fatigue data are presented in full in the appendices and summarised within the body of the report. The raw-data are supplied on the enclosed discs as Excel files. The files are filed under:

- **MATERIAL NAME** 8552
  E7T1
  F584
  - **DATA TYPE** compcal (compliance calibration)
    fatigue (compliance versus cycles data)
    static (reduced quasi-static data)
    - **SPECIMEN NUMBER**

6.1 Frequency Effects

For all tests conducted, see Table 5.1, even at 30Hz at amplitudes sufficiently close to static toughness to cause crack growth, no significant temperature rise was detected. The ambient lab temperature was approximately 24°C. The temperature of the test specimens was 1-2°C higher over the whole specimen (caused by radiated heat of the servo-hydraulic test stand) with no increase in temperature at the delamination tip region. In conclusion, because of the small area of the composite that is loaded ahead of the crack tip and the lack of friction or any other heat raising mechanism, heat build up in the unidirectional S2/8552 DCB specimens does not occur within the parameters tested. The comparison of *G-N* data generated at 5Hz and 20Hz is discussed below. In summary, the long term tests of DCB specimens may be conducted at frequencies up to 30Hz with no significant heat build up effects.

6.2 Static Results

The data sheets for all the static tests are given in Appendix 1. This consists of the following:

- The load displacement curve
- Table of data and data reduction
- R-curve.

6.2.1 S2/E7T1 (with fabric layer)

A typical load displacement curve is shown in Figure 6.1. Although these specimens contained a fabric layer, the curve had no signs of crack growth jumping across the weaves (observed as a ratchetting effect) but did show evidence of fibre bridging (load still increases after delamination initiation) [12]. Fibre bridging is evident on examination of the delaminated surfaces, Figure 6.2, where the bridged fibres appear lighter in colour. The R-curve for the four

S2/E7T1 (with fabric layer) specimens is shown in Figure 6.3. The scatter between the four samples tested is low. The data has the classical increase in crack growth resistance from the effects of fibre bridging. This increase occurs over the first 5-10mm of delamination growth where the values reach a plateau approximately twice that at initiation. The actual loads and values are given along with the fatigue data in the section 6.3.

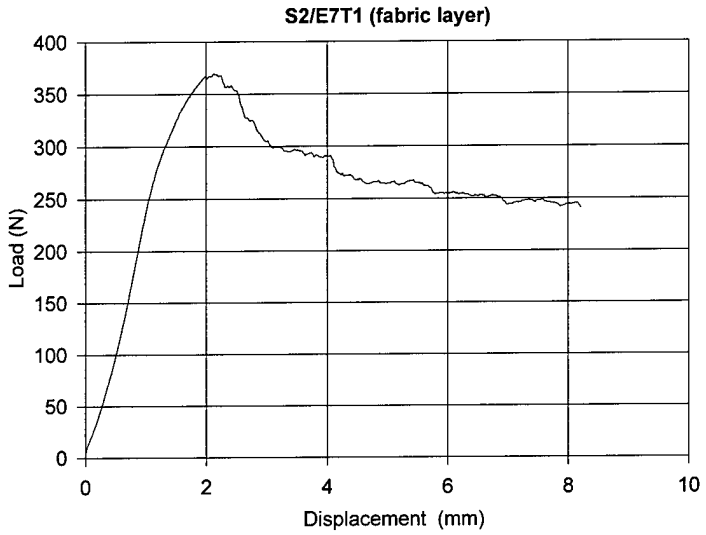

Figure 6.1 Typical Load Displacement Curve for S2/E7T1 with a fabric layer

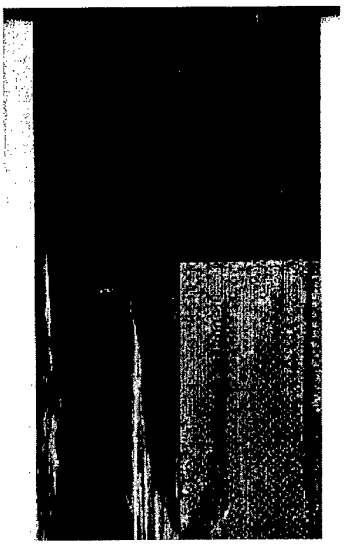

Figure 6.2 Digital scan of failure surface

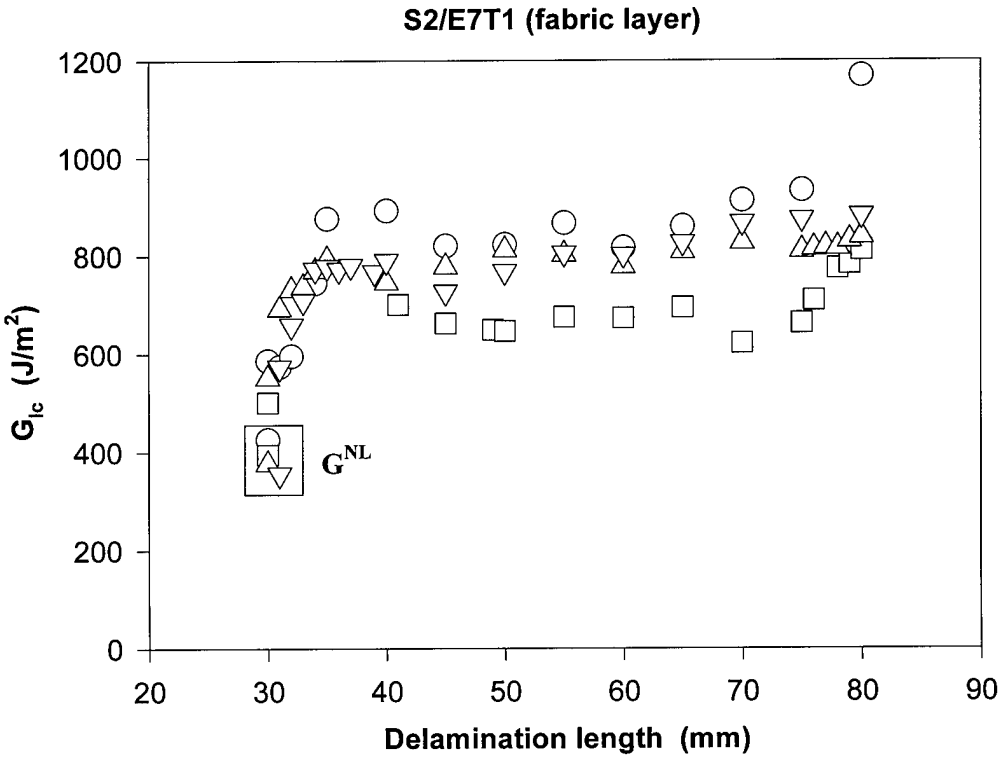

Figure 6.3 R-Curve for S2/E7T1 Material (with fabric layer)

6.2.2 S2/F584

A typical load displacement curve for the S2/F584 is shown in Figure 6.4. The actual values are given in Appendix 1. The G_{Ic}^{NL} values are given along with the fatigue data in section 6.3. The loading portion is linear but at the point of initiation, there was a jump in the load displacement

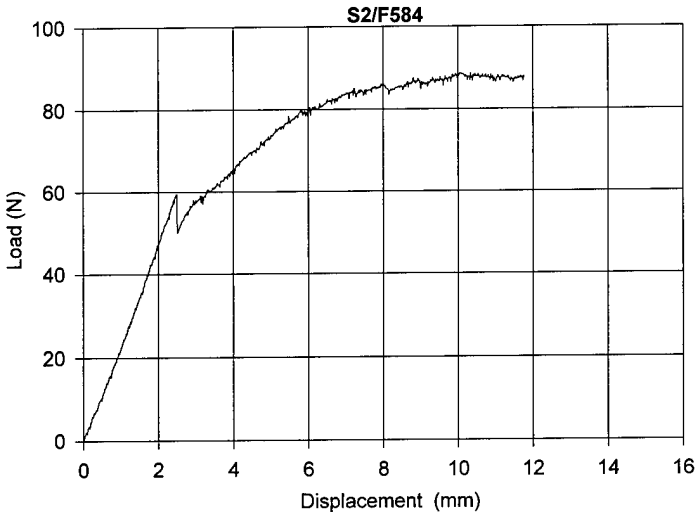

Figure 6.4 Typical Load Displacement Curve for S2/F584

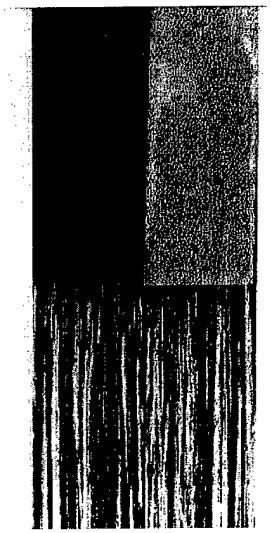

Figure 6.5 Digital scan of failure surface

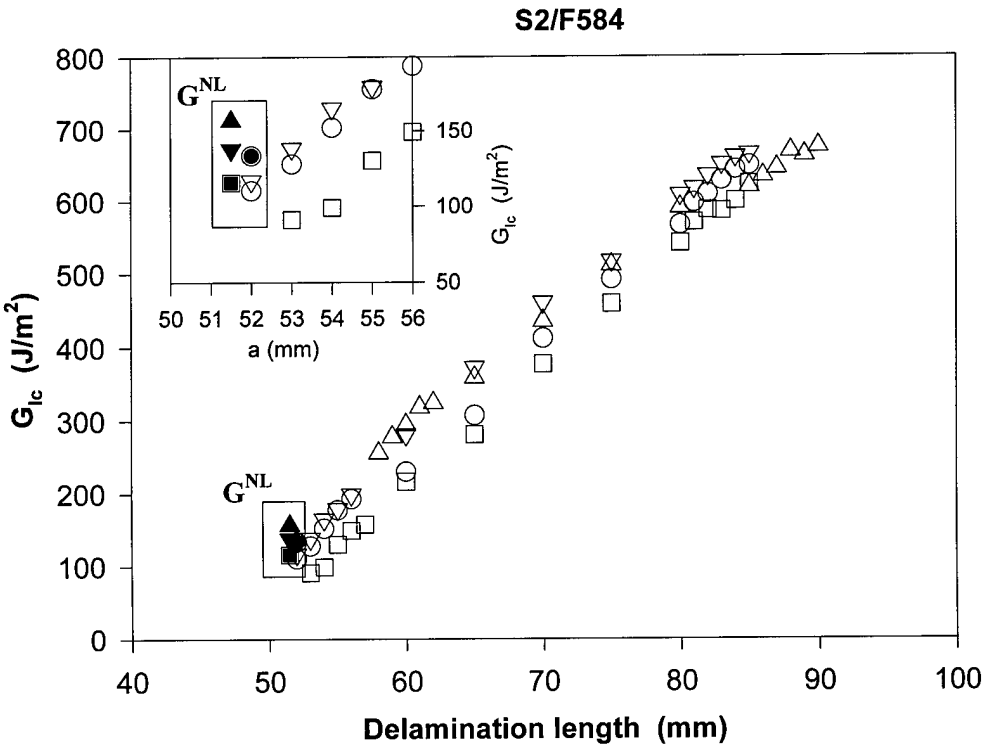

Figure 6.6 R-Curve for S2/F584 Material

curve, indicating unstable growth. This jump is a result of a thick insert being used creating a blunt crack. This results in artificially high values of G_{Ic}. According to ASTM 5528 these values are invalid. The magnitude of the jump was similar for all four specimens. On further delamination growth, the load continues to increase indicating substantial fibre bridging. Fibre bridging is evident on examination of the delaminated surfaces, Figure 6.5 where the bridged fibres appear lighter in colour. The R-curve for the S2/F584 is shown in Figure 6.6. The scatter between the four samples tested is low. The data shows the classical increase in crack growth resistance from the effects of fibre bridging. This increase occurs over the first 5-10mm of delamination growth where the values reach a plateau. The inset graph in Figure 6.6 shows the higher values of G_{Ic} at the insert.

6.2.3 S2/8552

A typical load displacement curve for the S2/8552 is shown in Figure 6.7. The G_{Ic}^{NL} values are given along with the fatigue data in the fatigue section below. The loading portion is linear and once the crack initiates the load continues to increase for a substantial amount of delamination growth. This is indicative of fibre bridging occurring. Fibre bridging is evident on examination of the delaminated surfaces, Figure 6.8. The R-curve for the S2/8552 is shown in Figure 6.9. The scatter between the four samples tested is low. The data increases from the initial values and appears to be approaching a plateau value. After 50mm of delamination growth, the values of G_{Ic} are seven times larger than that at initiation from the insert. the classical increase in crack growth resistance from the effects of fibre bridging.

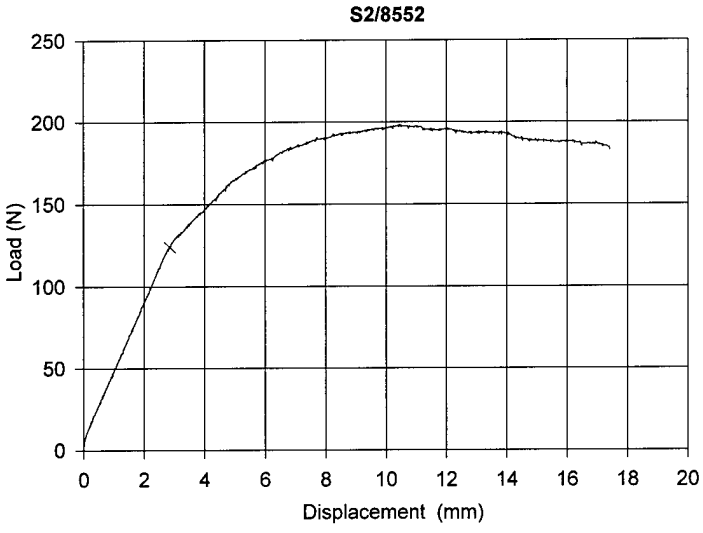

Figure 6.7 Typical Load Displacement Curve for S2/F584

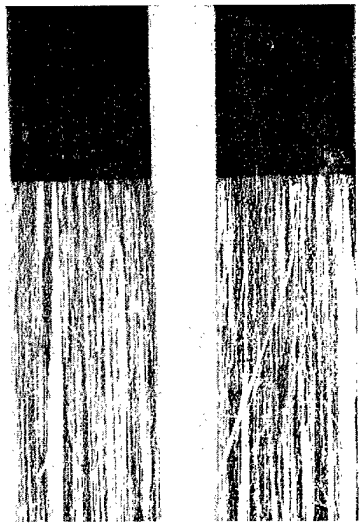

Figure 6.8 Digital scan of failure surface

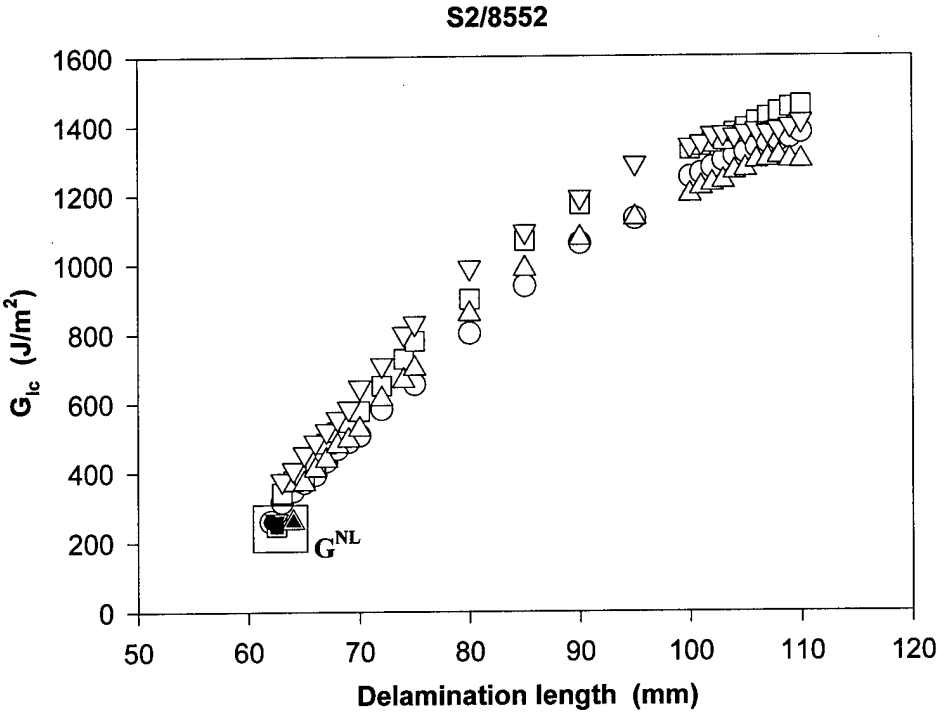

Figure 6.9 R-Curve for S2/8552 Material

6.3 FATIGUE RESULTS

The fatigue results are shown as measured compliance versus cycles monitored during the fatigue tests in Appendix 2. The number of cycles to delamination onset, taken as a 5% increase in compliance, are given in the subsequent tables and plots. The number of cycles to give a 5% increase in compliance was obtained graphically as illustrated in Figure 6.10.

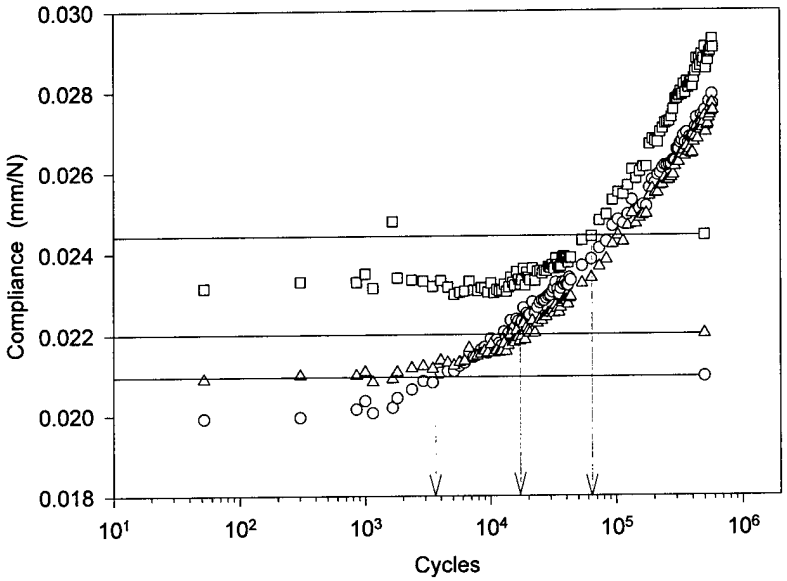

Figure 6.10 Determination of cycles to onset after a 5% increase in compliance for a S2/8552 DCB specimen

6.3.1 S2/E7T1 (with fabric layer)

The cycles to delamination onset for the S2/E7T1 specimens are shown in Figure 6.11 and Table 6.1. The data are plotted on a log-log scale with the quasi-static data (G_{Ic}^{NL}) plotted at 10^0 cycles. A linear fit to all the data is shown. Because of the fabric layer in the DCB specimens, the fatigue data had limited use, hence, these tests were not taken beyond 10^6 cycles. Also, post fatigue compliance calibrations for the fatigue specimens were not conducted and the average value of Δ from the four static tests were used to calculate G_{Imax}.

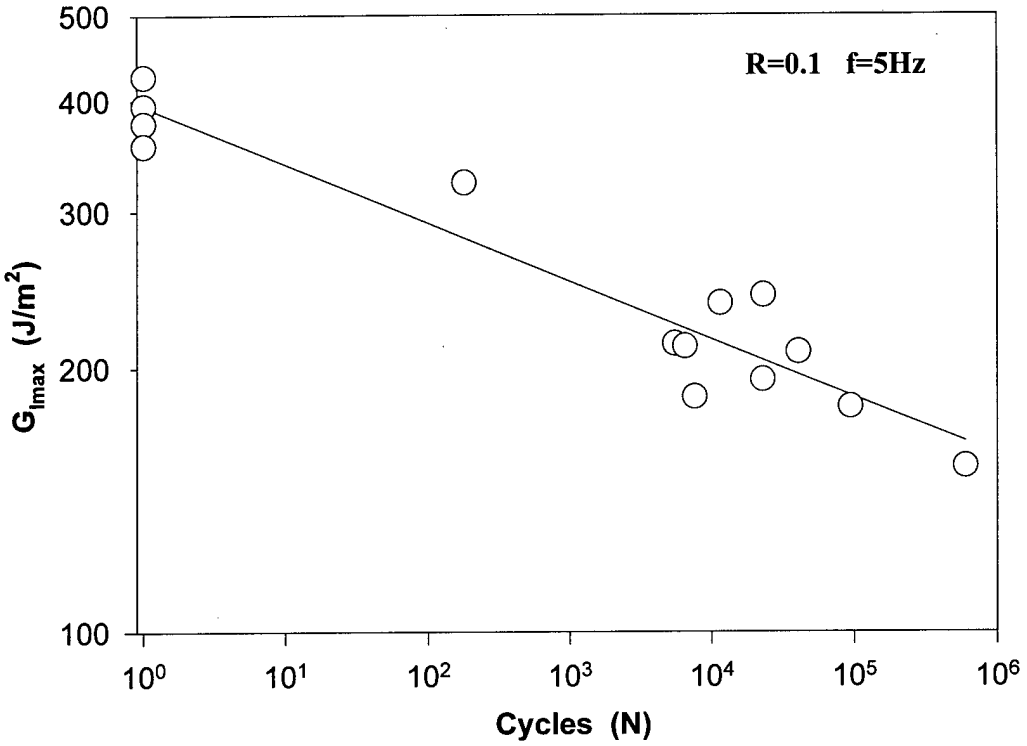

Figure 6.11 G-N curve for S2/E7T1 with a fabric layer

Sample	Width (mm)	Crack Length (a_0) (mm)	f (Hz)	P_{max} (N)	δ_{max} (mm)	G_{Imax} (J/m^2)	$N^{5\%}$
4A	25.36	30.0	-	273.3 NL	1.14 NL	425.7 NL	static
7A	25.80	30.0	-	269.3 NL	1.18 NL	394.4 NL	static
8B	25.84	30.0	-	260.0 NL	1.00 NL	376.6 NL	static
9A	25.85	31.0	-	237.4 NL	1.12 NL	355.4 NL	static
1B	25.07	32.4	5	175	0.77	154.2	600,000
9B	25.81	27.5	5	221	0.77	208.5	40,700
11B	25.51	29.0	5	195	0.77	180.6	94,200
10A	25.50	28.9	5	209	0.77	193.9	22,900
2B	25.35	28.0	5	203	0.74	185.4	7,600
3A	25.19	26.6	5	225	0.74	213.0	5,500
6B	25.63	24.7	5	248	0.74	241.6	23,100
8A	25.7	26.2	5	226	0.74	211.6	6,500
6A	25.49	27.1	5	272	0.95	323.3	180
5B	25.40	29.3	5	210	0.94	236.7	11,500

Table 6.1 Quasi-static and fatigue results for S2/E7T1 specimens

6.3.2 S2/F584

The cycles to delamination onset for the S2/F584 specimens are shown in Figure 6.12 and Table 6.2. The data are plotted on a log-log scale with the quasi-static data (G_{Ic}^{NL}) plotted at 10^0 cycles. These data were taken out to 10^8 cycles. A linear fit to all the data is shown. Post fatigue test compliance calibrations were conducted and the value for Δ from individual specimens used to calculate G_{Imax}. Note: the longer term tests were conducted at 17Hz because the fatigue machine was less resonant than at 20 Hz.

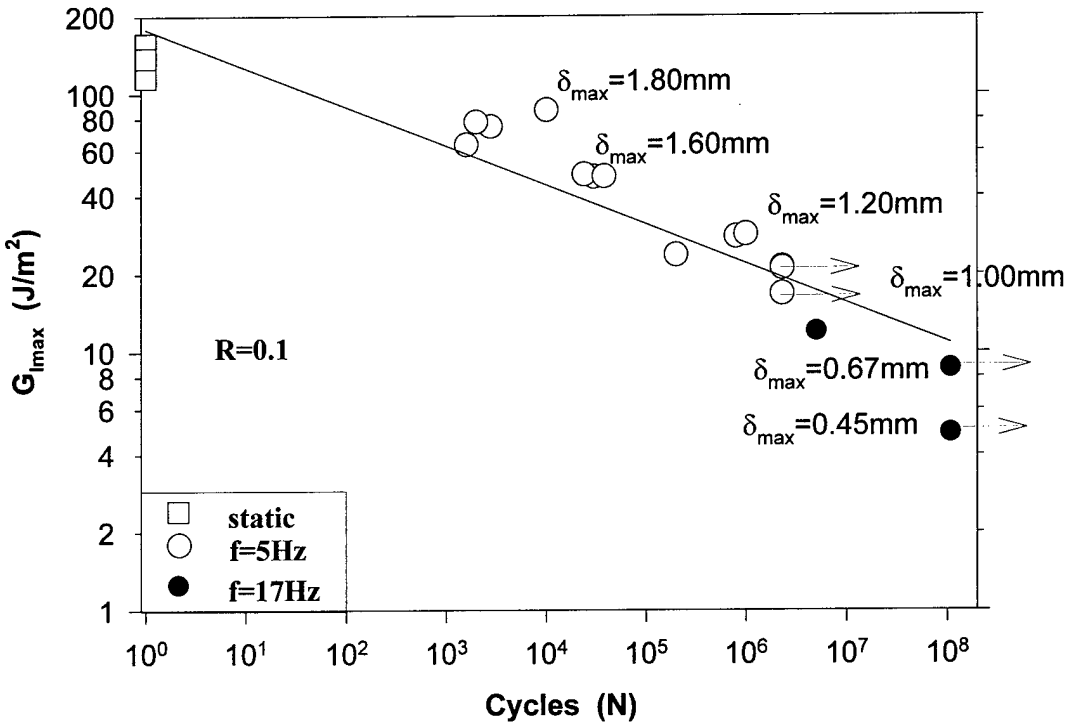

Figure 6.12 G-N curve for S2/F584

Spec #	b (mm)	Δ (mm)	m x10^{-3}	a (mm)	f (Hz)	δ_{max} (mm)	P_{max} (N)	C_0 (mm/N)	G_{Imax} (J/m^2)	N5%
13	20.05	29.44	4.70	52.0	-	2.60	56.0	-	133.6	static
14	20.05	22.43	5.01	51.5	-	2.20	52.0	-	115.7	static
17	20.06	19.96	5.16	51.5	-	2.50	60.0	-	156.8	static
22	20.01	30.02	4.47	51.5	-	2.50	60.0	-	137.8	static
01	20.25	22.25	4.79	51.0	5	1.60	46.1	0.034	74.6	2,800
03	20.20	26.24	4.68	51.0	5	1.60	50.6	0.036	77.8	2,000
10	19.98	35.42	4.33	51.0	5	1.60	45.6	0.037	63.4	1,600
12	20.06	19.85	5.08	51.0	5	1.60	51.2	0.033	86.5	10,100
05	20.24	27.58	4.56	52.0	5	1.20	42.5	0.034	47.5	30,000
08	20.19	23.50	4.88	51.0	5	1.20	40.5	0.035	48.5	24,000
09	20.16	22.87	4.79	52.0	5	1.20	40.0	0.035	47.7	38,000
11	20.16	22.69	4.96	51.0	5	1.20	-	-	-	lost data
02	20.29	27.25	4.73	52.0	5	1.00	-	-	-	lost data
06	20.01	27.54	4.66	50.0	5	1.00	28.9	0.036	27.9	800,000
07	20.16	25.87	4.66	52.0	5	1.00	29.8	0.035	28.5	1,000,000
15	20.12	24.50	4.84	52.0	5	0.80	30.4	0.035	23.7	200,000
19	19.72	30.64	4.53	52.0	5	0.80	29.0	0.034	21.3	2,300,000
21	20.12	28.81	4.68	52.0	5	0.80	22.8	0.041	16.8	2,300,000
24	19.93	19.80	5.11	52.0	5	0.80	25.2	0.037	21.1	2,300,000
26	20.00	21.67	5.09	52.0	17	0.43	11.1	0.038	4.86	108,000,000
29	20.04	20.53	5.14	52.0	17	0.67	12.5	0.048	8.64	108,000,000
30	20.15	26.82	4.58	52.0	17	0.67	19.0	0.031	12.02	5,000,000

underlined indicates a run out

Table 6.2 Quasi-static and fatigue results for S2/F584 specimens

6.3.3 S2/8552

The cycles to delamination onset for the S2/8552 specimens are shown in Figure 6.13 and Table 6.3. The data are plotted on a log-log scale with the quasi-static data (G_{Ic}^{NL}) plotted at 10^0 cycles. These data were taken out to 10^8 cycles. The tests conduced at 5 Hz are shown as open symbols. The tests conducted at higher frequencies (20Hz on MTS machine and 17Hz on multi-station machine) are shown as solid symbols. Because the two sets are largely coincident, then it can be concluded that within this range the frequency does not have an effect on the number of cycles to delamination onset. For the three specimens undergoing the long term tests, one station developed a fault during the test. The data were not recovered. On another specimen very early on in the test, the hinge pin came out. This was replaced and the test restarted. For this specimen a 5% change in compliance was achieved at approximately 10^8 cycles determined graphically. For the third specimen, the compliance fluctuates up and down. The cause for this was not identified but possibly caused from the fixture becoming loose during the fatigue test. However, because the overall compliance does not increase this test is considered a run out.

A linear fit including the static and run out data is shown. Post fatigue test compliance calibrations were conducted and the value for Δ from individual specimens used to calculate G_{Imax}.

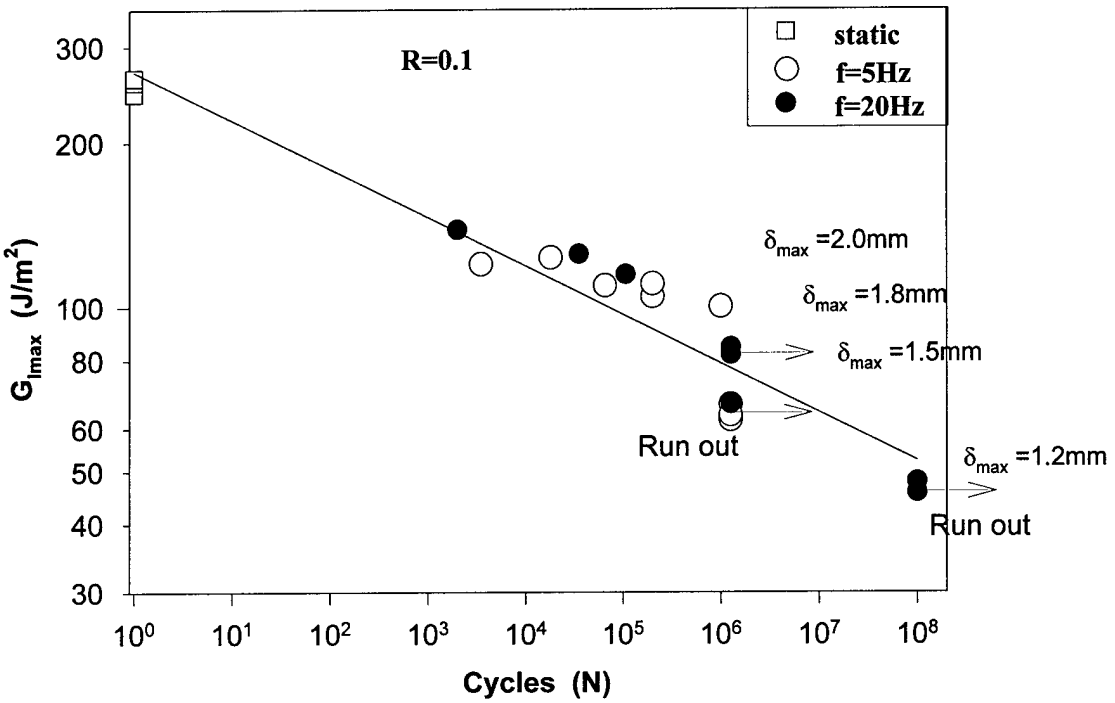

Figure 6.13 G-N curve for S2/8552

Spec #	b (mm)	Δ (mm)	m $x10^{-3}$	a (mm)	f (Hz)	δ_{max} (mm)	P_{max} (N)	C_0 (mm/N)	G_{Imax} (J/m^2)	N5%
05	25.40	20.86	3.47	62.0	1	2.80	130.0	-	259.3	1
12	25.40	19.94	3.51	62.5	1	2.80	123.0	-	246.0	1
16	25.39	21.48	3.42	64.0	1	2.90	129.0	-	258.4	1
21	25.37	20.91	3.52	62.5	1	2.90	128.0		262.9	1
08	25.40	31.07	3.18	62.0	5	2.00	86.2	0.023	109.4	65,000
11	25.40	33.60	3.19	62.0	5	2.00	97.0	0.020	119.8	3,500
19	25.40	28.36	3.26	62.0	5	2.00	94.2	0.021	123.1	18,000
02	25.4	26.63	3.32	62.0	5	1.80	87.1	0.021	104.5	200,000
09	25.40	25.56	3.25	62.0	5	1.80	82.5	0.021	100.2	1,000,000
10	25.40	20.92	3.43	62.0	5	1.80	86.0	0.021	110.2	200,000
15	25.40	14.74	3.44	62.0	20	1.85	97.3	0.020	138.5	2,000
20	25.40	14.28	3.53	62.0	20	1.85	87.3	0.023	125.0	108,000
3	25.40	28.20	3.23	62.0	20	1.85	94.7	0.020	114.7	3,500
01	25.40	25.24	3.34	62.0	5	1.50	61.3	0.023	62.2	1,260,000
14	25.40	25.39	3.30	62.0	5	1.50	65.5	0.022	66.4	1,260,000
18	25.40	24.64	3.36	62.0	5	1.50	62.1	0.024	63.5	1,260,000
6	25.40	26.81	3.19	62.0	20	1.55	79.9	0.023	84.4	1,264,000
13	25.40	33.63	3.16	62.0	20	1.55	69.5	0.026	66.5	1,264,000
22	25.40	28.18	3.22	62.0	20	1.55	80.7	0.022	81.9	1,264,000
04	25.40	29.04	3.21	63.0	17	1.24	56.2	0.022	44.7	108,000,000
07	25.40	40.67	2.98	62.0	17	1.24	55.3	0.021	39.4	108,000,000
17	25.40	32.21	3.02	62.0	17	-	-	-	-	-

underlined indicates a run out

Table 6.3 Quasi-static and fatigue results for S2/8552 specimens

7.0 DISCUSSION

Although a direct comparison of the materials is not an objective of this work because it is useful to compare the relative fatigue performance with respect to the quasi-static performance. A comparison of the *G-N* curves is shown in Figure 7.1.

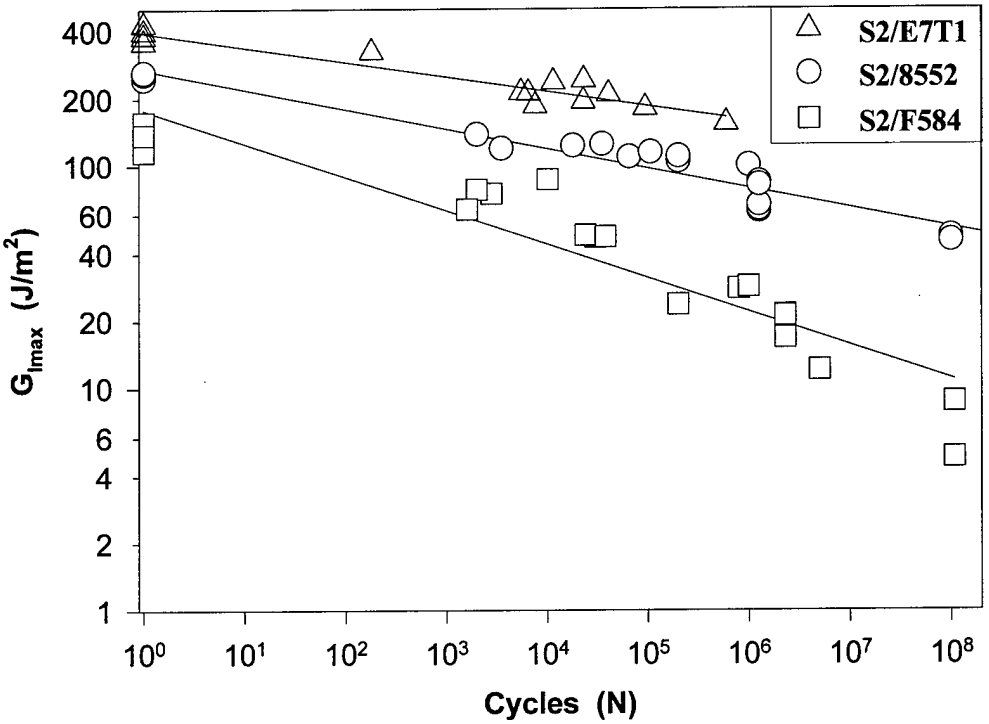

Figure 7.1 Comparison of delamination onset

For each material the decrease in G_c for delamination onset from the quasi-static value (plotted at 10^0) is of a similar degree as evident by the slopes of the curves in Figure 7.1. The slope of the linear fit in the F584 curve appears steeper, but is influenced by the run out tests. The numerical expression for this curve is given in Equation 7.1 and the values of the constants in Table 7.1

$$G_{\mathrm{I}max} = 10^{r} \left(N_{onset}\right)^{s} \tag{7.1}$$

Material	r	s
S2/E7T1	-0.0655	2.189
S2/F584	-0.1528	2.250
S2/8552	-0.0890	2.431

Table 7.1 Linear fit to fatigue data

The data represented in Figure 7.1 does not give any indication of turning to reach a fatigue limit below although several of the specimens were run outs. It is often the approach to plot fatigue data assymptoting to a lower bound. However, by actually generating the data to the typical duration of rotor craft structure, as in this work, an actual value of G_{Imax} can be determined as the true fatigue limit such that no delamination will initiate within the life of the structure.

8.0 CONCLUDING REMARKS

This work has illustrated that the combined use of a multi-station electro-mechanical fatigue machine and an increase in test frequency can be used to generate mode I interlaminar fracture fatigue data cost effectively. This work identified that increasing the frequency to 20Hz from the typical 5Hz had no effect on DCB delamination onset. This is largely because there is no temperature rise at the crack tip and the effect of time at load does not play a significant role with the small amplitudes and increase in frequency. Increasing the frequency to 20 Hz from 5Hz, reduces the test time four times. By testing all the required replicates, say four, at same time reduces the test time again by four times. It estimated that an electro-mechanical machine is at most 50% of the cost to operate a servo-hydraulic machine. Therefore, in total this approach in generating long term data is less than 5% of the costs of generating these data using conventional equipment.

The generation of a mode I interlaminar fatigue delamination criteria up to 10^8 cycles, offers the ability to make predictions of fatigue loaded structural parts with lives up to the same number of cycles. This must be based on a total G criteria where the individual modes are summed up and compared with the mode I fatigue and quasi-static properties. This enables a conservative prediction to be made if the delamination within a structure is also driven by shear loads. To further improve the failure criteria, a combination of mode I and II and ultimately mode III should be developed. Before this can be achieved, it is necessary to determine if the tests for mode II (4ENF) and mixed mode I/II (MMB) can be operated at 20 Hz or a higher frequency with no adverse effects on the data. This is research proposed for future work.

9.0 REFERENCES

1. O'Brien, T. K., "Towards a Damage Tolerance Philosophy for Composite Materials and Structures," *Composite Materials: Testing and Design,* Vol. 9, ASTM STP 1059, S.P. Garbo, Ed., American Society for Testing and Materials, Philadelphia, 1990, pp. 7-33.

2. O'Brien, T. K., Rigamonti, M., and Zanotti, C., "Tension Fatigue Analysis and Life Prediction for Composite Laminates," *International Journal of Fatigue*, Vol. 11, No. 6, Nov. 1989, pp. 379-393.

3. Murri, G. B., O'Brien, T. K., and Rousseau, C. Q., "Fatigue Life Prediction of Tapered Composite Laminates," American Helicopter Society, 53rd Annual Forum, April 29-May 1st, 1997, Virginia Beach, Virginia

4. Martin, R. H. "Interlaminar Fracture Characterization," Fracture of Composites, Key Engineering Materials Vols. 121-122 (1996), pp. 329-346, Transtec Publications, Switzerland.

5. Subramanian, S., and Chan, W. S., "Frequency Effects on Delamination Characteristics of Laminates with and without an Interleaf," Composites; Proceedings of the 8th, International Conference on Composite Materials, (ICCM/8), Honolulu, HI, July 15-19, 1991, Society for, the Advancement of Material and Process Engineering, Covina, CA, 1991, pp. 28-O-1 to 28-O-10.

6. Adams, D. F., Zimmerman, R. S., Odom, E. M., "Frequency and Load Ratio Effects on Critical Strain Energy Release Rate Gc Thresholds of Graphite/Epoxy Composites," *Toughened Composites*, ASTM STP 937, N. J. Johnston, Ed., American, Society for Testing and Materials, Philadelphia, 1987, p., 242-259.

7. Saff, C. R., "Effect of Load Frequency and Lay-up on Fatigue Life of Composites, *"Long-Term Behavior of Composites*, T. K. O'Brien, Ed., ASTM STP, American, Society for Testing and Materials, Philadelphia, 1983, p., 78-91.

8. Sun, C. T. and Chan W. S., "Frequency Effect on the Fatigue Life of a Laminated Composite," Composite Materials: Testing and Design, Fifth Conference, ASTM STP, American Society for Testing, and Materials, Philadelphia, 1979, p. 418-430.

9. Knauss, W. G., "A Study of the Time Dependence in Fracture Processes Relating to Service Prediction of Adhesive Joints and Advanced Composites," Final Technical Report, 15 Aug. 1983 - 30 Jun. 1984, California Inst. of Tech., Pasadena, CA.

10. Tsai, G. C., "A Study of Frequency Effects and Damage Accumulation During the Fatigue of Graphite/Epoxy and Glass/Epoxy Composite Materials - Ph.D. Thesis, Purdue Univ., West Lafayette, IN, 1984.

11. Hojo, M., Hayashi, R. Tanaka, K., and Gustafson, C. G., "Near-Threshold Propagation of Delamination Fatigue Cracks in Graphite/Peek Laminates," ICCM-VII; Proceedings of the 7th, International Conference on Composite Materials, Guangzhou, People's Republic of China, Nov., 22-24, 1989. Vol. 2, Beijing/Oxford, International Academic, Publishers/Pergamon Press, 1989, p. 511-516.

12. Martin, R. H., "Delamination Characterisation of Woven Glass/Polyester Composites," Journal of Composites Technology and Research, Vol. 19, No. 1, 1997, pp. 20-28.

APPENDIX A

QUASI-STATIC RESULTS

MERL	Bell E7T1 - 4A	Test Date: 02/07/96

Input					
Specimen thickness	2h [mm]	9.73	End block thickness	H [mm]	MISSING
Specimen width	B [mm]	25.36	End block length	l3 [mm]	MISSING
Starter foil material	[-]	MISSING	Temperature	[°C]	MISSING
Starter foil thickness	[µm]	MISSING	Relative humidity	[%]	MISSING
Starter foil length	A [mm]	30.00	Loading rate	[mm/min]	0.50
Hinge type	[-]	piano	Drying temperature	[°C]	MISSING
Fiber Volume Fraction	Vf [Vol%]	MISSING	Drying duration	[h]	MISSING
			% Change Compliance	[%]	MISSING

l1	2.43
l2	0.00

check	(a+l2)-A >= 0	OK

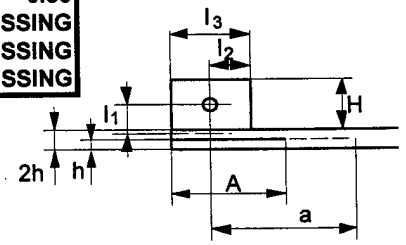

Text	Measure a [mm]	Load [N]	δ [mm]
NL	30.00	273.30	1.14
5%	30.00	308.90	1.39
Prop.	31.00	310.40	1.40
Prop.	32.00	318.80	1.46
Prop.	34.00	351.00	1.76
Prop.	35.00	366.70	2.04
Prop.	40.00	353.90	2.46
Prop.	45.00	319.40	2.82
Prop.	50.00	295.20	3.40
Prop.	55.00	290.80	4.00
Prop.	60.00	269.80	4.43
Prop.	65.00	263.70	5.17
Prop.	70.00	254.20	6.13
Prop.	75.00	244.00	7.00
Prop.	80.00	243.70	8.17

Results			
Gcbt [J/m2]	Gecm [J/m2]	Gmcc [J/m2]	E-Mod. [GPa]
366.2	425.7	366.4	83.1
504.5	586.4	492.3	76.9
500.7	574.4	497.9	81.5
526.0	596.0	530.6	85.0
672.4	744.5	683.1	86.9
799.3	875.6	799.0	82.7
853.2	891.7	863.4	85.8
815.1	820.2	824.9	85.8
843.7	822.5	841.3	82.1
912.8	866.6	918.9	84.5
879.6	816.3	890.2	85.9
944.5	859.5	957.1	86.2
1019.6	912.1	1020.9	83.1
1058.9	933.1	1056.0	82.1
1172.7	1019.6	1168.6	81.9
		average	83.6
		deviation	2.6

MERL	Bell E7T1 - 4A	Test Date: 02/07/96

Input					
Specimen thickness	2h [mm]	9.73	End block thickness	H [mm]	MISSING
Specimen width	B [mm]	25.36	End block length	l3 [mm]	MISSING
Starter foil material	[-]	MISSING	Temperature	[°C]	MISSING
Starter foil thickness	[µm]	MISSING	Relative humidity	[%]	MISSING
Starter foil length	A [mm]	30.00	Loading rate	[mm/min]	0.50
Hinge type	[-]	piano	Drying temperature	[°C]	MISSING
Fiber Volume Fraction	Vf [Vol%]	MISSING	Drying duration	[h]	MISSING
			% Change Compliance	[%]	MISSING

l1	2.43
l2	0.00

check	(a+l2)-A >= 0	OK

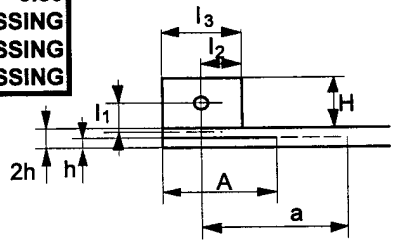

Text	Measure a [mm]	Load [N]	δ [mm]
NL	30.00	273.30	1.14
5%	30.00	308.90	1.39
Prop.	31.00	310.40	1.40
Prop.	32.00	318.80	1.46
Prop.	34.00	351.00	1.76
Prop.	35.00	366.70	2.04
Prop.	40.00	353.90	2.46
Prop.	45.00	319.40	2.82
Prop.	50.00	295.20	3.40
Prop.	55.00	290.80	4.00
Prop.	60.00	269.80	4.43
Prop.	65.00	263.70	5.17
Prop.	70.00	254.20	6.13
Prop.	75.00	244.00	7.00
Prop.	80.00	243.70	8.17

Results			
Gcbt [J/m2]	Gecm [J/m2]	Gmcc [J/m2]	E-Mod. [GPa]
366.2	425.7	366.4	83.1
504.5	586.4	492.3	76.9
500.7	574.4	497.9	81.5
526.0	596.0	530.6	85.0
672.4	744.5	683.1	86.9
799.3	875.6	799.0	82.7
853.2	891.7	863.4	85.8
815.1	820.2	824.9	85.8
843.7	822.5	841.3	82.1
912.8	866.6	918.9	84.5
879.6	816.3	890.2	85.9
944.5	859.5	957.1	86.2
1019.6	912.1	1020.9	83.1
1058.9	933.1	1056.0	82.1
1172.7	1019.6	1168.6	81.9
		average	83.6
		deviation	2.6

MERL	Bell E7T1 - 4A	Test Date: 02/07/96

Regression

Method	Gcbt		Gecm		Gmcc	
Value	slope	Y-axis	slope	Y-axis	slope	Y-axis
	0.00320058	0.06485084	2.08133821	-5.46474504	32.0688328	-2.07304546
Correction	Δ=	**-20.2622**	n=	**2.0813**	A1=	**32.0688**
Correl. coeff. r^2	0.998675		0.995310		0.998675	
Points for fit						
	x	y	x	y	x	y
Point 1	30.00	0.16	1.48	-2.39	0.16	3.10
Point 2	80.00	0.32	1.90	-1.50	0.32	8.29

Text	F [-]	N [-]	F/N [-]	C/N [mm/N]	(C/N)^1/3	log(C/N)	log(a)	δ/a < 0.4
NL	0.9949	0.9962	0.9988	0.0042	0.1612	-2.3781	1.4771	0.0380
0.05	0.9937	0.9952	0.9985	0.0045	0.1654	-2.3447	1.4771	0.0463
Prop.	0.9941	0.9955	0.9986	0.0045	0.1655	-2.3438	1.4914	0.0452
Prop.	0.9942	0.9956	0.9986	0.0046	0.1663	-2.3372	1.5051	0.0456
Prop.	0.9936	0.9951	0.9985	0.0050	0.1714	-2.2977	1.5315	0.0518
Prop.	0.9929	0.9946	0.9983	0.0056	0.1775	-2.2523	1.5441	0.0583
Prop.	0.9933	0.9948	0.9984	0.0070	0.1912	-2.1557	1.6021	0.0615
Prop.	0.9937	0.9952	0.9986	0.0089	0.2070	-2.0520	1.6532	0.0627
Prop.	0.9937	0.9951	0.9986	0.0116	0.2262	-1.9365	1.6990	0.0680
Prop.	0.9936	0.9950	0.9986	0.0138	0.2400	-1.8594	1.7404	0.0727
Prop.	0.9939	0.9952	0.9986	0.0165	0.2546	-1.7826	1.7782	0.0738
Prop.	0.9936	0.9950	0.9986	0.0197	0.2701	-1.7055	1.8129	0.0795
Prop.	0.9931	0.9946	0.9985	0.0242	0.2894	-1.6154	1.8451	0.0876
Prop.	0.9928	0.9944	0.9985	0.0289	0.3067	-1.5398	1.8751	0.0933
Prop.	0.9922	0.9938	0.9984	0.0337	0.3231	-1.4719	1.9031	0.1021

Bell E7T1 - 4A

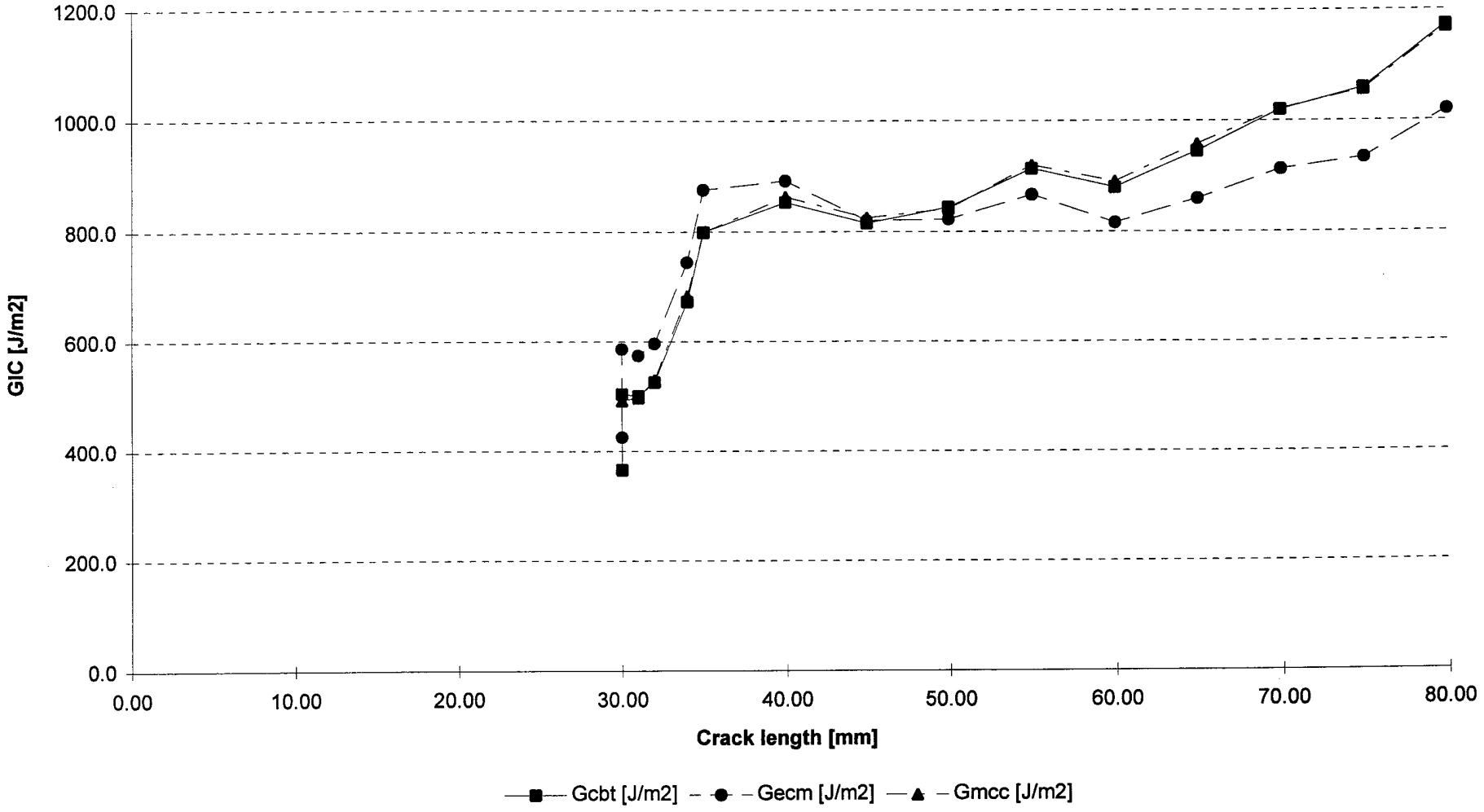

04/07/96 16:23

DCB Mode I from Insert

V1.02

MERL	Bell E7T1-7A	Test Date: 02/07/96

Input					
Specimen thickness	2h [mm]	9.89	End block thickness	H [mm]	MISSING
Specimen width	B [mm]	25.80	End block length	l3 [mm]	MISSING
Starter foil material	[-]	MISSING	Temperature	[°C]	MISSING
Starter foil thickness	[µm]	MISSING	Relative humidity	[%]	MISSING
Starter foil length	A [mm]	MISSING	Loading rate	[mm/min]	MISSING
Hinge type	[-]	MISSING	Drying temperature	[°C]	MISSING
Fiber Volume Fraction	Vf [Vol%]	MISSING	Drying duration	[h]	MISSING
			% Change Compliance	[%]	MISSING

l1	2.47
l2	0.00

check	(a+l2)-A >= 0	OK

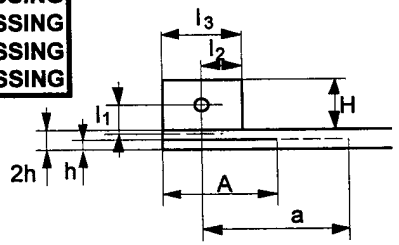

Text	Measure a [mm]	Load [N]	δ [mm]
NL	30.00	269.30	1.18
5%	30.00	297.00	1.36
Prop.	41.00	354.10	2.18
Prop.	45.00	336.50	2.38
Prop.	49.00	308.50	2.77
Prop.	50.00	302.60	2.87
Prop.	55.00	294.40	3.39
Prop.	60.00	284.80	3.81
Prop.	65.00	269.60	4.50
Prop.	70.00	238.30	4.91
Prop.	75.00	241.20	5.54
Prop.	76.00	245.90	5.89
Prop.	78.00	252.80	6.42
Prop.	79.00	252.40	6.59
Prop.	80.00	250.50	6.96

Results			
Gcbt [J/m2]	Gecm [J/m2]	Gmcc [J/m2]	E-Mod. [GPa]
331.4	394.4	321.7	100.6
421.1	501.2	402.8	96.2
672.1	700.9	697.6	123.0
657.9	662.6	691.1	127.5
664.4	649.3	681.1	118.5
666.3	646.7	679.6	116.7
718.3	675.6	732.1	116.5
735.4	673.4	757.2	120.1
776.9	694.9	786.4	114.1
710.1	622.4	707.0	108.6
770.7	663.4	778.7	113.5
827.1	709.5	832.3	112.1
908.9	774.7	914.6	112.0
922.6	783.9	928.7	112.1
957.8	811.3	953.4	108.4
		average	113.3
		deviation	8.0

MERL	Bell E7T1-7A	Test Date: 02/07/96

Regression

Method	Gcbt		Gecm		Gmcc	
Value	slope	Y-axis	slope	Y-axis	slope	Y-axis
	0.00282947	0.07267419	1.92351568	-5.25554278	35.445013	-2.52757049
Correction	Δ=	**-25.6847**	n=	**1.9235**	A1=	**35.4450**
Correl. coeff. r^2	0.991874		0.976330		0.991874	
Points for fit						
	x	y	x	y	x	y
Point 1	30.00	0.16	1.48	-2.41	0.16	3.28
Point 2	80.00	0.30	1.90	-1.59	0.30	8.23

Text	F [-]	N [-]	F/N [-]	C/N [mm/N]	(C/N)^1/3	log(C/N)	log(a)	δ/a < 0.4
NL	0.9947	0.9960	0.9987	0.0044	0.1639	-2.3566	1.4771	0.0393
0.05	0.9938	0.9953	0.9985	0.0046	0.1663	-2.3372	1.4771	0.0453
Prop.	0.9943	0.9957	0.9987	0.0062	0.1835	-2.2088	1.6128	0.0532
Prop.	0.9948	0.9960	0.9988	0.0071	0.1922	-2.1487	1.6532	0.0529
Prop.	0.9948	0.9960	0.9988	0.0090	0.2081	-2.0450	1.6902	0.0565
Prop.	0.9948	0.9960	0.9988	0.0095	0.2120	-2.0212	1.6990	0.0574
Prop.	0.9947	0.9959	0.9988	0.0116	0.2261	-1.9370	1.7404	0.0616
Prop.	0.9949	0.9960	0.9988	0.0134	0.2377	-1.8719	1.7782	0.0635
Prop.	0.9946	0.9958	0.9988	0.0168	0.2559	-1.7757	1.8129	0.0692
Prop.	0.9948	0.9959	0.9989	0.0207	0.2745	-1.6843	1.8451	0.0701
Prop.	0.9947	0.9959	0.9988	0.0231	0.2847	-1.6371	1.8751	0.0739
Prop.	0.9944	0.9956	0.9988	0.0241	0.2887	-1.6187	1.8808	0.0775
Prop.	0.9941	0.9953	0.9987	0.0255	0.2944	-1.5932	1.8921	0.0823
Prop.	0.9940	0.9953	0.9987	0.0262	0.2971	-1.5811	1.8976	0.0834
Prop.	0.9937	0.9950	0.9987	0.0279	0.3034	-1.5540	1.9031	0.0870

E7T1-7AN.XLS

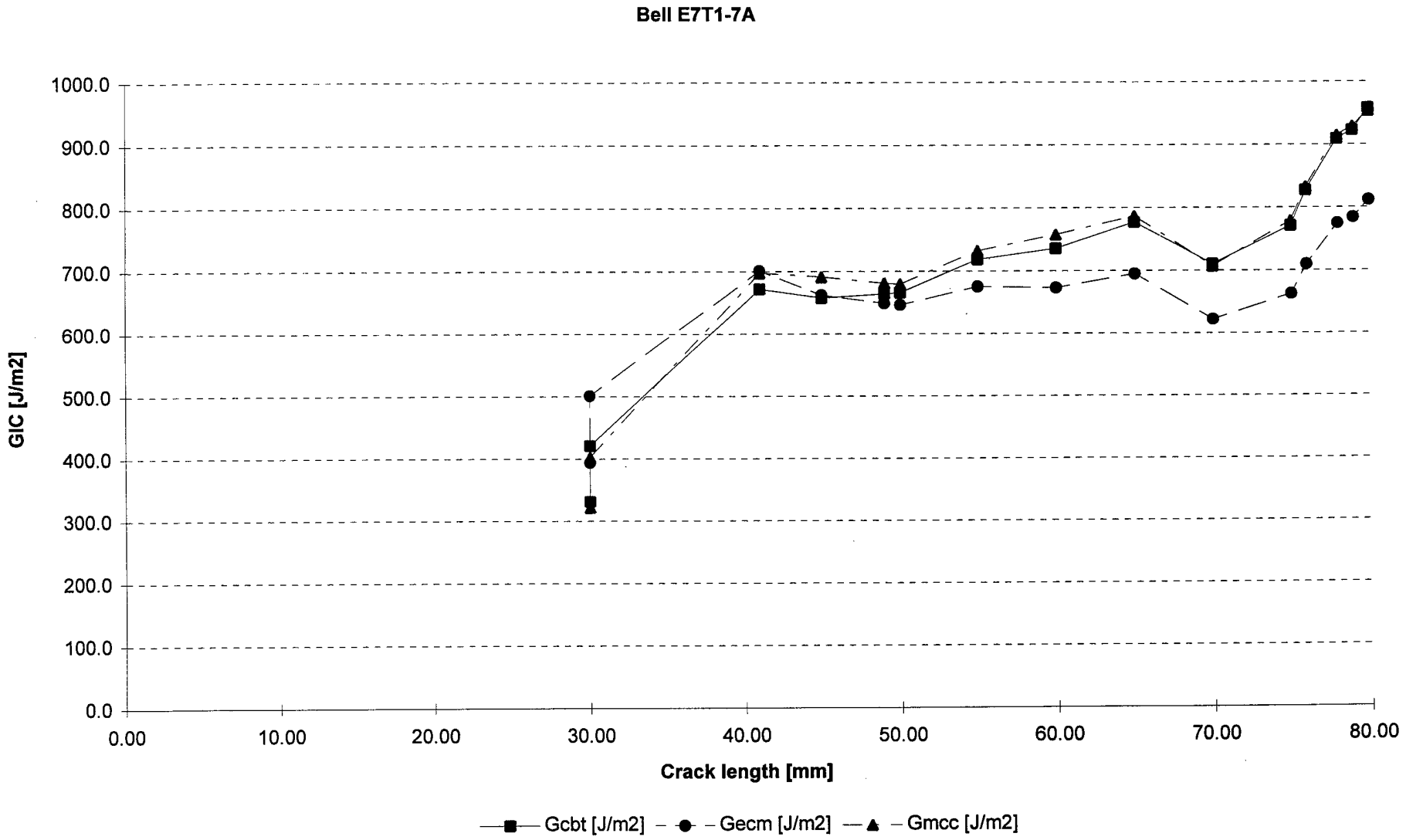

04/07/96 16:25

DCB Mode I from Insert

V1.02

MERL	Bell E7T1-8B	Test Date: 02/07/96

Input					
Specimen thickness	2h [mm]	9.77	End block thickness	H [mm]	MISSING
Specimen width	B [mm]	25.84	End block length	l3 [mm]	MISSING
Starter foil material	[-]	MISSING	Temperature	[°C]	MISSING
Starter foil thickness	[µm]	MISSING	Relative humidity	[%]	MISSING
Starter foil length	A [mm]	MISSING	Loading rate	[mm/min]	MISSING
Hinge type	[-]	MISSING	Drying temperature	[°C]	MISSING
Fiber Volume Fraction	Vf [Vol%]	MISSING	Drying duration	[h]	MISSING
			% Change Compliance	[%]	MISSING

l1	2.44
l2	0.00

check	(a+l2)-A >= 0	OK

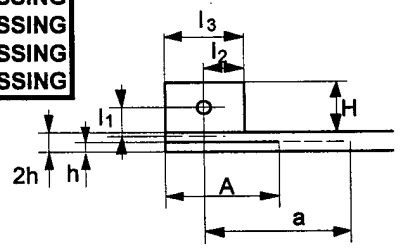

Text	Measure a [mm]	Load [N]	δ [mm]
NL	30.00	260.00	1.00
5%	30.00	309.40	1.23
Prop.	31.00	338.20	1.46
Prop.	32.00	347.60	1.55
Prop.	33.00	348.00	1.61
Prop.	34.00	352.30	1.71
Prop.	35.00	353.10	1.81
Prop.	40.00	330.20	2.08
Prop.	45.00	313.60	2.57
Prop.	50.00	298.50	3.13
Prop.	55.00	277.60	3.66
Prop.	60.00	252.40	4.26
Prop.	65.00	246.80	4.90
Prop.	70.00	232.40	5.74
Prop.	75.00	215.80	6.48
Prop.	76.00	215.20	6.62
Prop.	77.00	213.10	6.80
Prop.	78.00	210.40	6.96
Prop.	79.00	211.20	7.15
Prop.	80.00	209.50	7.37

Results			
Gcbt [J/m2]	Gecm [J/m2]	Gmcc [J/m2]	E-Mod. [GPa]
331.6	376.6	329.5	64.7
485.2	551.1	476.9	62.5
615.9	691.8	601.9	61.4
657.9	731.3	649.7	63.4
670.0	737.4	667.4	65.1
705.9	769.6	706.2	65.9
734.0	793.1	735.7	66.3
717.8	745.9	738.2	71.7
772.7	778.0	793.6	71.3
827.3	811.7	847.4	70.8
835.9	802.5	853.8	70.2
826.0	778.5	832.1	67.3
871.2	808.2	886.6	69.4
904.8	827.8	909.3	66.8
896.0	809.9	893.1	65.2
902.9	814.3	902.5	65.7
908.4	817.5	906.9	65.5
908.2	815.5	905.5	65.2
926.6	830.3	926.6	65.8
937.5	838.3	935.3	65.3
		average	66.5
		deviation	2.8

MERL	Bell E7T1-8B	Test Date: 02/07/96

Regression

Method	Gcbt		Gecm		Gmcc	
Value	slope	Y-axis	slope	Y-axis	slope	Y-axis
	0.00341801	0.05287603	2.24800156	-5.75245558	29.8912684	-1.57056149
Correction	Δ=	**-15.4698**	n=	**2.2480**	A1=	**29.8913**
Correl. coeff. r^2	0.998188		0.994760		0.998188	
Points for fit						
	x	y	x	y	x	y
Point 1	30.00	0.16	1.48	-2.43	0.16	3.12
Point 2	80.00	0.33	1.90	-1.47	0.33	8.24

Text	F [-]	N [-]	F/N [-]	C/N [mm/N]	(C/N)^1/3	log(C/N)	log(a)	δ/a < 0.4
NL	0.9956	0.9967	0.9989	0.0039	0.1569	-2.4135	1.4771	0.0333
0.05	0.9945	0.9958	0.9987	0.0040	0.1586	-2.3988	1.4771	0.0410
Prop.	0.9938	0.9953	0.9985	0.0043	0.1631	-2.3628	1.4914	0.0471
Prop.	0.9938	0.9952	0.9985	0.0045	0.1649	-2.3487	1.5051	0.0484
Prop.	0.9939	0.9953	0.9985	0.0046	0.1669	-2.3327	1.5185	0.0488
Prop.	0.9938	0.9953	0.9985	0.0049	0.1696	-2.3119	1.5315	0.0503
Prop.	0.9938	0.9953	0.9985	0.0052	0.1727	-2.2882	1.5441	0.0517
Prop.	0.9944	0.9957	0.9987	0.0063	0.1849	-2.1989	1.6021	0.0520
Prop.	0.9944	0.9957	0.9987	0.0082	0.2019	-2.0846	1.6532	0.0571
Prop.	0.9942	0.9956	0.9987	0.0105	0.2192	-1.9775	1.6990	0.0626
Prop.	0.9942	0.9955	0.9987	0.0132	0.2366	-1.8780	1.7404	0.0665
Prop.	0.9942	0.9955	0.9987	0.0170	0.2569	-1.7707	1.7782	0.0710
Prop.	0.9940	0.9954	0.9987	0.0199	0.2712	-1.7001	1.8129	0.0754
Prop.	0.9937	0.9951	0.9986	0.0248	0.2917	-1.6052	1.8451	0.0820
Prop.	0.9935	0.9949	0.9986	0.0302	0.3113	-1.5203	1.8751	0.0864
Prop.	0.9935	0.9949	0.9986	0.0309	0.3139	-1.5098	1.8808	0.0871
Prop.	0.9935	0.9948	0.9986	0.0321	0.3177	-1.4938	1.8865	0.0883
Prop.	0.9934	0.9948	0.9986	0.0333	0.3216	-1.4782	1.8921	0.0892
Prop.	0.9933	0.9947	0.9986	0.0340	0.3241	-1.4681	1.8976	0.0905
Prop.	0.9932	0.9947	0.9986	0.0354	0.3282	-1.4514	1.9031	0.0921

Bell E7T1-8B

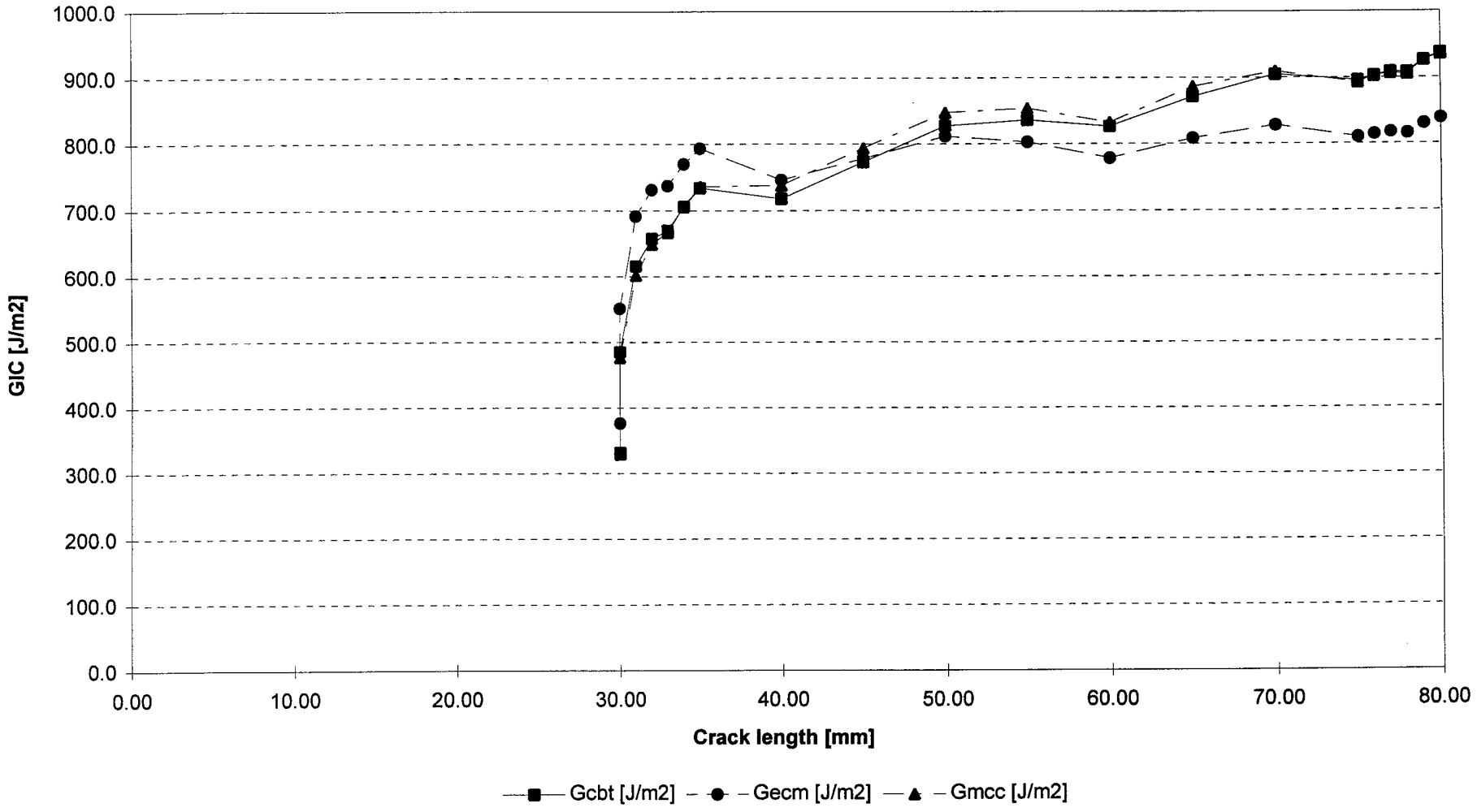

04/07/96 16:27

DCB Mode I from Insert

V1.02

MERL	Bell E7T1-9A	Test Date: 02/07/96

Input					
Specimen thickness	2h [mm]	9.65	End block thickness	H [mm]	MISSING
Specimen width	B [mm]	25.85	End block length	l3 [mm]	MISSING
Starter foil material	[-]	MISSING	Temperature	[°C]	MISSING
Starter foil thickness	[µm]	MISSING	Relative humidity	[%]	MISSING
Starter foil length	A [mm]	MISSING	Loading rate	[mm/min]	MISSING
Hinge type	[-]	MISSING	Drying temperature	[°C]	MISSING
Fiber Volume Fraction	Vf [Vol%]	MISSING	Drying duration	[h]	MISSING
			% Change Compliance	[%]	MISSING

l1	2.41
l2	0.00

check	(a+l2)-A >= 0	OK

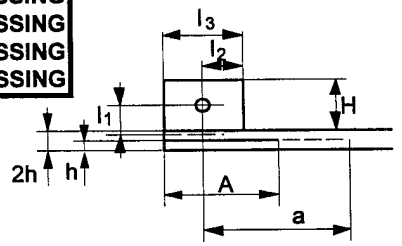

Text	Measure a [mm]	Load [N]	δ [mm]
NL	31.00	237.40	1.12
5%	31.00	300.00	1.43
Prop.	32.00	318.00	1.60
Prop.	33.00	330.20	1.71
Prop.	34.00	342.80	1.85
Prop.	35.00	338.90	1.94
Prop.	36.00	333.80	2.01
Prop.	37.00	323.90	2.15
Prop.	39.00	318.20	2.27
Prop.	40.00	320.30	2.38
Prop.	45.00	292.20	2.70
Prop.	50.00	287.80	3.22
Prop.	55.00	273.90	3.90
Prop.	60.00	257.50	4.51
Prop.	65.00	243.20	5.33
Prop.	70.00	237.10	6.18
Prop.	75.00	224.50	7.05
Prop.	80.00	213.40	7.98

Results			
Gcbt [J/m2]	Gecm [J/m2]	Gmcc [J/m2]	E-Mod. [GPa]
312.4	355.4	309.6	69.9
503.9	573.3	497.7	69.1
585.7	658.6	579.7	69.5
637.3	708.7	637.2	71.6
702.1	772.6	705.8	72.8
714.2	778.1	717.5	72.6
715.5	772.0	720.0	73.0
729.2	779.6	723.4	70.0
730.0	767.2	732.6	72.4
757.2	789.4	762.7	73.2
721.9	726.3	734.1	75.4
785.9	767.9	809.1	78.2
844.1	804.6	860.6	75.9
859.1	801.8	873.2	75.2
901.3	826.1	904.4	72.4
961.1	867.1	964.9	72.5
982.5	874.1	979.4	70.9
1003.4	881.7	994.2	69.6
		average	72.5
		deviation	2.5

MERL	Bell E7T1-9A	Test Date: 02/07/96

Regression

Method	Gcbt		Gecm		Gmcc	
Value	slope	Y-axis	slope	Y-axis	slope	Y-axis
	0.00336226	0.06163591	2.14476435	-5.54737579	30.7524299	-1.88464839
Correction	Δ=	**-18.3317**	n=	**2.1448**	A1=	**30.7524**
Correl. coeff. r^2	0.997787		0.994143		0.997787	
Points for fit						
	x	y	x	y	x	y
Point 1	31.00	0.17	1.49	-2.35	0.17	3.28
Point 2	80.00	0.33	1.90	-1.47	0.34	8.42

Text	F [-]	N [-]	F/N [-]	C/N [mm/N]	(C/N)^1/3	log(C/N)	log(a)	δ/a < 0.4
NL	0.9954	0.9965	0.9989	0.0047	0.1679	-2.3247	1.4914	0.0361
0.05	0.9940	0.9954	0.9986	0.0048	0.1686	-2.3198	1.4914	0.0461
Prop.	0.9936	0.9951	0.9985	0.0051	0.1716	-2.2962	1.5051	0.0500
Prop.	0.9935	0.9950	0.9985	0.0052	0.1733	-2.2836	1.5185	0.0518
Prop.	0.9933	0.9949	0.9984	0.0054	0.1757	-2.2656	1.5315	0.0544
Prop.	0.9933	0.9949	0.9984	0.0058	0.1792	-2.2401	1.5441	0.0554
Prop.	0.9935	0.9950	0.9985	0.0061	0.1822	-2.2181	1.5563	0.0558
Prop.	0.9933	0.9949	0.9984	0.0067	0.1883	-2.1757	1.5682	0.0581
Prop.	0.9936	0.9951	0.9985	0.0072	0.1928	-2.1445	1.5911	0.0582
Prop.	0.9936	0.9951	0.9985	0.0075	0.1955	-2.1268	1.6021	0.0595
Prop.	0.9941	0.9955	0.9986	0.0093	0.2102	-2.0323	1.6532	0.0600
Prop.	0.9941	0.9954	0.9987	0.0112	0.2240	-1.9492	1.6990	0.0644
Prop.	0.9938	0.9952	0.9986	0.0143	0.2428	-1.8444	1.7404	0.0709
Prop.	0.9938	0.9951	0.9986	0.0176	0.2601	-1.7545	1.7782	0.0752
Prop.	0.9934	0.9948	0.9986	0.0220	0.2803	-1.6570	1.8129	0.0820
Prop.	0.9931	0.9946	0.9985	0.0262	0.2970	-1.5816	1.8451	0.0883
Prop.	0.9928	0.9943	0.9985	0.0316	0.3161	-1.5006	1.8751	0.0940
Prop.	0.9925	0.9941	0.9984	0.0376	0.3351	-1.4246	1.9031	0.0998

E7T1-9AN.XLS

Bell E7T1-9A

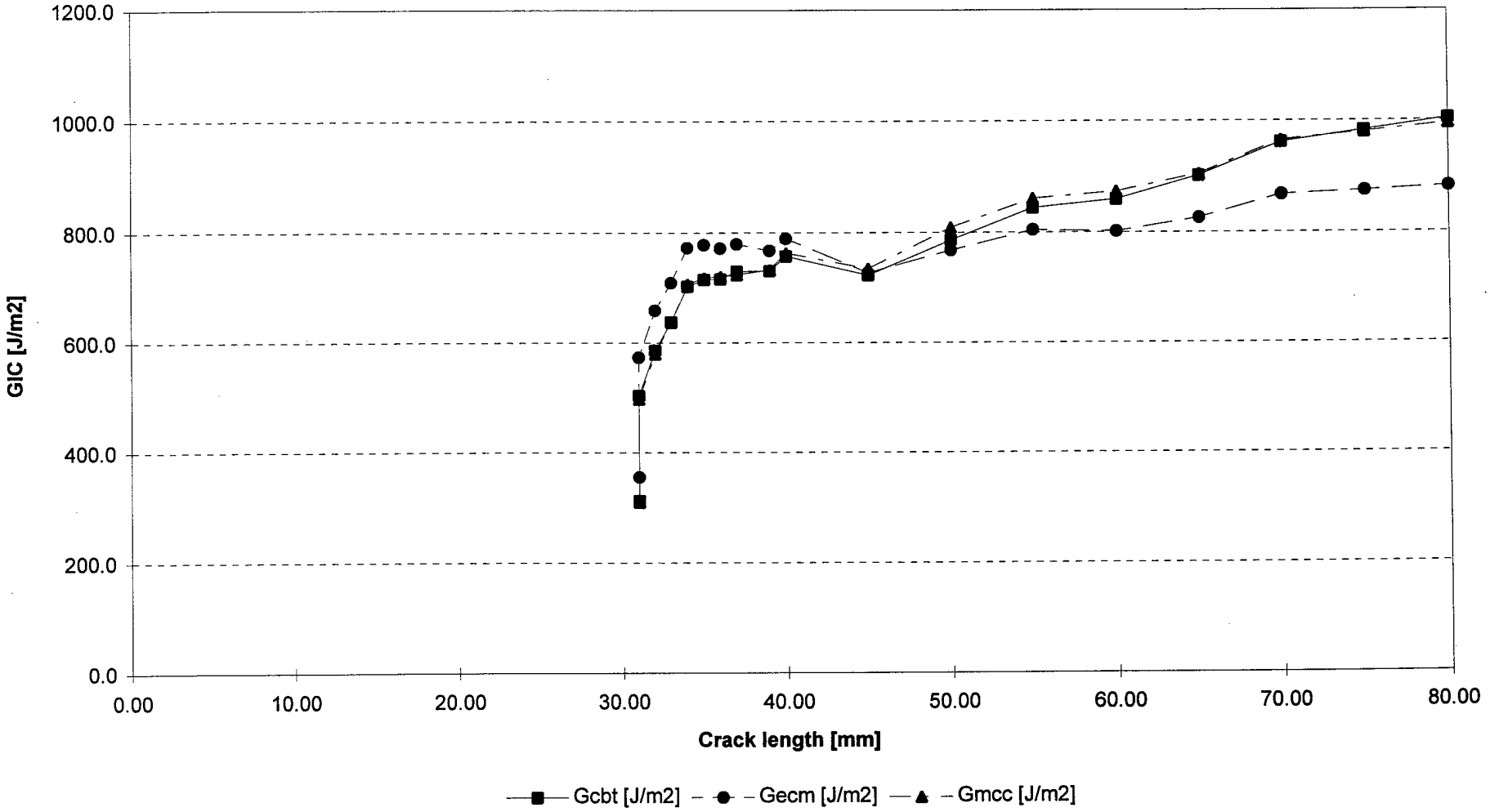

04/07/96 16:28

DCB Mode I from Insert

V1.02

MERL	S2/F584 13 ERO	Test Date: 01/01/04

Input					
Specimen thickness	2h [mm]	6.72	End block thickness	H [mm]	MISSING
Specimen width	B [mm]	20.05	End block length	l3 [mm]	MISSING
Starter foil material	[-]	Teflon	Temperature	[°C]	23.00
Starter foil thickness	[µm]	13.00	Relative humidity	[%]	MISSING
Starter foil length	A [mm]	MISSING	Loading rate	[mm/min]	0.50
Hinge type	[-]	MS20001-6	Drying temperature	[°C]	MISSING
Fiber Volume Fraction	Vf [Vol%]	MISSING	Drying duration	[h]	MISSING
			% Change Compliance	[%]	MISSING

l1	1.68
l2	0.00

check	(a+l2)-A >= 0	OK

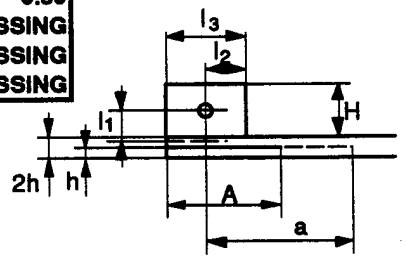

Text	Measure a [mm]	Load [N]	δ [mm]
NL	52.00	56.00	2.60
Prop.	52.00	45.00	2.67
Prop.	53.00	48.00	2.94
Prop.	54.00	52.00	3.27
Prop.	55.00	55.00	3.65
Prop.	56.00	57.00	3.87
Prop.	60.00	61.00	4.52
Prop.	65.00	68.00	5.71
Prop.	70.00	74.00	7.41
Prop.	75.00	77.00	8.93
Prop.	80.00	79.00	10.51
Prop.	81.00	79.00	11.18
Prop.	82.00	79.00	11.51
Prop.	83.00	80.00	11.82
Prop.	84.00	80.00	12.21
Prop.	85.00	80.00	12.43

Results Gcbt [J/m2]	Gecm [J/m2]	Gmcc [J/m2]	E-Mod. [GPa]
133.6	144.9	144.7	122.1
110.3	119.6	110.0	95.5
128.0	137.8	127.9	96.0
152.3	163.0	152.7	96.9
177.7	188.9	177.1	95.1
193.0	203.9	193.1	96.3
230.4	237.8	234.4	101.2
307.2	309.1	316.6	105.0
411.9	405.2	421.5	102.7
491.7	474.2	503.2	102.6
566.5	536.7	580.3	102.9
597.1	563.8	604.7	99.3
609.2	573.3	616.5	99.1
627.9	589.0	638.1	100.4
642.9	601.2	652.1	99.7
648.7	604.8	659.9	100.6
		average	101.0
		deviation	6.4

MERL	S2/F584 13 ERO	Test Date: 01/01/04

Regression

Method	Gcbt		Gecm		Gmcc	
Value	slope	Y-axis	slope	Y-axis	slope	Y-axis
	0.00470885	0.13864757	2.07733005	-4.81690886	31.1443264	-4.17164758
Correction	Δ=	**-29.4440**	n=	**2.0773**	A1=	**31.1443**
Correl. coeff. r^2	0.985515		0.979481		0.985515	
Points for fit						
	x	y	x	y	x	y
Point 1	52.00	0.38	1.72	-1.25	0.36	7.03
Point 2	85.00	0.54	1.93	-0.81	0.54	12.62

Text	F [-]	N [-]	F/N [-]	C/N [mm/N]	(C/N)^1/3	log(C/N)	log(a)	δ/a < 0.4
NL	0.9968	0.9975	0.9993	0.0465	0.3597	-1.3321	1.7160	0.0500
Prop.	0.9967	0.9975	0.9993	0.0595	0.3904	-1.2256	1.7160	0.0513
Prop.	0.9964	0.9972	0.9992	0.0614	0.3946	-1.2117	1.7243	0.0555
Prop.	0.9961	0.9969	0.9991	0.0631	0.3981	-1.2001	1.7324	0.0606
Prop.	0.9956	0.9966	0.9990	0.0666	0.4053	-1.1766	1.7404	0.0664
Prop.	0.9955	0.9964	0.9990	0.0681	0.4084	-1.1666	1.7482	0.0691
Prop.	0.9951	0.9962	0.9990	0.0744	0.4206	-1.1285	1.7782	0.0753
Prop.	0.9943	0.9955	0.9988	0.0844	0.4386	-1.0739	1.8129	0.0878
Prop.	0.9928	0.9943	0.9986	0.1007	0.4653	-0.9969	1.8451	0.1059
Prop.	0.9917	0.9934	0.9984	0.1167	0.4887	-0.9327	1.8751	0.1191
Prop.	0.9907	0.9925	0.9982	0.1340	0.5118	-0.8727	1.9031	0.1314
Prop.	0.9900	0.9919	0.9981	0.1427	0.5225	-0.8456	1.9085	0.1380
Prop.	0.9898	0.9917	0.9981	0.1469	0.5277	-0.8329	1.9138	0.1404
Prop.	0.9896	0.9915	0.9980	0.1490	0.5302	-0.8268	1.9191	0.1424
Prop.	0.9893	0.9913	0.9980	0.1540	0.5360	-0.8126	1.9243	0.1454
Prop.	0.9892	0.9912	0.9980	0.1567	0.5392	-0.8048	1.9294	0.1462

S2/F584 13 ERO

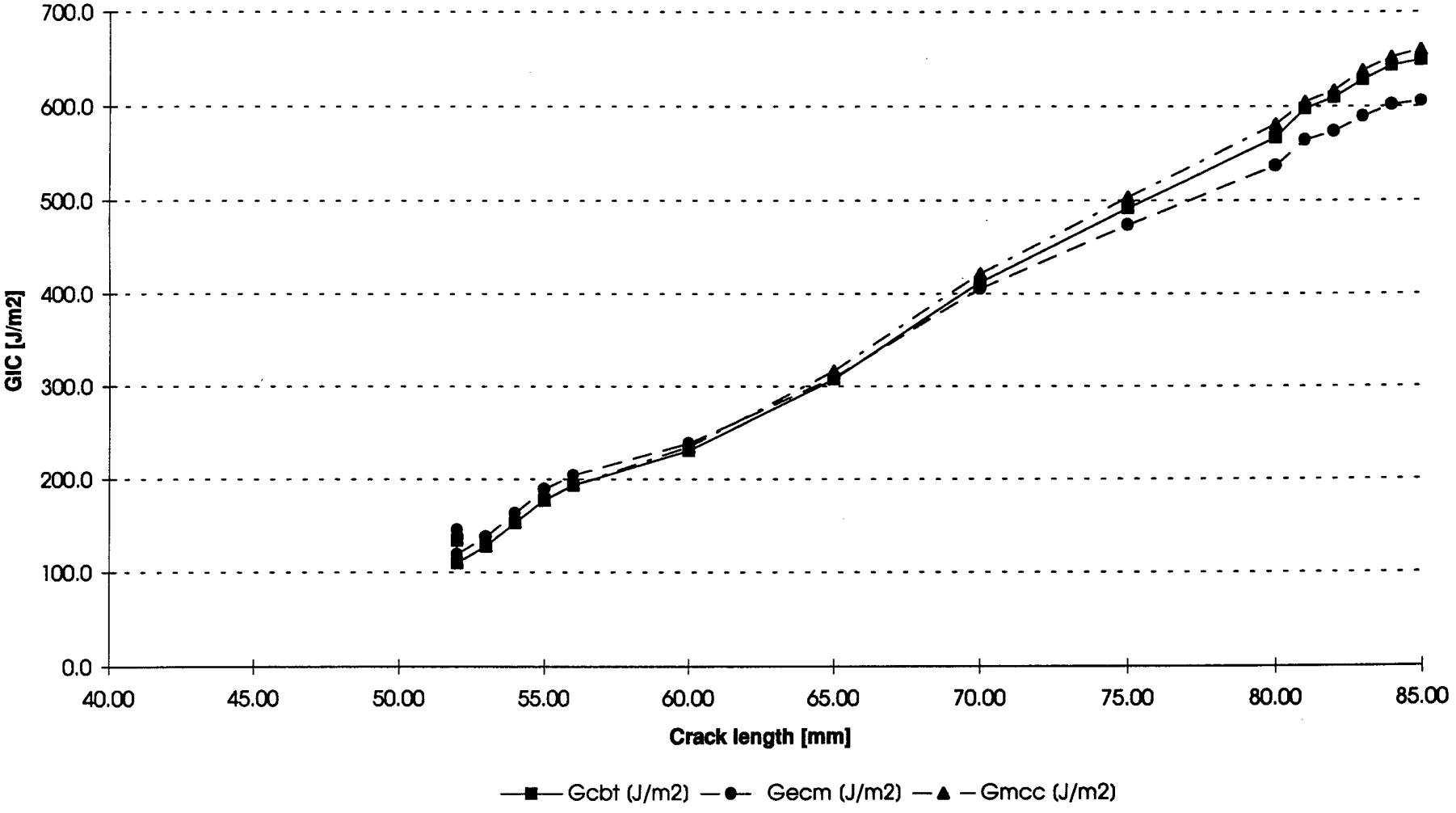

17/09/97 12:40

DCB Mode I from Insert

V1.02

MERL	S2/F584 14 ERO	Test Date: 01/01/04

Input			End block thickness	H [mm]	MISSING
Specimen thickness	2h [mm]	6.72	End block length	l3 [mm]	MISSING
Specimen width	B [mm]	20.05	Temperature	[°C]	23.00
Starter foil material	[-]	Teflon	Relative humidity	[%]	MISSING
Starter foil thickness	[µm]	13.00	Loading rate	[mm/min]	0.50
Starter foil length	A [mm]	MISSING	Drying temperature	[°C]	MISSING
Hinge type	[-]	MS20001-6	Drying duration	[h]	MISSING
Fiber Volume Fraction	Vf [Vol%]	MISSING	% Change Compliance	[%]	MISSING

l1	1.68
l2	0.00

check	(a+l2)-A >= 0	OK

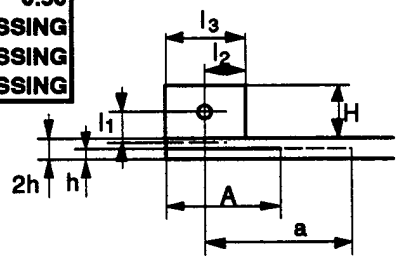

Text	Measure a [mm]	Load [N]	δ [mm]
NL	51.50	52.00	2.20
Prop.	53.00	40.00	2.30
Prop.	54.00	42.00	2.41
Prop.	55.00	47.00	2.87
Prop.	56.00	50.00	3.13
Prop.	57.00	51.00	3.29
Prop.	60.00	57.00	4.19
Prop.	65.00	63.00	5.22
Prop.	70.00	69.00	6.76
Prop.	75.00	72.00	8.31
Prop.	80.00	75.00	9.90
Prop.	81.00	75.00	10.53
Prop.	82.00	76.00	10.80
Prop.	83.00	75.00	11.03
Prop.	84.00	75.00	11.39
Prop.	85.00	76.00	11.79

Results			
Gcbt [J/m2]	Gecm [J/m2]	Gmcc [J/m2]	E-Mod. [GPa]
115.7	124.8	124.5	100.3
91.2	97.6	90.4	78.4
99.0	105.3	99.5	81.7
130.2	137.8	129.8	79.8
149.2	157.0	149.4	80.9
157.9	165.4	158.6	81.5
216.5	223.6	216.1	79.9
281.1	284.2	285.8	84.5
377.0	374.2	383.3	84.4
458.7	447.9	465.5	83.8
541.4	521.0	552.3	85.1
570.2	547.3	575.4	82.3
586.9	561.9	595.6	83.7
585.9	559.5	593.4	83.2
599.4	570.8	606.3	82.9
622.8	591.7	631.4	83.4
		average	83.5
		deviation	4.9

MERL	S2/F584 14 ERO	Test Date: 01/01/04

Regression

Method	Gcbt		Gecm		Gmcc	
Value	slope	Y-axis	slope	Y-axis	slope	Y-axis
	0.00501688	0.11255306	2.25486553	-5.15771424	29.3490403	-3.19630012
Correction	Δ=	**-22.4349**	n=	**2.2549**	A1=	**29.3490**
Correl. coeff. r^2	0.989457		0.985355		0.989457	
Points for fit						
	x	y	x	y	x	y
Point 1	51.50	0.37	1.71	-1.30	0.35	7.04
Point 2	85.00	0.54	1.93	-0.81	0.54	12.62

Text	F [-]	N [-]	F/N [-]	C/N [mm/N]	(C/N)^1/3	log(C/N)	log(a)	/a < 0.4
NL	0.9974	0.9980	0.9994	0.0424	0.3487	-1.3727	1.7118	0.0427
Prop.	0.9974	0.9980	0.9994	0.0576	0.3862	-1.2394	1.7243	0.0434
Prop.	0.9973	0.9979	0.9994	0.0575	0.3860	-1.2403	1.7324	0.0446
Prop.	0.9968	0.9975	0.9993	0.0612	0.3941	-1.2131	1.7404	0.0522
Prop.	0.9965	0.9973	0.9992	0.0628	0.3974	-1.2023	1.7482	0.0559
Prop.	0.9964	0.9972	0.9992	0.0647	0.4014	-1.1892	1.7559	0.0577
Prop.	0.9956	0.9965	0.9991	0.0738	0.4194	-1.1322	1.7782	0.0698
Prop.	0.9950	0.9960	0.9989	0.0832	0.4365	-1.0799	1.8129	0.0803
Prop.	0.9937	0.9950	0.9987	0.0985	0.4618	-1.0067	1.8451	0.0966
Prop.	0.9926	0.9941	0.9985	0.1161	0.4879	-0.9351	1.8751	0.1108
Prop.	0.9915	0.9931	0.9984	0.1329	0.5103	-0.8764	1.9031	0.1238
Prop.	0.9909	0.9926	0.9983	0.1414	0.5210	-0.8494	1.9085	0.1300
Prop.	0.9907	0.9925	0.9982	0.1432	0.5231	-0.8441	1.9138	0.1317
Prop.	0.9907	0.9924						

S2/F584 14 ERO

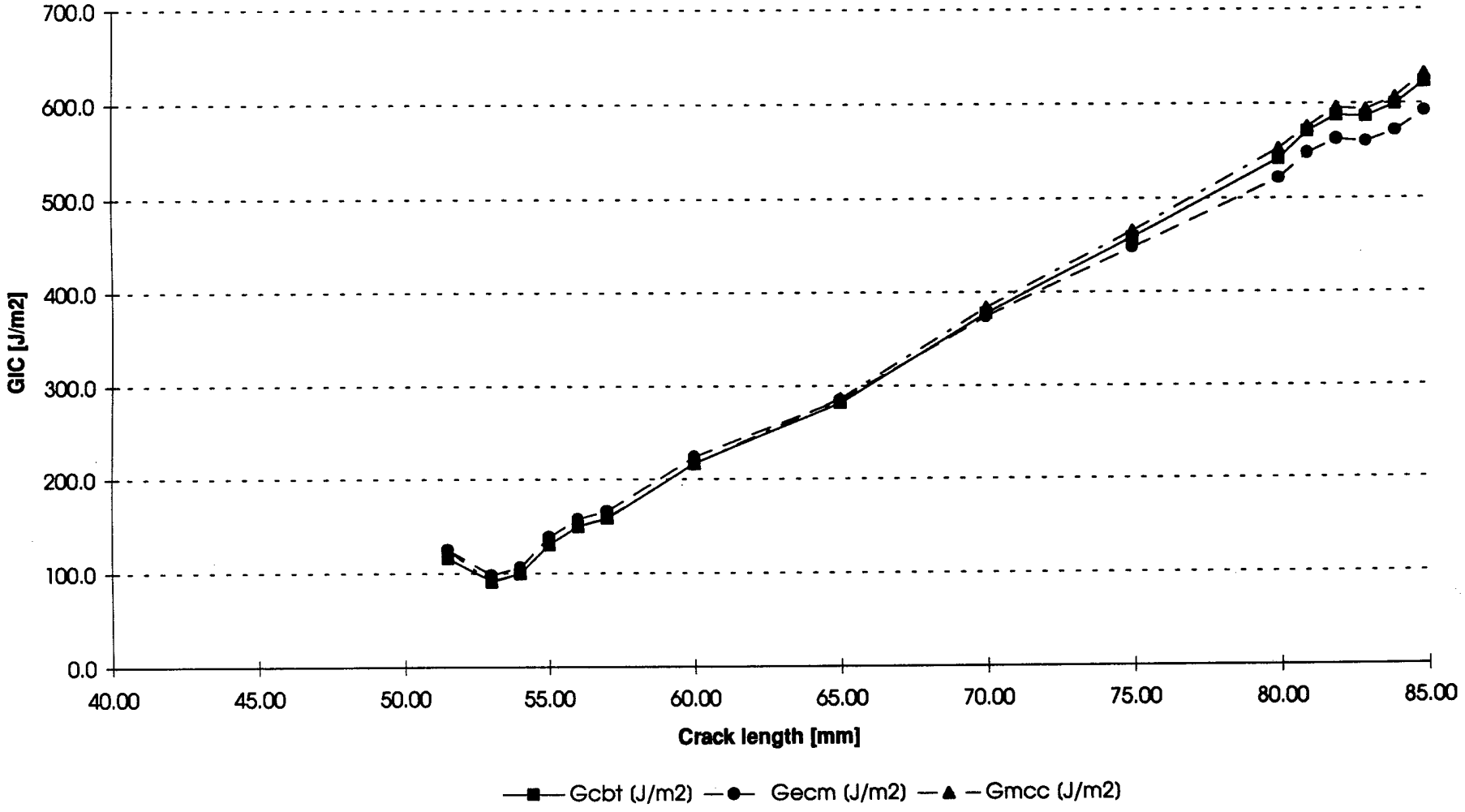

17/09/97 12:37

DCB Mode I from Insert

V1.02

MERL	S2/F584 17 ERO	Test Date: 01/01/04

Input					
Specimen thickness	2h [mm]	6.80	End block thickness	H [mm]	MISSING
Specimen width	B [mm]	20.06	End block length	l3 [mm]	MISSING
Starter foil material	[-]	Teflon	Temperature	[°C]	23.00
Starter foil thickness	[µm]	13.00	Relative humidity	[%]	MISSING
Starter foil length	A [mm]	MISSING	Loading rate	[mm/min]	0.50
Hinge type	[-]	MS20001-6	Drying temperature	[°C]	MISSING
Fiber Volume Fraction	Vf [Vol%]	MISSING	Drying duration	[h]	MISSING
			% Change Compliance	[%]	MISSING

l1	1.70
l2	0.00

check	(a+l2)-A >= 0	OK

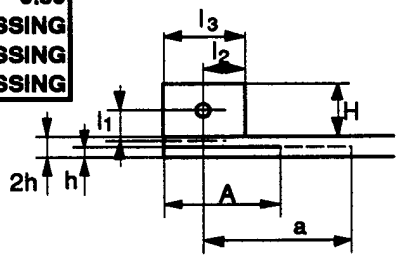

Text	Measure a [mm]	Load [N]	δ [mm]
NL	51.50	60.00	2.50
Prop.	58.00	62.00	4.31
Prop.	59.00	64.00	4.59
Prop.	60.00	65.00	4.85
Prop.	61.00	67.00	5.15
Prop.	62.00	68.00	5.23
Prop.	65.00	70.00	5.83
Prop.	70.00	74.00	7.08
Prop.	75.00	76.00	8.55
Prop.	80.00	78.00	10.13
Prop.	85.00	76.00	11.45
Prop.	86.00	75.00	11.99
Prop.	87.00	74.00	12.48
Prop.	88.00	74.00	13.06
Prop.	89.00	73.00	13.25
Prop.	90.00	74.00	13.43

Results			
Gcbt [J/m2]	Gecm [J/m2]	Gmcc [J/m2]	E-Mod. [GPa]
156.8	170.7	169.3	88.7
256.0	270.0	254.1	68.9
277.9	291.7	276.5	69.4
294.5	307.9	292.8	69.2
318.3	331.4	317.3	69.7
324.1	336.1	327.0	72.3
358.7	367.8	365.4	74.4
434.9	438.4	447.8	76.8
510.9	507.4	526.1	76.8
590.1	578.4	609.7	77.5
618.8	599.5	639.0	77.3
633.4	612.2	647.4	74.9
644.4	621.5	653.1	73.0
668.0	642.9	673.1	71.7
662.4	636.2	667.4	71.7
674.4	646.4	685.7	73.7
		average	74.1
		deviation	4.9

MERL	S2/F584 17 ERO	Test Date: 01/01/04

Regression

Method	Gcbt		Gecm		Gmcc	
Value	slope	Y-axis	slope	Y-axis	slope	Y-axis
	0.00515863	0.10297058	2.35343232	-5.33929202	28.0907878	-2.73586246
Correction	Δ=	**-19.9608**	n=	**2.3534**	A1=	**28.0908**
Correl. coeff. r^2	0.985388		0.981751		0.985388	
Points for fit						
	x	y	x	y	x	y
Point 1	51.50	0.37	1.71	-1.31	0.35	7.01
Point 2	90.00	0.57	1.95	-0.74	0.57	13.22

Text	F [-]	N [-]	F/N [-]	C/N [mm/N]	(C/N)^1/3	log(C/N)	log(a)	δ/a < 0.4
NL	0.9969	0.9976	0.9993	0.0418	0.3470	-1.3792	1.7118	0.0485
Prop.	0.9951	0.9961	0.9989	0.0698	0.4117	-1.1562	1.7634	0.0743
Prop.	0.9948	0.9959	0.9989	0.0720	0.4160	-1.1426	1.7709	0.0778
Prop.	0.9946	0.9957	0.9989	0.0749	0.4216	-1.1253	1.7782	0.0808
Prop.	0.9943	0.9955	0.9988	0.0772	0.4258	-1.1123	1.7853	0.0844
Prop.	0.9944	0.9956	0.9988	0.0773	0.4259	-1.1121	1.7924	0.0844
Prop.	0.9941	0.9953	0.9988	0.0837	0.4374	-1.0774	1.8129	0.0897
Prop.	0.9932	0.9946	0.9986	0.0962	0.4582	-1.0168	1.8451	0.1011
Prop.	0.9922	0.9938	0.9985	0.1132	0.4838	-0.9461	1.8751	0.1140
Prop.	0.9912	0.9928	0.9983	0.1308	0.5076	-0.8834	1.9031	0.1266
Prop.	0.9905	0.9923	0.9982	0.1518	0.5335	-0.8187	1.9294	0.1347
Prop.	0.9900	0.9919	0.9981	0.1612	0.5442	-0.7927	1.9345	0.1394
Prop.	0.9896	0.9916	0.9981	0.1701	0.5541	-0.7693	1.9395	0.1434
Prop.	0.9891	0.9911	0.9980	0.1781	0.5626	-0.7494	1.9445	0.1484
Prop.	0.9891	0.9911	0.9980	0.1831	0.5679	-0.7372	1.9494	0.1489
Prop.	0.9891	0.9911	0.9980	0.1831	0.5679	-0.7373	1.9542	0.1492

S2/F584 17 ERO

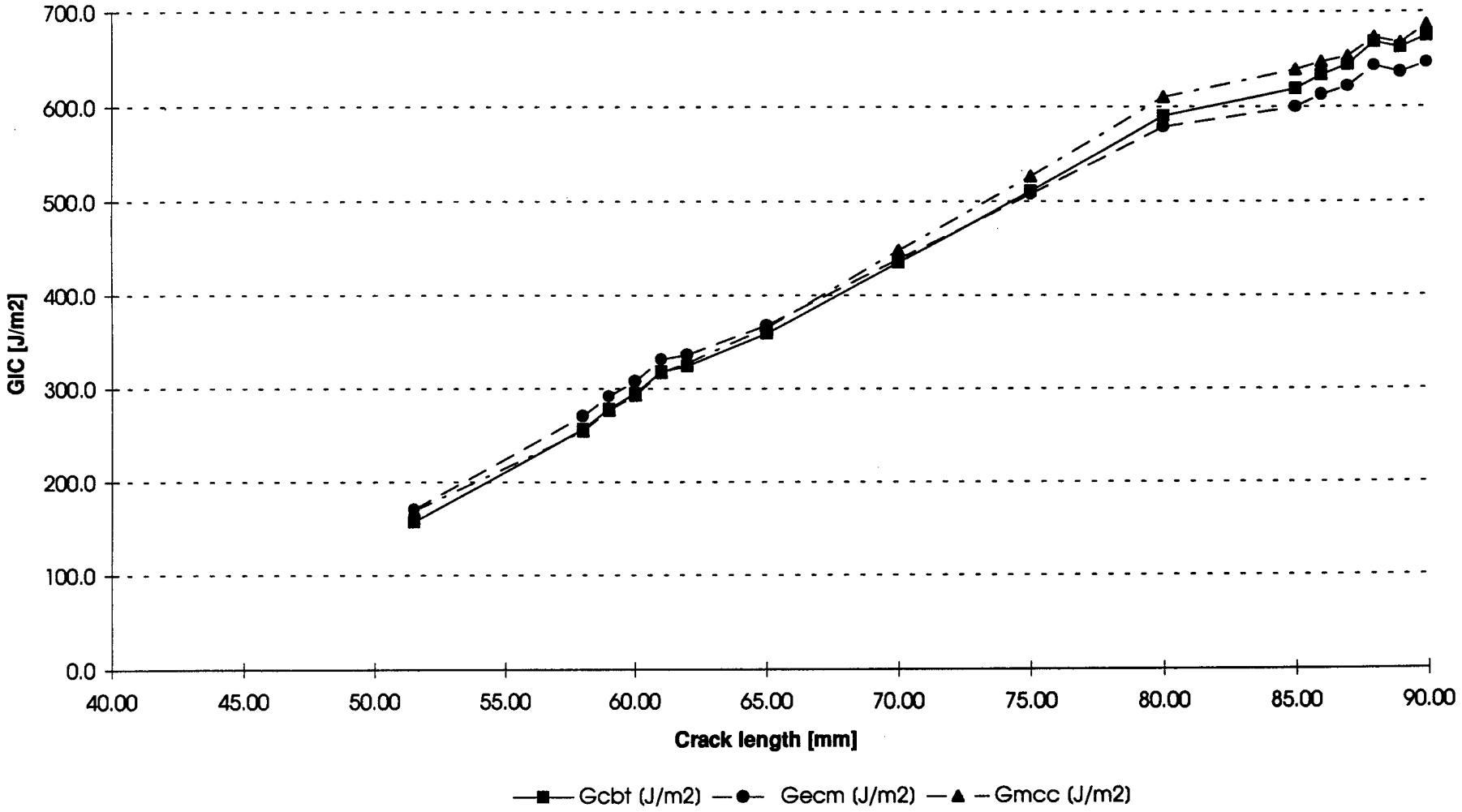

17/09/97 12:45

DCB Mode I from Insert

V1.02

MERL	S2/F584 22 ERO	Test Date: 01/01/04

Input					
Specimen thickness	2h [mm]	6.81	End block thickness	H [mm]	MISSING
Specimen width	B [mm]	20.01	End block length	l3 [mm]	MISSING
Starter foil material	[-]	Teflon	Temperature	[°C]	23.00
Starter foil thickness	[µm]	13.00	Relative humidity	[%]	MISSING
Starter foil length	A [mm]	MISSING	Loading rate	[mm/min]	0.50
Hinge type	[-]	MS20001-6	Drying temperature	[°C]	MISSING
Fiber Volume Fraction	Vf [Vol%]	MISSING	Drying duration	[h]	MISSING
			% Change Compliance	[%]	MISSING

l1	1.70
l2	0.00

check	(a+l2)-A >= 0	OK

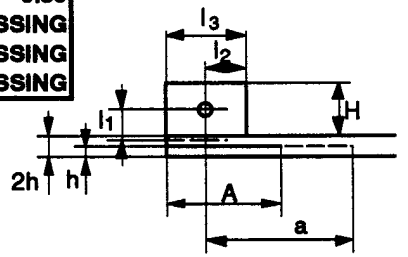

Text	Measure a [mm]	Load [N]	δ [mm]
NL	51.50	60.00	2.50
Prop.	52.00	50.00	2.56
Prop.	53.00	55.00	2.79
Prop.	54.00	58.00	3.19
Prop.	55.00	60.00	3.39
Prop.	56.00	62.00	3.69
Prop.	60.00	71.00	4.76
Prop.	65.00	79.00	5.98
Prop.	70.00	84.00	7.32
Prop.	75.00	85.00	8.53
Prop.	80.00	88.00	10.16
Prop.	81.00	87.00	10.53
Prop.	82.00	87.00	10.93
Prop.	83.00	87.00	11.30
Prop.	84.00	87.00	11.58
Prop.	85.00	87.00	11.75

Results			
Gcbt [J/m2]	Gecm [J/m2]	Gmcc [J/m2]	E-Mod. [GPa]
137.8	150.4	146.2	131.4
116.9	127.1	116.5	108.9
138.4	149.5	140.1	114.0
164.9	176.9	164.4	108.9
179.2	190.9	179.1	109.8
199.2	210.9	198.0	108.0
281.1	290.7	281.0	109.8
372.2	375.0	377.2	114.2
460.2	453.2	468.4	115.6
516.7	498.7	526.8	116.2
608.1	576.4	619.9	116.0
617.5	583.3	625.2	113.7
635.2	598.1	640.9	112.5
650.8	610.8	655.3	111.7
661.1	618.5	666.0	111.9
665.0	620.2	672.6	113.2
		average	113.5
		deviation	5.5

MERL	S2/F584 22 ERO	Test Date: 01/01/04

Regression

Method	Gcbt		Gecm		Gmcc	
Value	slope	Y-axis	slope	Y-axis	slope	Y-axis
	0.0044709	0.13423744	2.0677186	-4.85894725	32.5492201	-4.27978081
Correction	Δ=	**-30.0247**	n=	**2.0677**	A1=	**32.5492**
Correl. coeff. r^2	0.991020		0.988109		0.991020	
Points for fit						
	x	y	x	y	x	y
Point 1	51.50	0.36	1.71	-1.32	0.35	7.01
Point 2	85.00	0.51	1.93	-0.87	0.51	12.47

Text	F [-]	N [-]	F/N [-]	C/N [mm/N]	(C/N)^1/3	log(C/N)	log(a)	δ/a < 0.4
NL	0.9969	0.9976	0.9993	0.0418	0.3470	-1.3792	1.7118	0.0485
Prop.	0.9969	0.9976	0.9993	0.0513	0.3716	-1.2897	1.7160	0.0492
Prop.	0.9966	0.9974	0.9992	0.0509	0.3705	-1.2936	1.7243	0.0526
Prop.	0.9962	0.9970	0.9991	0.0552	0.3807	-1.2583	1.7324	0.0591
Prop.	0.9960	0.9969	0.9991	0.0567	0.3841	-1.2466	1.7404	0.0616
Prop.	0.9957	0.9966	0.9991	0.0597	0.3909	-1.2239	1.7482	0.0659
Prop.	0.9947	0.9958	0.9989	0.0673	0.4068	-1.1718	1.7782	0.0793
Prop.	0.9938	0.9951	0.9987	0.0761	0.4237	-1.1188	1.8129	0.0920
Prop.	0.9929	0.9943	0.9986	0.0876	0.4442	-1.0573	1.8451	0.1046
Prop.	0.9922	0.9938	0.9985	0.1010	0.4657	-0.9958	1.8751	0.1137
Prop.	0.9911	0.9928	0.9983	0.1163	0.4881	-0.9345	1.9031	0.1270
Prop.	0.9908	0.9926	0.9982	0.1219	0.4959	-0.9139	1.9085	0.1300
Prop.	0.9905	0.9923	0.9982	0.1266	0.5021	-0.8975	1.9138	0.1333
Prop.	0.9903	0.9921	0.9981	0.1309	0.5078	-0.8830	1.9191	0.1361
Prop.	0.9901	0.9920	0.9981	0.1342	0.5120	-0.8723	1.9243	0.1379
Prop.	0.9901	0.9920	0.9981	0.1362	0.5144	-0.8660	1.9294	0.1382

S2/F584 22 ERO

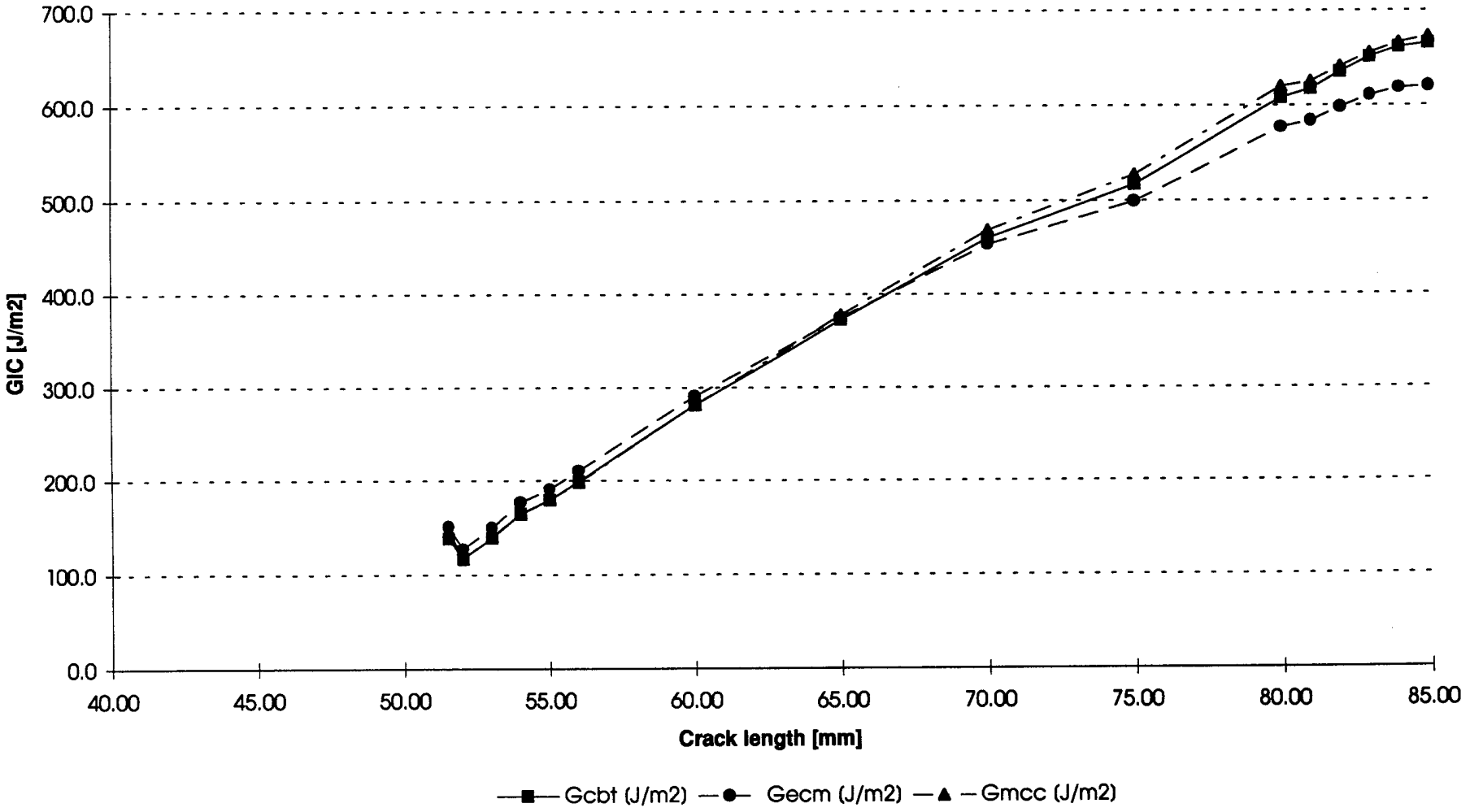

17/09/97 12:34

DCB Mode I from Insert

V1.02

MERL	S2/8552 - ERO	Test Date: 01/01/04

Input			End block thickness	H [mm]	MISSING
Specimen thickness	2h [mm]	9.45	End block length	l3 [mm]	MISSING
Specimen width	B [mm]	25.40	Temperature	[°C]	24.00
Starter foil material	[-]	MISSING	Relative humidity	[%]	MISSING
Starter foil thickness	[µm]	MISSING	Loading rate	[mm/min]	0.50
Starter foil length	A [mm]	MISSING	Drying temperature	[°C]	MISSING
Hinge type	[-]	ms20001-6	Drying duration	[h]	MISSING
Fiber Volume Fraction	Vf [Vol%]	MISSING	% Change Compliance	[%]	MISSING

DCB Mode I

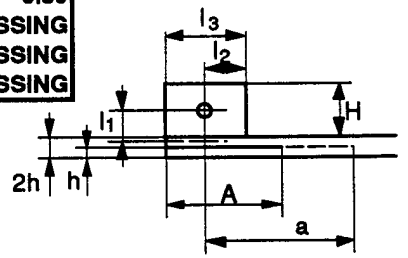

l1	2.36
l2	0.00

check	(a+l2)-A >= 0	OK

Text	Measure a [mm]	Load [N]	δ [mm]
NL	62.00	130.00	2.80
Prop.	63.00	134.00	3.35
Prop.	64.00	139.00	3.60
Prop.	65.00	142.00	3.81
Prop.	66.00	145.00	4.00
Prop.	67.00	150.00	4.30
Prop.	68.00	155.00	4.55
Prop.	69.00	156.00	4.77
Prop.	70.00	158.00	4.94
Prop.	72.00	165.00	5.56
Prop.	75.00	170.00	6.26
Prop.	80.00	181.00	7.58
Prop.	85.00	187.00	9.00
Prop.	90.00	188.00	10.60
Prop.	95.00	187.00	11.88
Prop.	100.00	187.00	13.72
Prop.	101.00	187.00	13.95
Prop.	102.00	187.00	14.25
Prop.	103.00	187.00	14.58
Prop.	104.00	186.00	14.93

Results			
Gcbt [J/m2]	Gecm [J/m2]	Gmcc [J/m2]	E-Mod. [GPa]
259.3	276.8	268.1	78.7
315.9	335.9	314.5	70.2
347.9	368.5	346.5	70.2
371.8	392.3	370.2	70.2
394.0	414.2	393.2	70.7
433.1	453.7	431.7	70.4
468.2	488.8	468.3	71.1
488.5	508.2	487.4	70.6
506.8	525.5	507.5	71.3
582.8	600.4	581.7	70.6
654.8	668.6	655.1	71.1
802.2	807.9	809.0	72.7
937.4	932.7	947.2	73.1
1059.7	1042.8	1063.8	71.6
1130.3	1101.2	1139.5	72.5
1251.1	1208.0	1254.1	71.2
1261.7	1216.1	1268.1	71.8
1278.3	1230.0	1286.2	72.0
1297.3	1246.2	1305.9	72.1
1310.7	1257.1	1317.2	71.7

MERL	S2/8552 - ERO	Test Date: 01/01/04

Regression

Method	Gcbt		Gecm		Gmcc	
Value	slope	Y-axis	slope	Y-axis	slope	Y-axis
	0.00346801	0.07232651	2.39669936	-5.92529484	30.4759899	-2.19307535
Correction	Δ=	**-20.8553**	n=	**2.3967**	A1=	**30.4760**
Correl. coeff. r^2	0.998781		0.998092		0.998781	
Points for fit						
	x	y	x	y	x	y
Point 1	62.00	0.29	1.79	-1.63	0.28	6.29
Point 2	110.00	0.45	2.04	-1.03	0.46	11.69

Text	F [-]	N [-]	F/N [-]	C/N [mm/N]	(C/N)^1/3	log(C/N)	log(a)	δ/a < 0.4
NL	0.9968	0.9975	0.9993	0.0216	0.2785	-1.6657	1.7924	0.0452
Prop.	0.9962	0.9970	0.9991	0.0251	0.2927	-1.6008	1.7993	0.0532
Prop.	0.9959	0.9969	0.9991	0.0260	0.2962	-1.5853	1.8062	0.0563
Prop.	0.9958	0.9967	0.9991	0.0269	0.2997	-1.5699	1.8129	0.0586
Prop.	0.9956	0.9966	0.9990	0.0277	0.3025	-1.5578	1.8195	0.0606
Prop.	0.9954	0.9964	0.9990	0.0288	0.3064	-1.5411	1.8261	0.0642
Prop.	0.9952	0.9962	0.9989	0.0295	0.3089	-1.5307	1.8325	0.0669
Prop.	0.9950	0.9961	0.9989	0.0307	0.3131	-1.5129	1.8388	0.0691
Prop.	0.9949	0.9960	0.9989	0.0314	0.3155	-1.5032	1.8451	0.0706
Prop.	0.9944	0.9956	0.9988	0.0338	0.3235	-1.4705	1.8573	0.0772
Prop.	0.9940	0.9953	0.9987	0.0370	0.3332	-1.4318	1.8751	0.0835
Prop.	0.9931	0.9945	0.9986	0.0421	0.3479	-1.3756	1.9031	0.0948
Prop.	0.9922	0.9938	0.9984	0.0484	0.3645	-1.3149	1.9294	0.1059
Prop.	0.9912	0.9930	0.9982	0.0568	0.3844	-1.2458	1.9542	0.1178
Prop.	0.9906	0.9925	0.9981	0.0640	0.4000	-1.1937	1.9777	0.1251
Prop.	0.9895	0.9915	0.9980	0.0740	0.4198	-1.1308	2.0000	0.1372
Prop.	0.9894	0.9915	0.9980	0.0752	0.4222	-1.1235	2.0043	0.1381
Prop.	0.9893	0.9913	0.9979	0.0769	0.4252	-1.1142	2.0086	0.1397
Prop.	0.9891	0.9912	0.9979	0.0787	0.4285	-1.1042	2.0128	0.1416
Prop.	0.9889	0.9910	0.9979	0.0810	0.4327	-1.0915	2.0170	0.1436

8552-5.XLW

S2/8552 - ERO

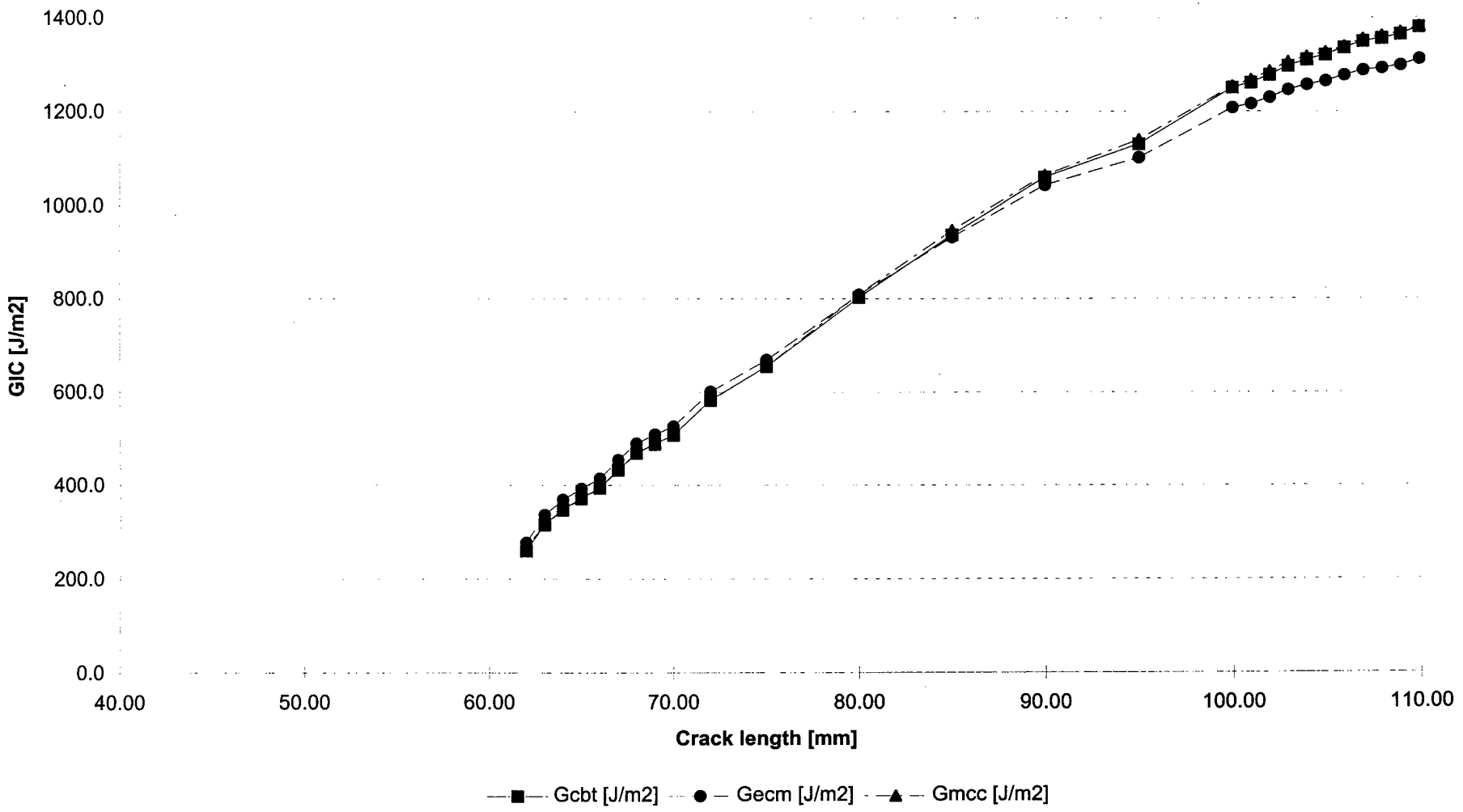

05/01/98 10:36

DCB Mode I from Insert

V1.02

MERL	S2/8552 ERO	Test Date: 01/01/04

Input					
Specimen thickness	2h [mm]	9.28	End block thickness	H [mm]	MISSING
Specimen width	B [mm]	25.45	End block length	l3 [mm]	MISSING
Starter foil material	[-]	MISSING	Temperature	[°C]	24.00
Starter foil thickness	[µm]	MISSING	Relative humidity	[%]	MISSING
Starter foil length	A [mm]	MISSING	Loading rate	[mm/min]	0.50
Hinge type	[-]	MS20001-6	Drying temperature	[°C]	MISSING
Fiber Volume Fraction	Vf [Vol%]	MISSING	Drying duration	[h]	MISSING
			% Change Compliance	[%]	MISSING

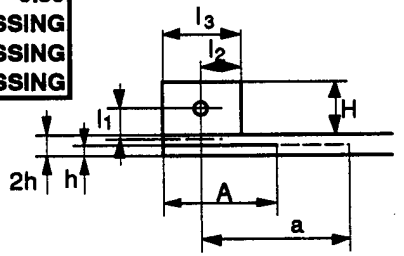

l1	2.32
l2	0.00

check	(a+l2)-A >= 0	OK

Text	Measure a [mm]	Load [N]	δ [mm]
NL	62.50	123.00	2.80
Prop.	63.00	138.00	3.48
Prop.	64.00	143.00	3.75
Prop.	65.00	145.00	3.93
Prop.	66.00	151.00	4.17
Prop.	67.00	157.00	4.55
Prop.	68.00	162.00	4.77
Prop.	69.00	165.00	5.00
Prop.	70.00	168.00	5.25
Prop.	72.00	174.00	5.84
Prop.	74.00	181.00	6.42
Prop.	75.00	184.00	6.83
Prop.	80.00	190.00	8.04
Prop.	85.00	196.00	9.70
Prop.	90.00	197.00	11.11
Prop.	100.00	192.00	14.13
Prop.	101.00	190.00	14.51
Prop.	102.00	189.00	14.80
Prop.	103.00	189.00	15.00
Prop.	104.00	188.00	15.45

Results			
Gcbt [J/m2]	Gecm [J/m2]	Gmcc [J/m2]	E-Mod. [GPa]
246.0	261.5	251.6	77.3
340.9	361.7	339.0	71.0
376.1	397.6	373.7	70.8
395.0	416.0	392.7	70.9
431.4	452.7	431.2	72.1
483.7	505.8	481.4	71.1
517.3	539.1	518.0	72.4
546.0	567.2	547.7	72.8
577.2	597.7	579.5	73.0
650.5	669.5	651.9	72.5
728.0	744.8	731.8	73.2
779.0	794.7	779.5	72.2
899.4	905.5	907.0	73.8
1065.8	1060.5	1071.1	73.0
1171.1	1152.9	1180.4	73.6
1330.2	1285.8	1338.6	73.1
1340.6	1293.7	1343.6	72.2
1349.0	1299.7	1351.8	72.2
1356.1	1304.5	1364.0	73.0
1378.1	1323.6	1381.3	72.2

MERL	S2/8552 ERO	Test Date: 01/01/04

Regression

Method	Gcbt		Gecm		Gmcc	
Value	slope	Y-axis	slope	Y-axis	slope	Y-axis
	0.0035131	0.07008529	2.41753561	-5.95999584	30.6510824	-2.14147808
Correction	Δ=	**-19.9497**	n=	**2.4175**	A1=	**30.6511**
Correl. coeff. r^2	0.999272		0.998718		0.999272	
Points for fit						
	x	y	x	y	x	y
Point 1	62.50	0.29	1.80	-1.62	0.28	6.55
Point 2	110.00	0.46	2.04	-1.02	0.46	11.85

Text	F [-]	N [-]	F/N [-]	C/N [mm/N]	(C/N)^1/3	log(C/N)	log(a)	δ/a < 0.4
NL	0.9969	0.9976	0.9993	0.0228	0.2836	-1.6417	1.7959	0.0448
Prop.	0.9960	0.9969	0.9991	0.0253	0.2935	-1.5970	1.7993	0.0552
Prop.	0.9958	0.9967	0.9991	0.0263	0.2974	-1.5799	1.8062	0.0586
Prop.	0.9957	0.9966	0.9990	0.0272	0.3007	-1.5655	1.8129	0.0605
Prop.	0.9955	0.9965	0.9990	0.0277	0.3026	-1.5573	1.8195	0.0632
Prop.	0.9951	0.9962	0.9989	0.0291	0.3076	-1.5362	1.8261	0.0679
Prop.	0.9949	0.9960	0.9989	0.0296	0.3092	-1.5293	1.8325	0.0701
Prop.	0.9948	0.9959	0.9989	0.0304	0.3122	-1.5167	1.8388	0.0725
Prop.	0.9946	0.9958	0.9988	0.0314	0.3154	-1.5033	1.8451	0.0750
Prop.	0.9941	0.9954	0.9987	0.0337	0.3231	-1.4721	1.8573	0.0811
Prop.	0.9937	0.9950	0.9987	0.0356	0.3291	-1.4480	1.8692	0.0868
Prop.	0.9933	0.9947	0.9986	0.0373	0.3342	-1.4281	1.8751	0.0911
Prop.	0.9926	0.9941	0.9985	0.0426	0.3492	-1.3709	1.9031	0.1005
Prop.	0.9914	0.9931	0.9983	0.0498	0.3680	-1.3025	1.9294	0.1141
Prop.	0.9907	0.9925	0.9981	0.0568	0.3844	-1.2455	1.9542	0.1234
Prop.	0.9891	0.9912	0.9979	0.0742	0.4203	-1.1293	2.0000	0.1413
Prop.	0.9889	0.9910	0.9979	0.0771	0.4255	-1.1132	2.0043	0.1437
Prop.	0.9887	0.9909	0.9978	0.0790	0.4291	-1.1022	2.0086	0.1451
Prop.	0.9887	0.9909	0.9978	0.0801	0.4311	-1.0964	2.0128	0.1456
Prop.	0.9884	0.9906	0.9978	0.0830	0.4361	-1.0811	2.0170	0.1486

8552-12.XLW

S2/8552 ERO

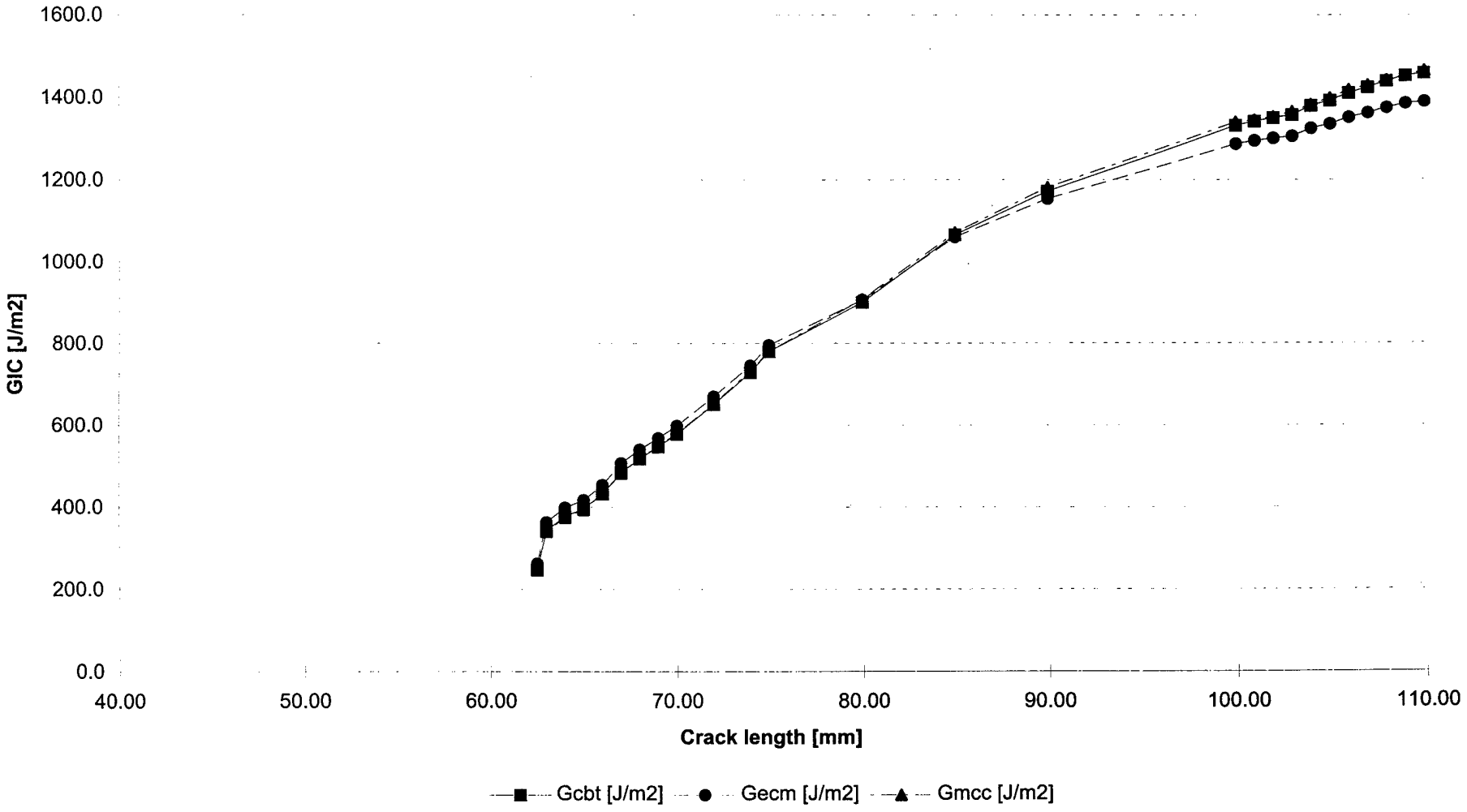

05/01/98 10:37

DCB Mode I from Insert

V1.02

MERL	S2/8552 ERO	Test Date: 01/01/04

Input					
Specimen thickness	2h [mm]	9.46	End block thickness	H [mm]	MISSING
Specimen width	B [mm]	25.39	End block length	l3 [mm]	MISSING
Starter foil material	[-]	MISSING	Temperature	[°C]	24.00
Starter foil thickness	[µm]	MISSING	Relative humidity	[%]	MISSING
Starter foil length	A [mm]	MISSING	Loading rate	[mm/min]	0.50
Hinge type	[-]	MS20001-6	Drying temperature	[°C]	MISSING
Fiber Volume Fraction	Vf [Vol%]	MISSING	Drying duration	[h]	MISSING
			% Change Compliance	[%]	MISSING

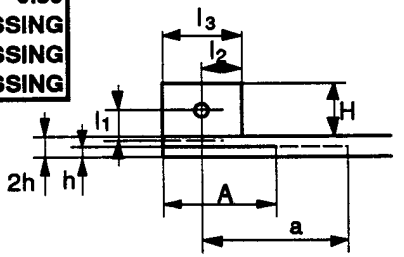

l1	2.37
l2	0.00

check	(a+l2)-A >= 0	OK

Text	Measure a [mm]	Load [N]	δ [mm]
NL	64.00	129.00	2.90
Prop.	65.00	143.00	3.78
Prop.	66.00	149.00	4.06
Prop.	67.00	152.00	4.30
Prop.	68.00	158.00	4.59
Prop.	69.00	159.00	4.76
Prop.	70.00	163.00	5.00
Prop.	72.00	171.00	5.68
Prop.	74.00	176.00	6.12
Prop.	75.00	179.00	6.40
Prop.	80.00	189.00	7.80
Prop.	85.00	193.00	9.22
Prop.	90.00	193.00	10.51
Prop.	95.00	189.00	11.82
Prop.	100.00	187.00	13.20
Prop.	101.00	187.00	13.55
Prop.	102.00	186.00	13.85
Prop.	103.00	185.00	14.12
Prop.	104.00	185.00	14.55
Prop.	105.00	185.00	14.75

Results			
Gcbt [J/m2]	Gecm [J/m2]	Gmcc [J/m2]	E-Mod. [GPa]
258.4	275.0	268.1	82.5
368.9	391.1	366.9	72.6
408.1	431.0	406.5	72.9
435.9	458.7	433.7	72.7
478.3	501.5	477.0	73.2
493.6	515.8	492.8	73.4
525.7	547.5	526.3	74.0
613.0	634.2	610.8	72.9
665.6	684.3	667.0	74.2
700.5	718.1	702.9	74.4
856.9	866.2	862.1	75.0
985.6	983.9	990.9	74.8
1073.0	1059.1	1081.2	75.2
1130.9	1104.9	1137.0	74.7
1198.1	1159.7	1206.5	75.0
1219.7	1178.7	1227.7	74.9
1230.0	1186.5	1236.9	74.7
1237.2	1191.5	1243.9	74.6
1264.7	1215.9	1269.0	74.2
1271.9	1220.9	1280.6	74.9

MERL	S2/8552 ERO	Test Date: 01/01/04

Regression

Method	Gcbt		Gecm		Gmcc	
Value	slope	Y-axis	slope	Y-axis	slope	Y-axis
	0.00342002	0.07348197	2.3904408	-5.92408486	30.8557585	-2.2514527
Correction	Δ=	**-21.4858**	n=	**2.3904**	A1=	**30.8558**
Correl. coeff. r^2	0.998288		0.997446		0.998288	
Points for fit						
	x	y	x	y	x	y
Point 1	64.00	0.29	1.81	-1.61	0.28	6.46
Point 2	110.00	0.45	2.04	-1.04	0.45	11.68

Text	F [-]	N [-]	F/N [-]	C/N [mm/N]	(C/N)^1/3	log(C/N)	log(a)	δ/a < 0.4
NL	0.9969	0.9976	0.9993	0.0225	0.2825	-1.6471	1.8062	0.0453
Prop.	0.9958	0.9967	0.9991	0.0265	0.2982	-1.5764	1.8129	0.0582
Prop.	0.9956	0.9965	0.9990	0.0273	0.3013	-1.5632	1.8195	0.0615
Prop.	0.9954	0.9964	0.9990	0.0284	0.3051	-1.5468	1.8261	0.0642
Prop.	0.9951	0.9962	0.9989	0.0292	0.3078	-1.5352	1.8325	0.0675
Prop.	0.9950	0.9961	0.9989	0.0301	0.3109	-1.5221	1.8388	0.0690
Prop.	0.9948	0.9960	0.9989	0.0308	0.3135	-1.5115	1.8451	0.0714
Prop.	0.9942	0.9955	0.9988	0.0334	0.3219	-1.4767	1.8573	0.0789
Prop.	0.9940	0.9953	0.9987	0.0349	0.3269	-1.4567	1.8692	0.0827
Prop.	0.9938	0.9951	0.9987	0.0359	0.3300	-1.4445	1.8751	0.0853
Prop.	0.9928	0.9943	0.9985	0.0415	0.3462	-1.3819	1.9031	0.0975
Prop.	0.9919	0.9936	0.9984	0.0481	0.3636	-1.3180	1.9294	0.1085
Prop.	0.9913	0.9930	0.9983	0.0548	0.3799	-1.2609	1.9542	0.1168
Prop.	0.9907	0.9925	0.9982	0.0630	0.3979	-1.2006	1.9777	0.1244
Prop.	0.9901	0.9920	0.9981	0.0712	0.4144	-1.1478	2.0000	0.1320
Prop.	0.9899	0.9918	0.9980	0.0731	0.4180	-1.1363	2.0043	0.1342
Prop.	0.9897	0.9917	0.9980	0.0751	0.4219	-1.1245	2.0086	0.1358
Prop.	0.9896	0.9916	0.9980	0.0770	0.4254	-1.1137	2.0128	0.1371
Prop.	0.9894	0.9914	0.9980	0.0793	0.4297	-1.1006	2.0170	0.1399
Prop.	0.9893	0.9914	0.9980	0.0804	0.4316	-1.0946	2.0212	0.1405

8552-16.XLW

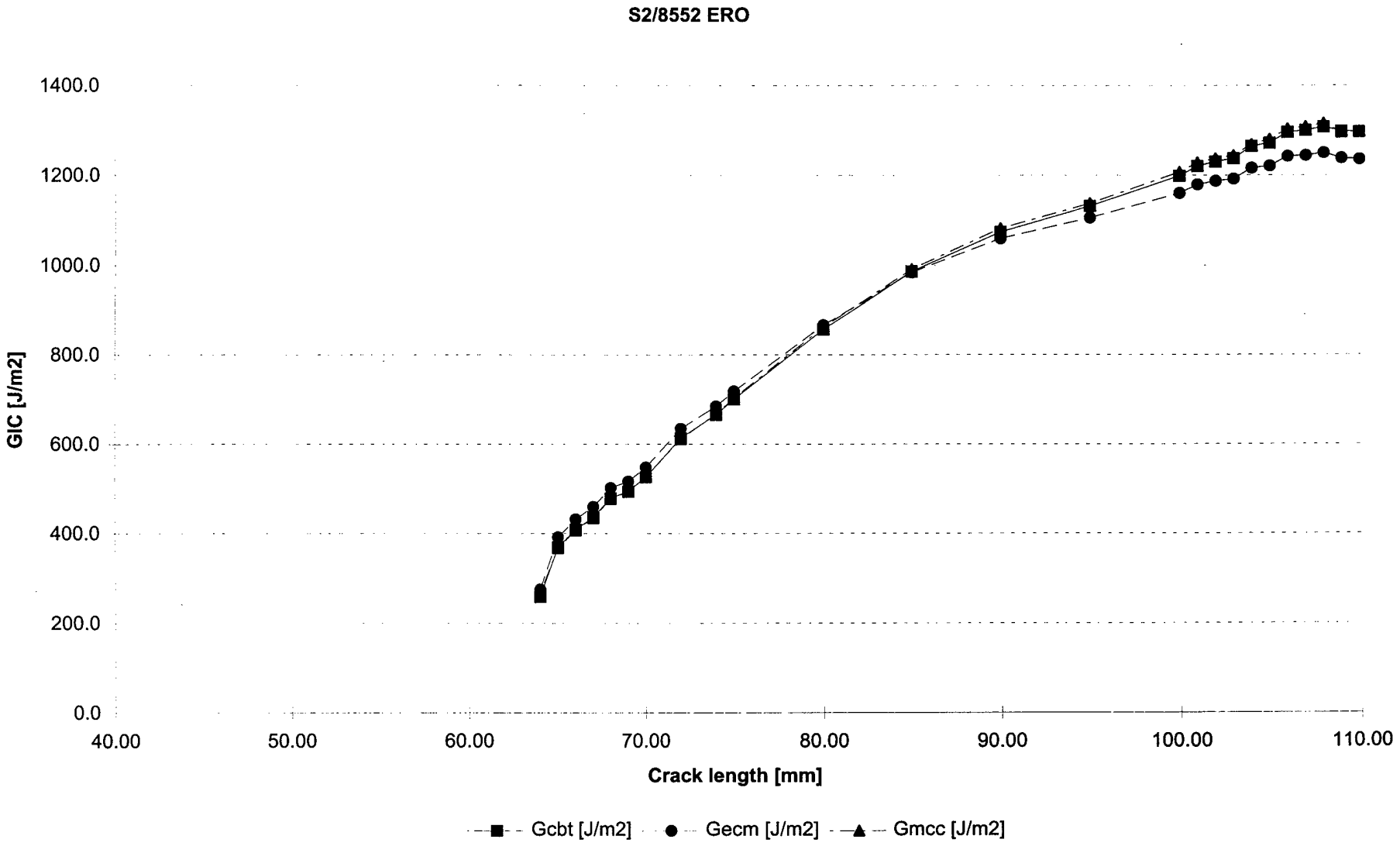

05/01/98 10:37

DCB Mode I from Insert

V1.02

MERL	S2/8552 ERO	Test Date: 01/01/04

Input					
Specimen thickness	2h [mm]	9.38	End block thickness	H [mm]	MISSING
Specimen width	B [mm]	25.37	End block length	l3 [mm]	MISSING
Starter foil material	[-]	MISSING	Temperature	[°C]	24.00
Starter foil thickness	[µm]	MISSING	Relative humidity	[%]	MISSING
Starter foil length	A [mm]	MISSING	Loading rate	[mm/min]	0.50
Hinge type	[-]	MS20001-6	Drying temperature	[°C]	MISSING
Fiber Volume Fraction	Vf [Vol%]	MISSING	Drying duration	[h]	MISSING
			% Change Compliance	[%]	MISSING

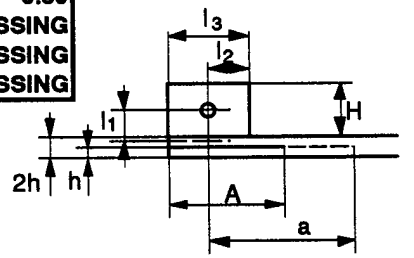

l1	2.35
l2	0.00

check	(a+l2)-A >= 0	OK

Text	Measure a [mm]	Load [N]	δ [mm]
NL	62.50	128.00	2.90
Prop.	63.00	143.00	3.76
Prop.	64.00	147.00	4.00
Prop.	65.00	154.00	4.30
Prop.	66.00	157.00	4.58
Prop.	67.00	161.00	4.82
Prop.	68.00	165.00	5.08
Prop.	69.00	168.00	5.31
Prop.	70.00	175.00	5.69
Prop.	72.00	180.00	6.21
Prop.	74.00	186.00	6.92
Prop.	75.00	188.00	7.18
Prop.	80.00	196.00	8.63
Prop.	85.00	196.00	10.00
Prop.	90.00	195.00	11.48
Prop.	95.00	194.00	13.05
Prop.	100.00	190.00	14.45
Prop.	101.00	189.00	14.75
Prop.	102.00	189.00	15.13
Prop.	103.00	188.00	15.36

Results			
Gcbt [J/m2]	Gecm [J/m2]	Gmcc [J/m2]	E-Mod. [GPa]
262.9	280.5	273.0	78.1
378.5	402.9	376.2	68.4
409.0	433.7	406.7	68.5
455.3	480.9	454.1	69.1
488.6	514.3	485.9	68.5
521.3	546.7	519.9	69.1
556.7	581.8	556.3	69.5
585.9	610.2	586.8	70.0
646.8	671.4	648.9	70.3
710.4	732.7	714.1	70.7
800.7	820.7	801.7	69.8
830.9	849.2	833.5	70.2
989.4	997.5	995.9	70.9
1092.2	1087.7	1098.5	70.7
1191.1	1173.2	1196.0	70.3
1288.7	1256.7	1293.7	70.1
1339.7	1294.6	1346.6	70.4
1349.1	1301.5	1355.5	70.3
1372.5	1321.9	1378.7	70.2
1374.8	1321.9	1382.8	70.5

MERL	S2/8552 ERO	Test Date: 01/01/04

Regression

Method	Gcbt		Gecm		Gmcc	
Value	slope	Y-axis	slope	Y-axis	slope	Y-axis
	0.00351766	0.07354279	2.39785108	-5.90850369	30.2675596	-2.21402012
Correction	Δ=	**-20.9068**	n=	**2.3979**	A1=	**30.2676**
Correl. coeff. r^2	0.998697		0.997865		0.998697	

Points for fit

	x	y	x	y	x	y
Point 1	62.50	0.29	1.80	-1.60	0.28	6.36
Point 2	110.00	0.46	2.04	-1.01	0.46	11.72

Text	F [-]	N [-]	F/N [-]	C/N [mm/N]	(C/N)^1/3	log(C/N)	log(a)	δ/a < 0.4
NL	0.9967	0.9975	0.9993	0.0227	0.2832	-1.6437	1.7959	0.0464
Prop.	0.9956	0.9966	0.9990	0.0264	0.2977	-1.5787	1.7993	0.0597
Prop.	0.9954	0.9964	0.9990	0.0273	0.3011	-1.5637	1.8062	0.0625
Prop.	0.9951	0.9962	0.9989	0.0280	0.3038	-1.5524	1.8129	0.0662
Prop.	0.9949	0.9960	0.9989	0.0293	0.3083	-1.5333	1.8195	0.0694
Prop.	0.9947	0.9958	0.9988	0.0301	0.3109	-1.5220	1.8261	0.0719
Prop.	0.9945	0.9957	0.9988	0.0309	0.3139	-1.5097	1.8325	0.0747
Prop.	0.9943	0.9955	0.9988	0.0317	0.3166	-1.4983	1.8388	0.0770
Prop.	0.9939	0.9952	0.9987	0.0327	0.3197	-1.4859	1.8451	0.0813
Prop.	0.9936	0.9949	0.9986	0.0347	0.3261	-1.4600	1.8573	0.0863
Prop.	0.9929	0.9944	0.9985	0.0374	0.3345	-1.4270	1.8692	0.0935
Prop.	0.9928	0.9943	0.9985	0.0384	0.3374	-1.4155	1.8751	0.0957
Prop.	0.9918	0.9935	0.9983	0.0443	0.3539	-1.3534	1.9031	0.1079
Prop.	0.9910	0.9928	0.9982	0.0514	0.3718	-1.2891	1.9294	0.1176
Prop.	0.9901	0.9921	0.9980	0.0593	0.3901	-1.2266	1.9542	0.1276
Prop.	0.9893	0.9913	0.9979	0.0679	0.4079	-1.1684	1.9777	0.1374
Prop.	0.9887	0.9908	0.9978	0.0768	0.4250	-1.1149	2.0000	0.1445
Prop.	0.9885	0.9907	0.9978	0.0788	0.4287	-1.1036	2.0043	0.1460
Prop.	0.9883	0.9905	0.9978	0.0808	0.4324	-1.0925	2.0086	0.1483
Prop.	0.9882	0.9905	0.9978	0.0825	0.4353	-1.0836	2.0128	0.1491

8552-21.XLW

S2/8552 ERO

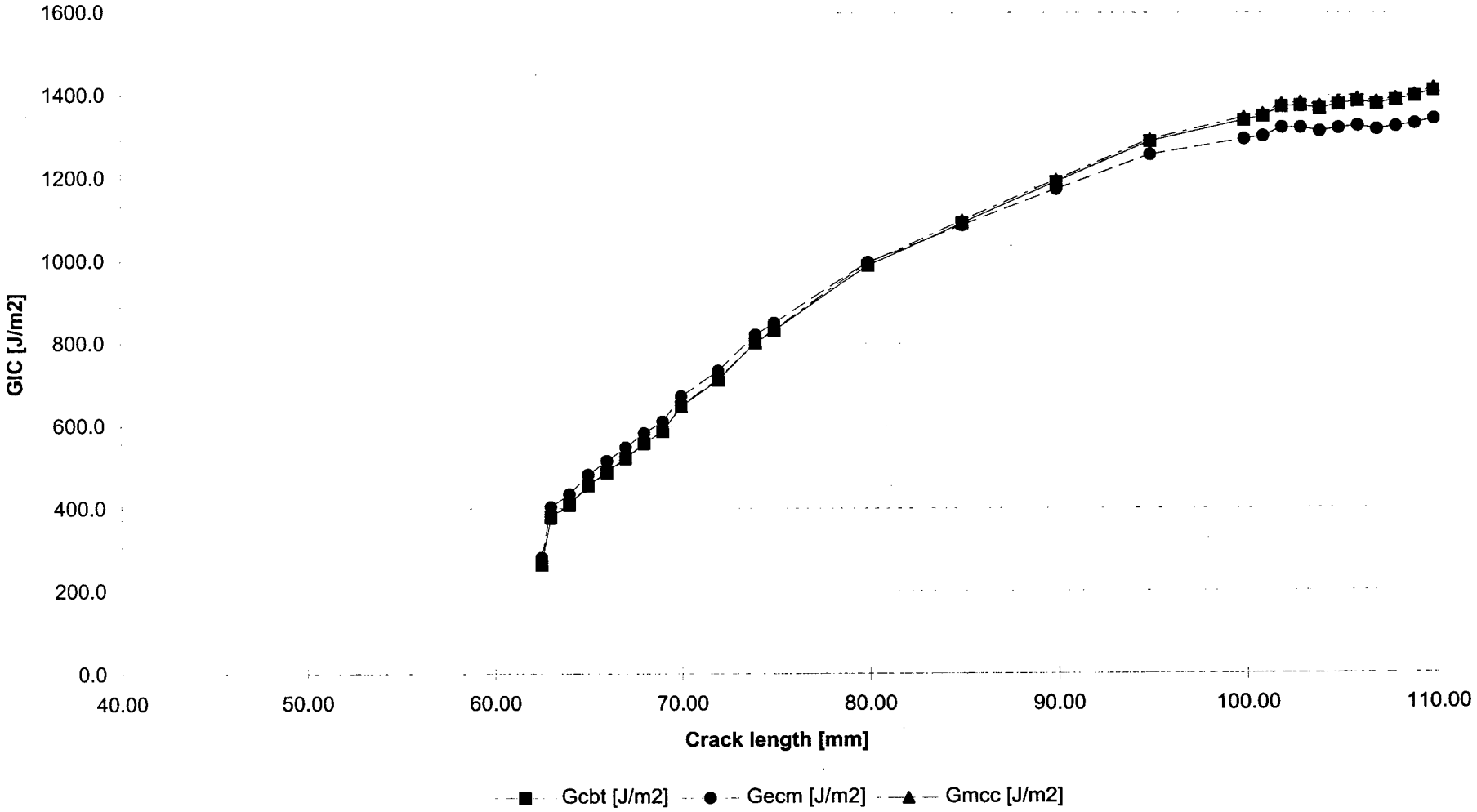

05/01/98 10:37

DCB Mode I from Insert

V1.02

APPENDIX B

FATIGUE COMPLIANCE RESULTS

E7T1 - 0.07 to 0.74mm (R=0.1) load approx 200 to 250N

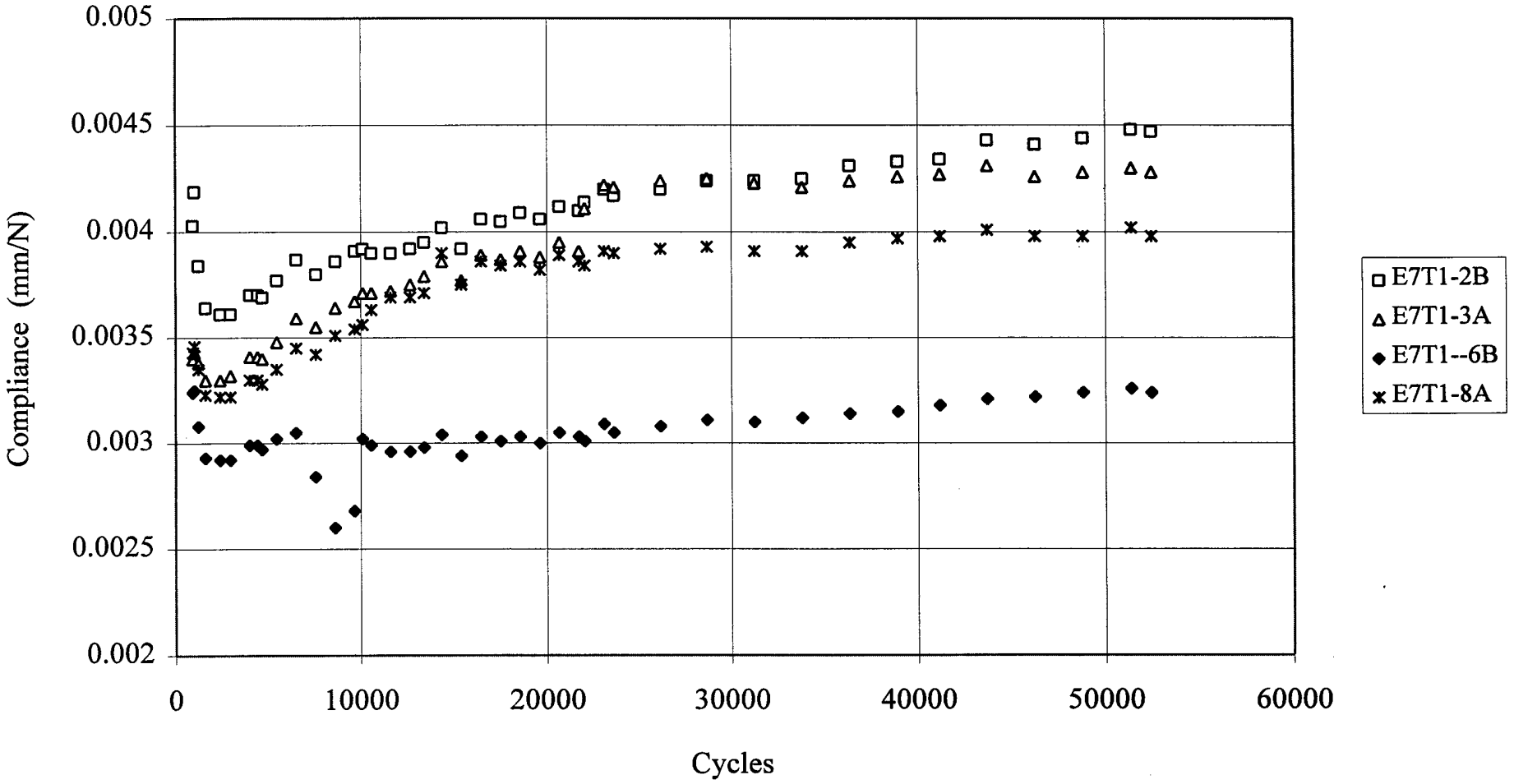

E7T1 - 0.08 to 0.75mm (R=0.1) load approx 175 to 220N

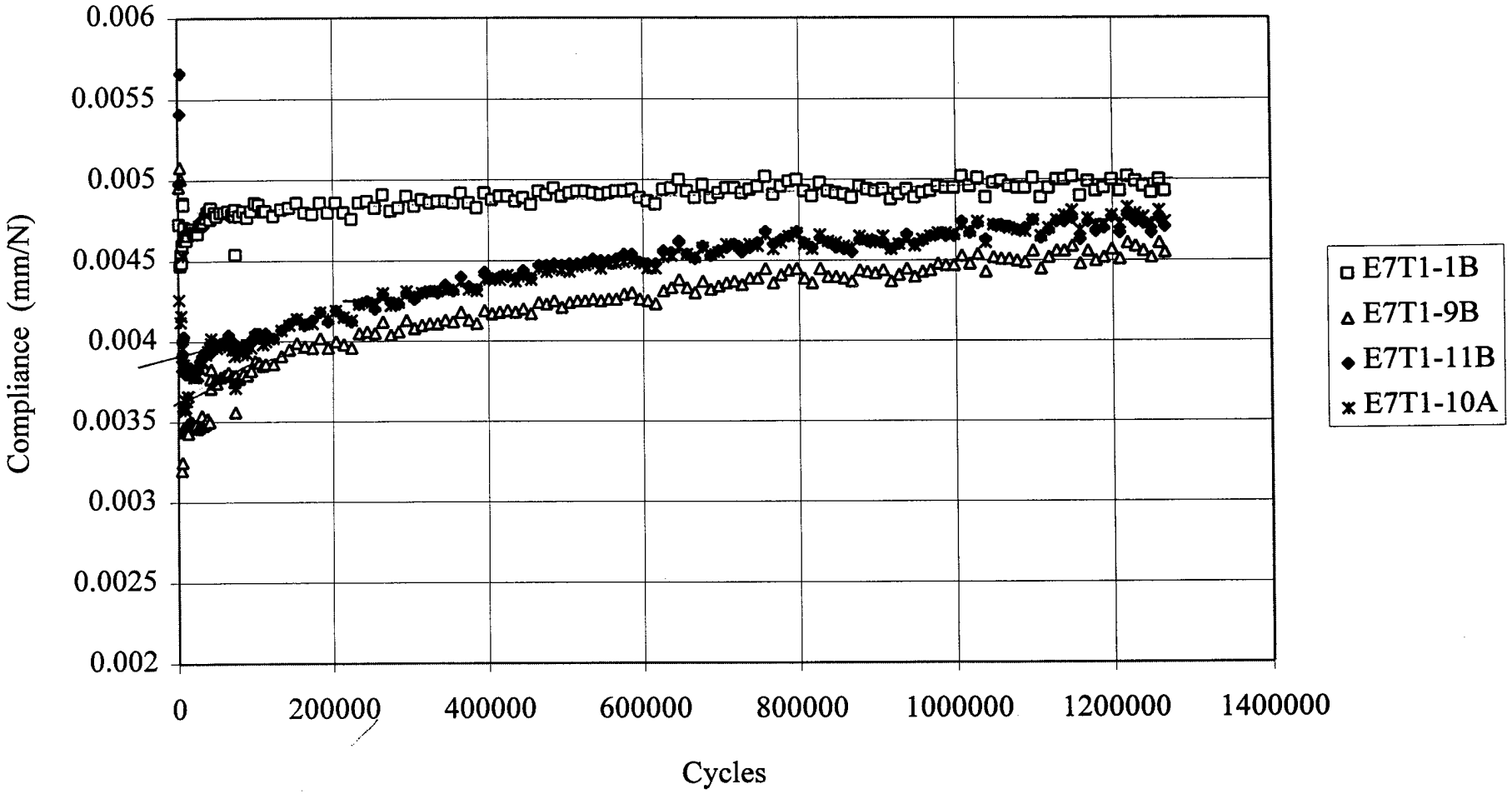

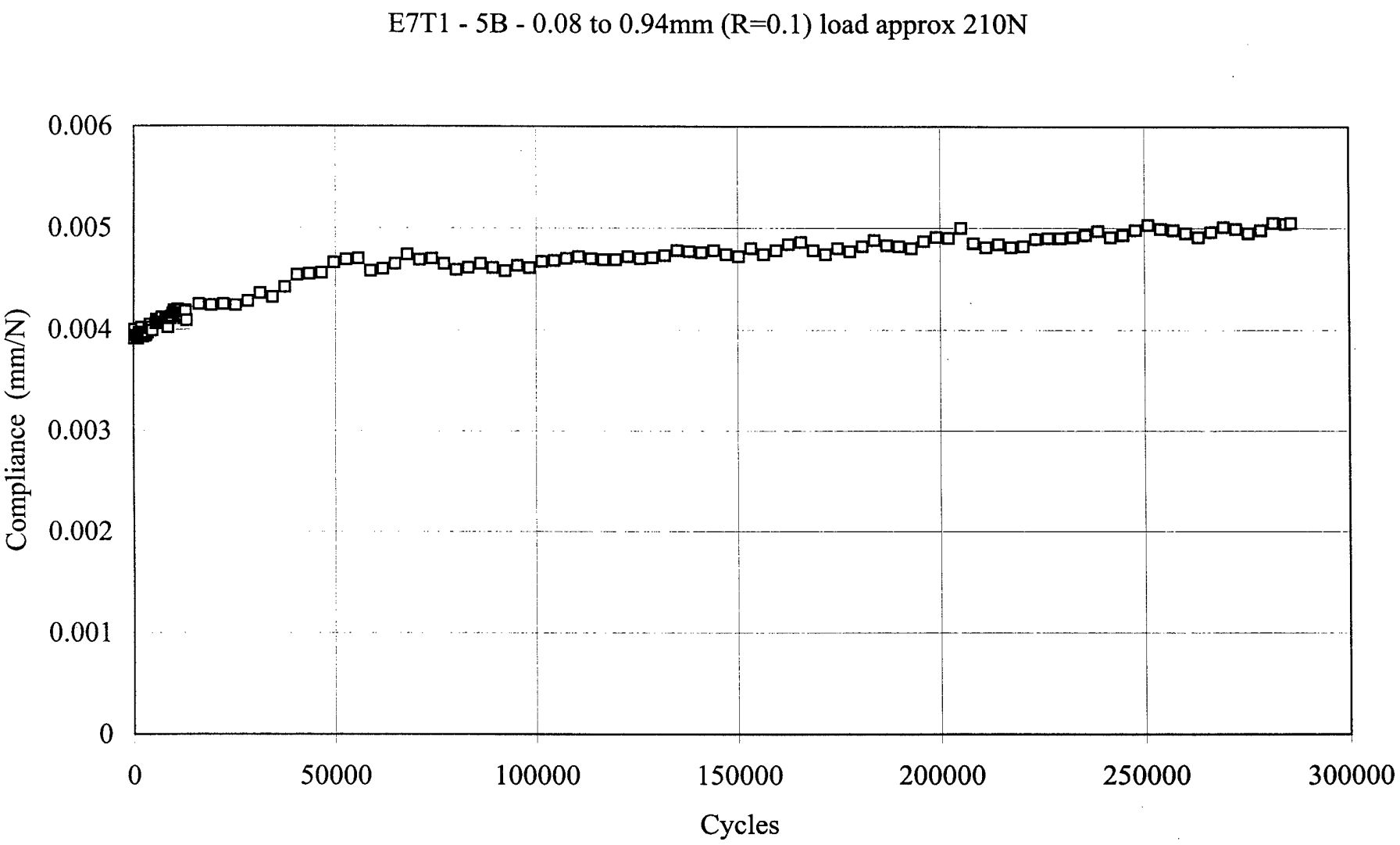
E7T1 - 5B - 0.08 to 0.94mm (R=0.1) load approx 210N
0.006
0.005
0.004
0.003
0.002
0.001
0
Compliance (mm/N)
0
50000
100000
150000
200000
250000
300000
Cycles

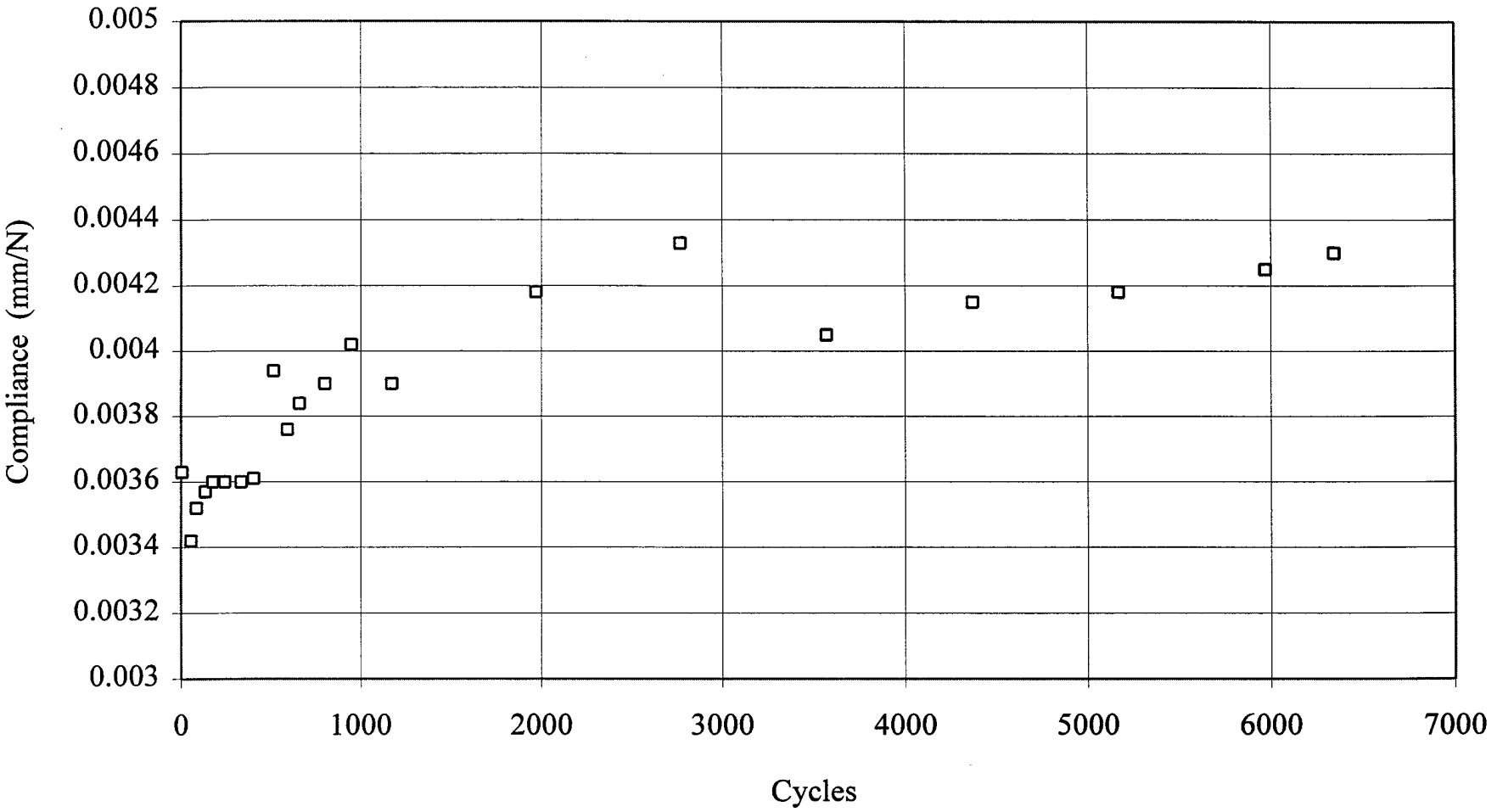
E7T1-6A - 0.1 to 0.95mm (R=0.1) load approx 270N
Compliance (mm/N)
0.005
0.0048
0.0046
0.0044
0.0042
0.004
0.0038
0.0036
0.0034
0.0032
0.003
0
1000
2000
3000
4000
5000
6000
7000
Cycles

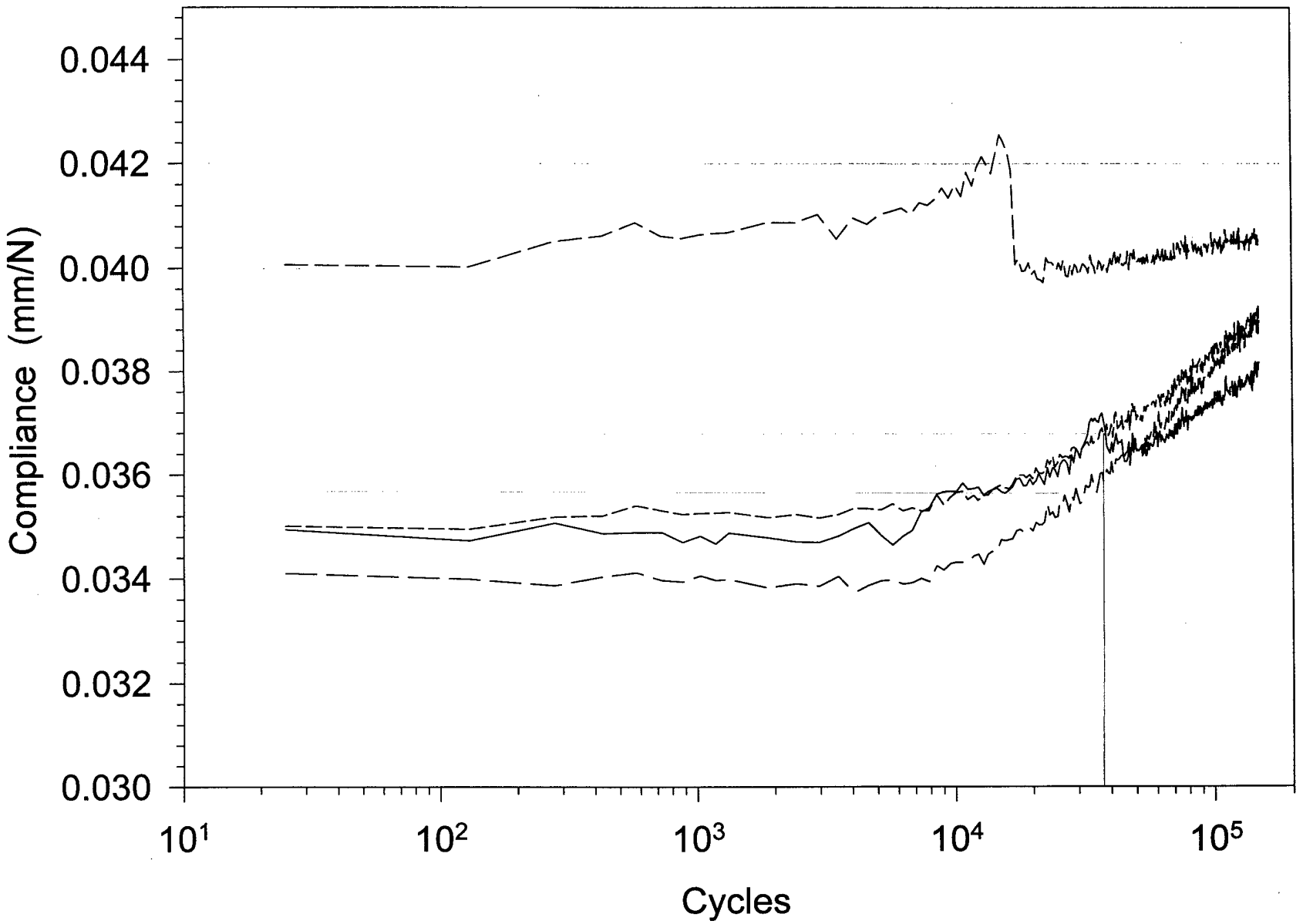
S2/F584 δ_{max} =1.2 mm
Compliance (mm/N)
0.044
0.042
0.040
0.038
0.036
0.034
0.032
0.030
10^1
10^2
10^3
10^4
10^5
Cycles

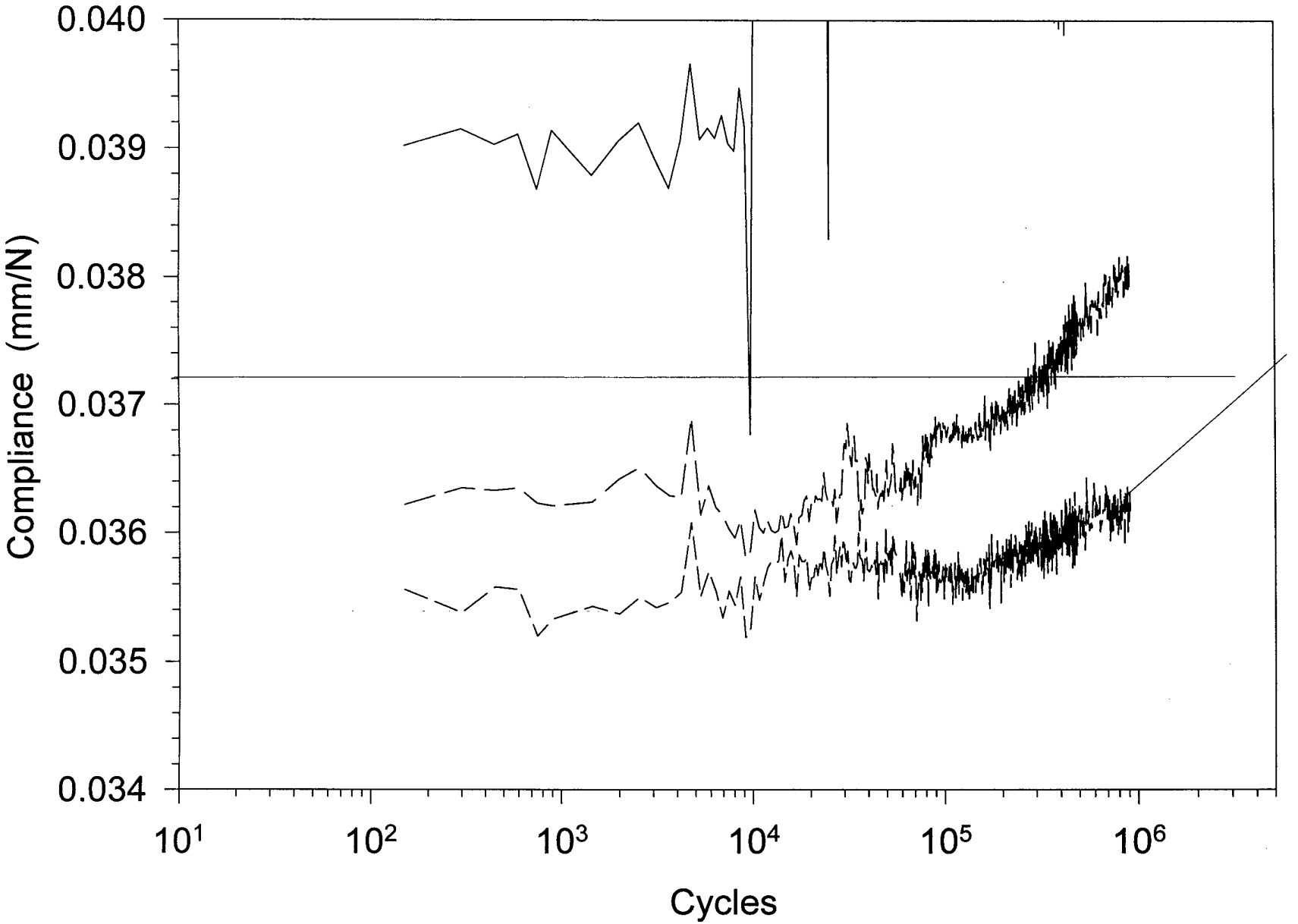
S2/F584 δ_{max} =1.0 mm
0.040
0.039
0.038
0.037
0.036
0.035
0.034
Compliance (mm/N)
10^1
10^2
10^3
10^4
10^5
10^6
Cycles

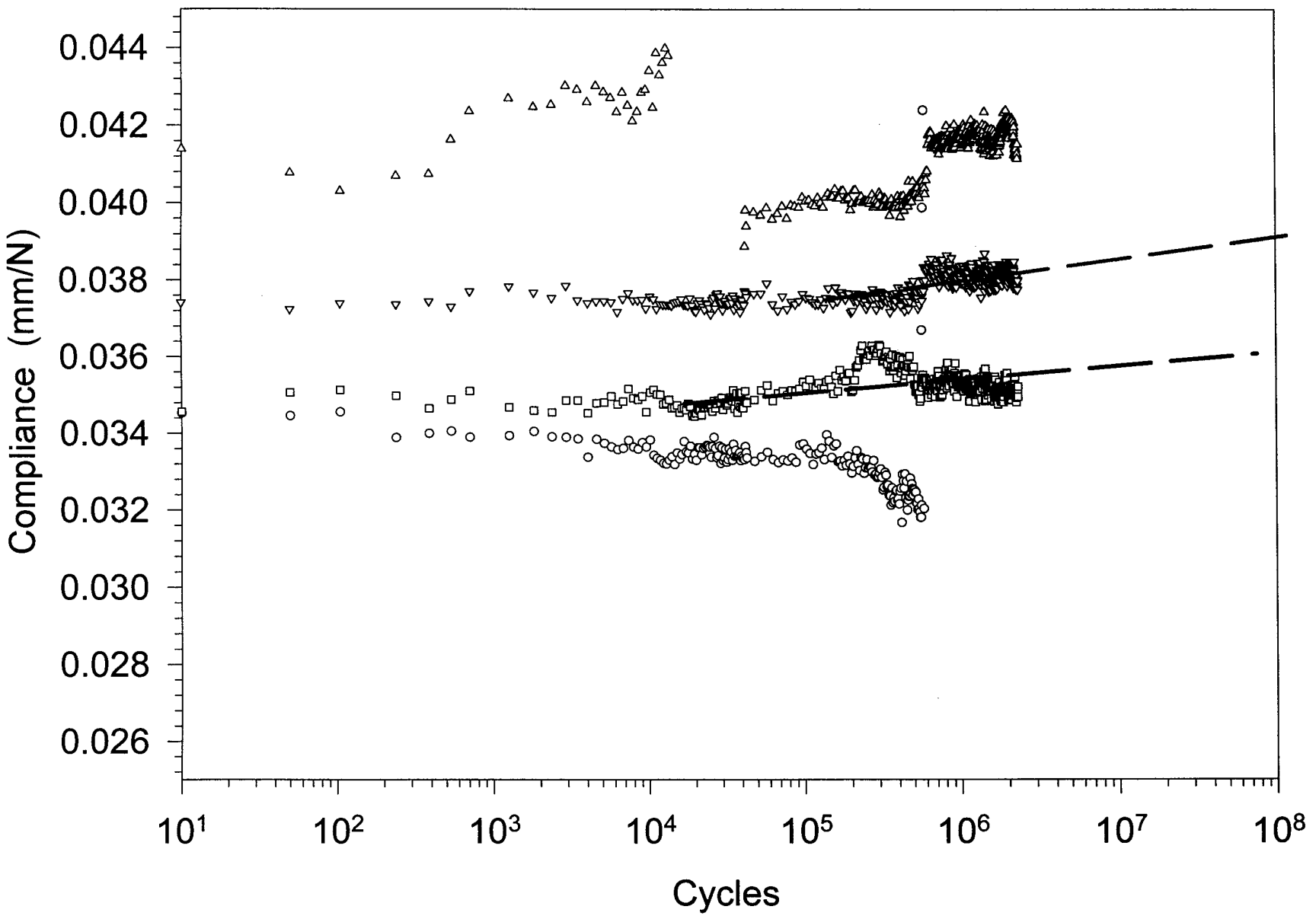
S2/F584 δ_{max} =0.8mm
Compliance (mm/N)
0.044
0.042
0.040
0.038
0.036
0.034
0.032
0.030
0.028
0.026
10^1
10^2
10^3
10^4
10^5
10^6
10^7
10^8
Cycles

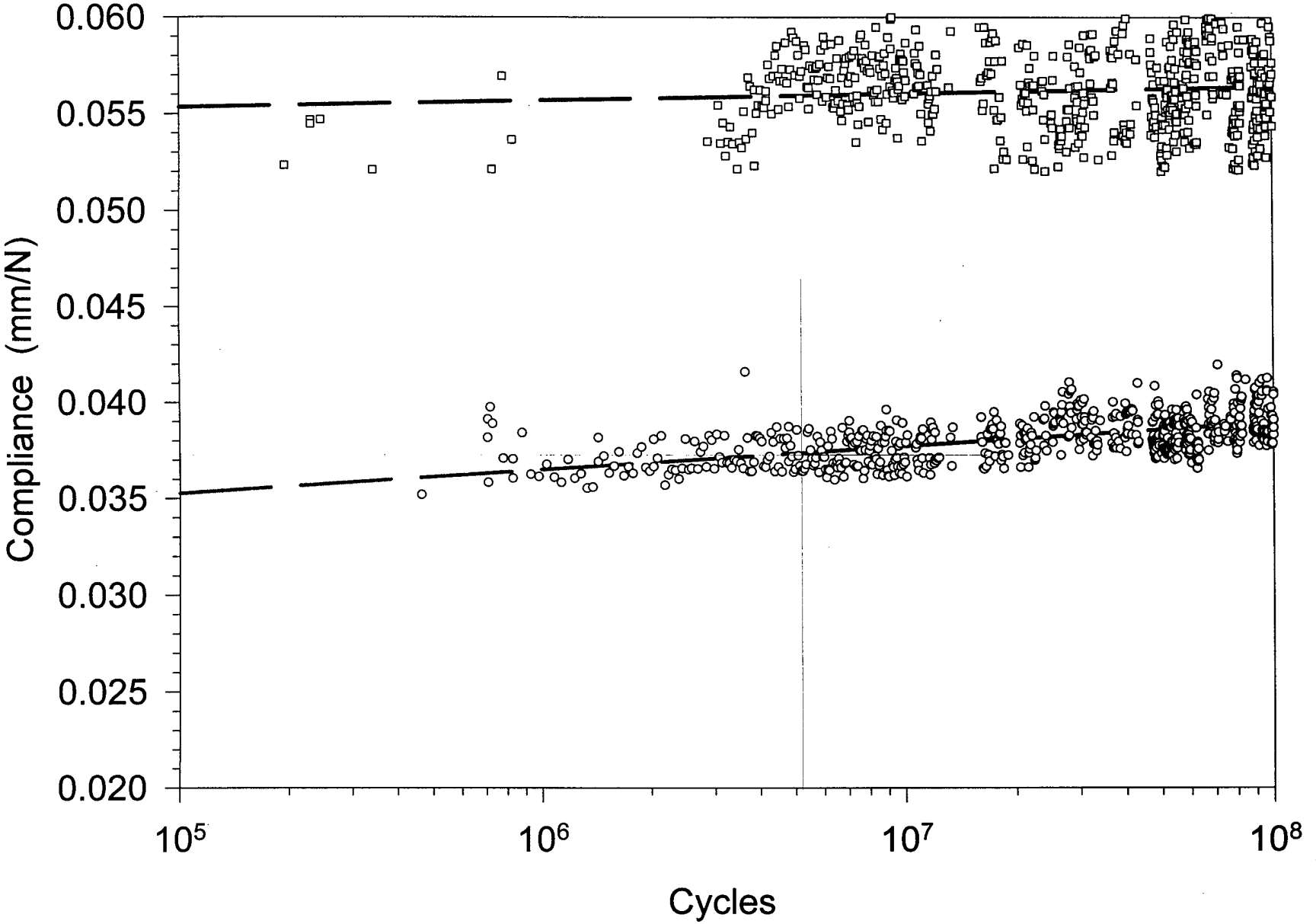
S2/F584 δ_{max} =0.6mm
0.060
0.055
0.050
0.045
0.040
0.035
0.030
0.025
0.020
Compliance (mm/N)
10^5
10^6
10^7
10^8
Cycles

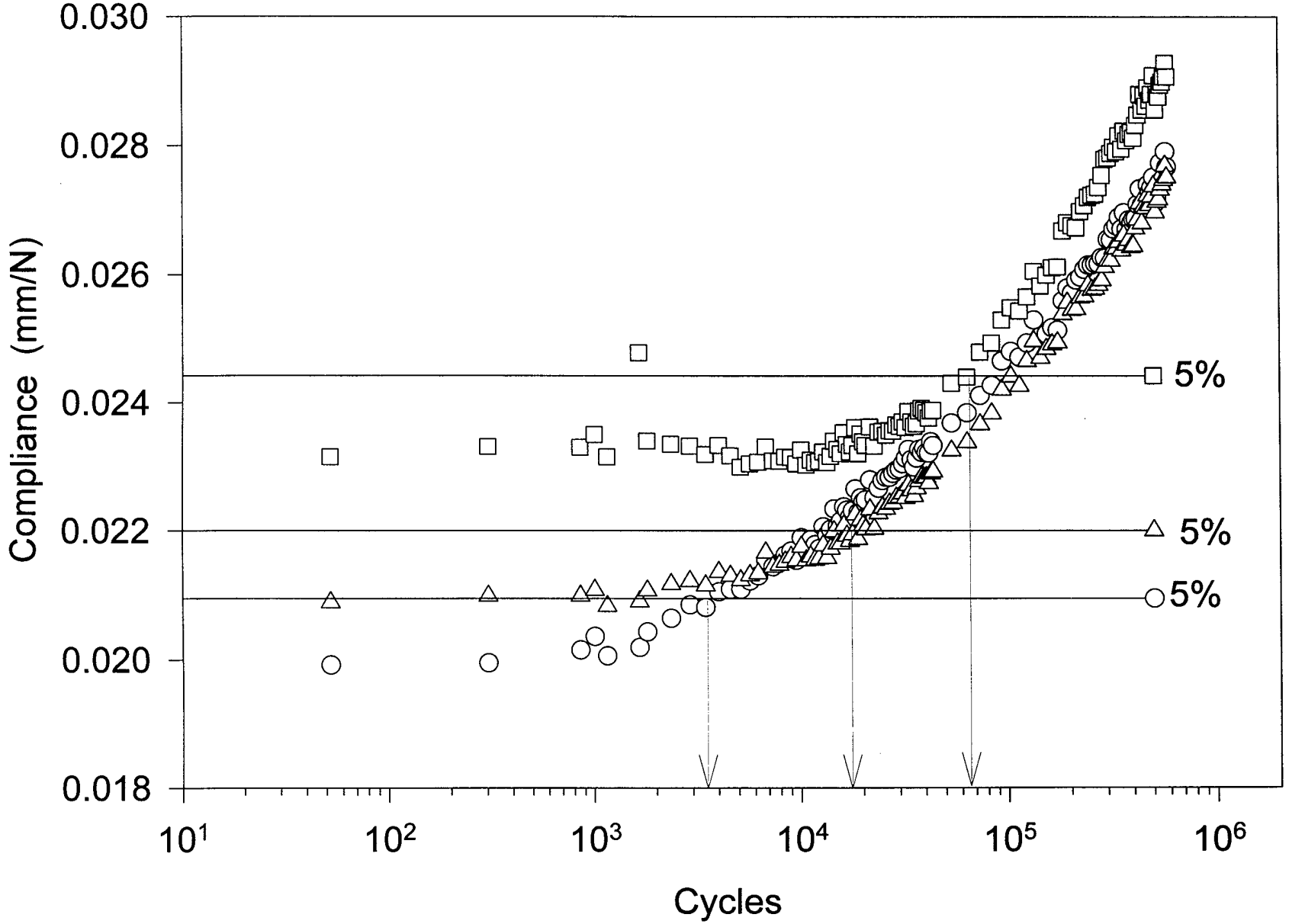
S2/8552 δ_{max} = 2.0mm f= 5Hz
0.030
0.028
0.026
0.024
0.022
0.020
0.018
Compliance (mm/N)
5%
5%
5%
10^1
10^2
10^3
10^4
10^5
10^6
Cycles

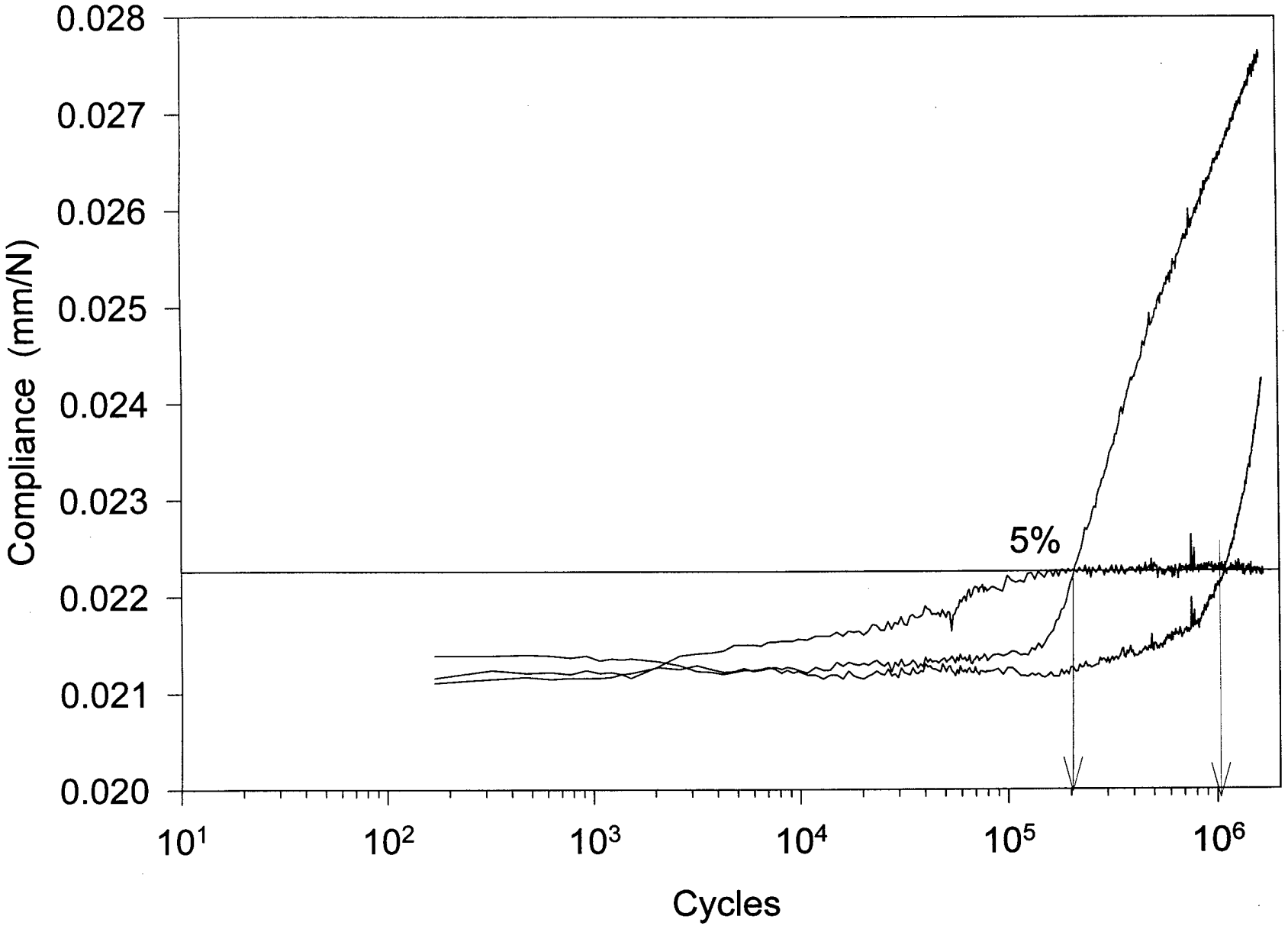
S2/8552 δ_{max} =1.8mm f=5Hz
0.028
0.027
0.026
0.025
0.024
0.023
0.022
0.021
0.020
Compliance (mm/N)
5%
10^1
10^2
10^3
10^4
10^5
10^6
Cycles

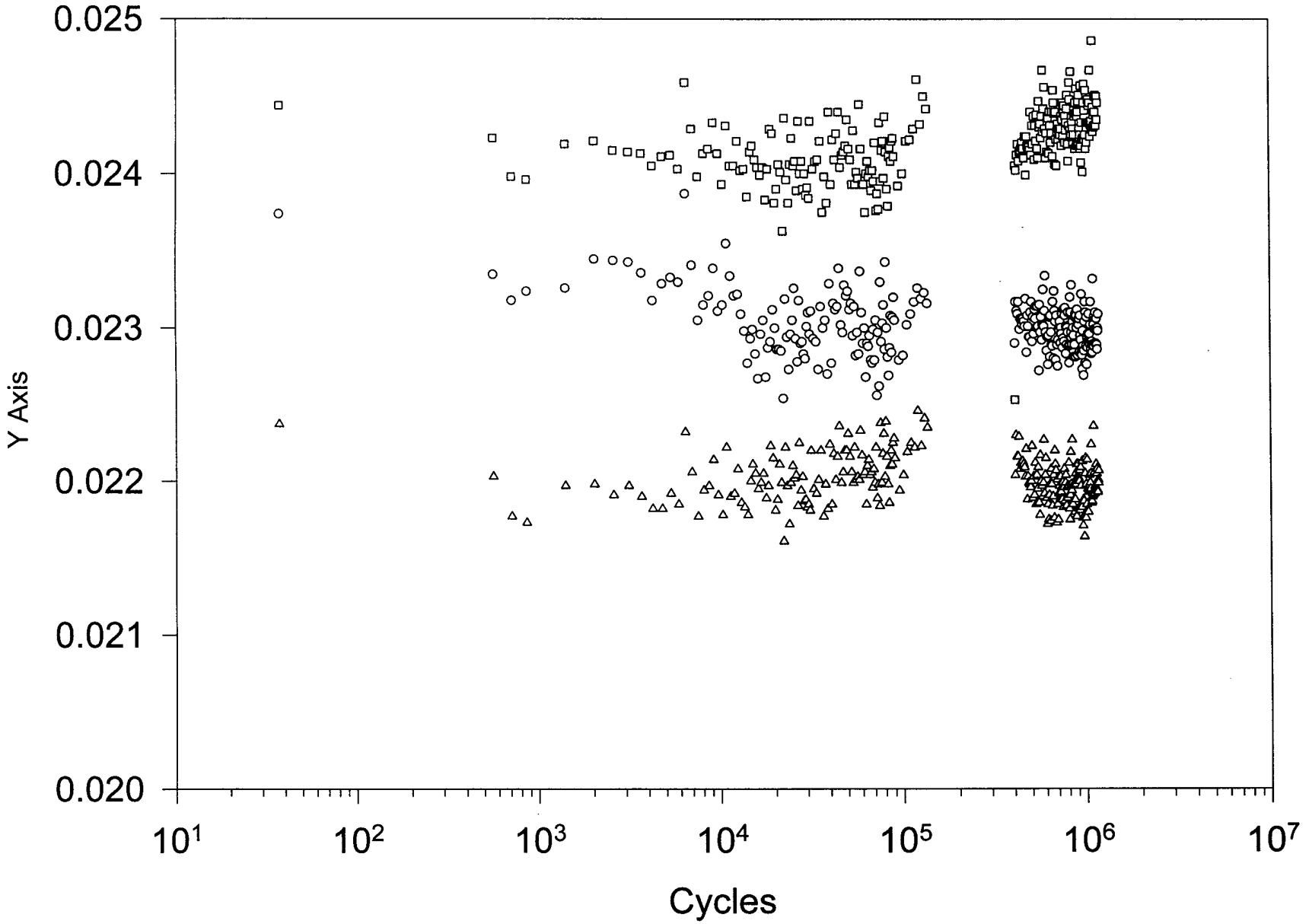
S2/8552 δ_{max} = 1.5mm f= 5Hz
0.025
0.024
0.023
0.022
0.021
0.020
Y Axis
10^1
10^2
10^3
10^4
10^5
10^6
10^7
Cycles

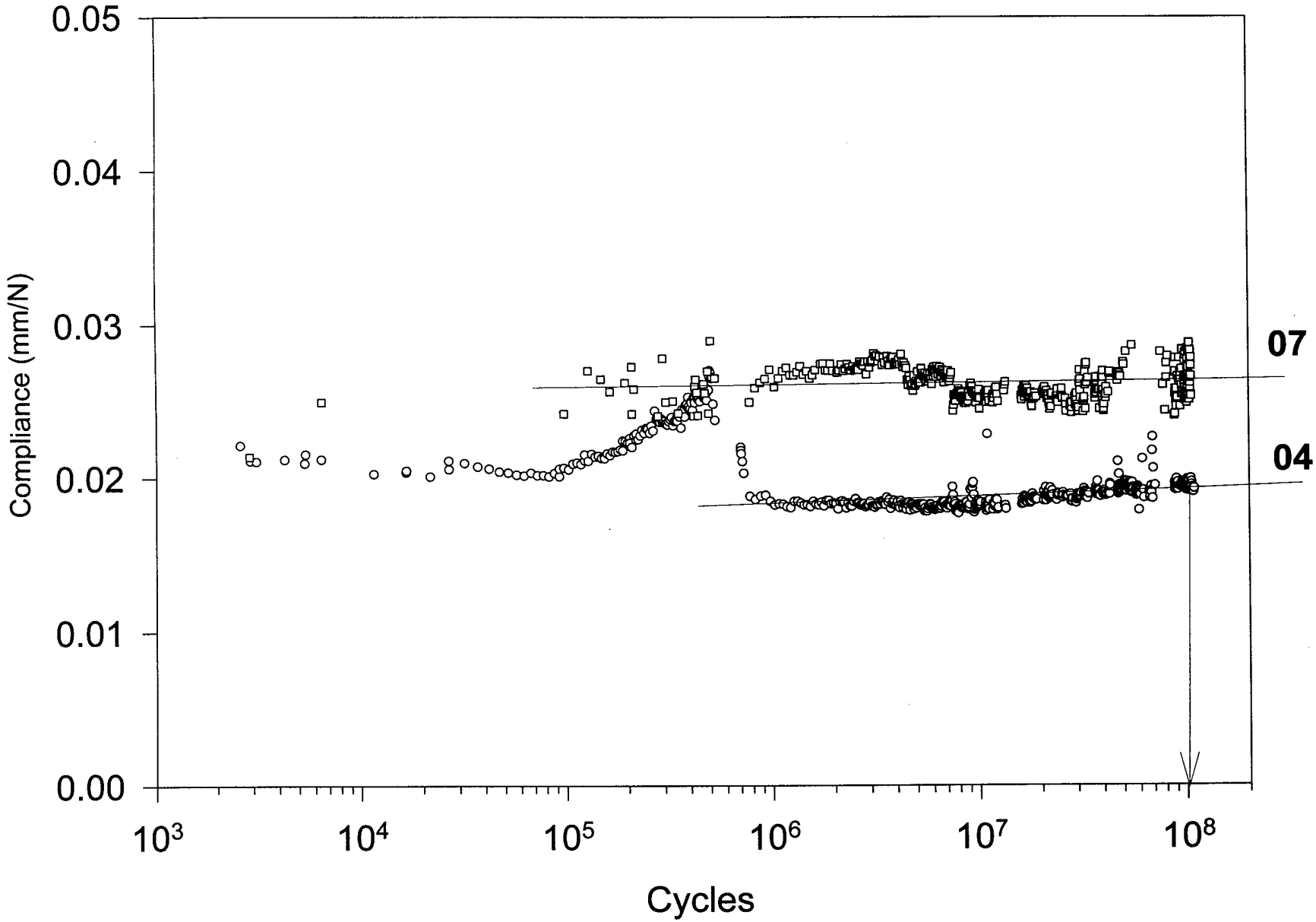
S2/8552 δ_{max} = 1.24mm f= 17Hz
0.05
0.04
0.03
0.02
0.01
0.00
Compliance (mm/N)
10^3
10^4
10^5
10^6
10^7
10^8
Cycles
07
04

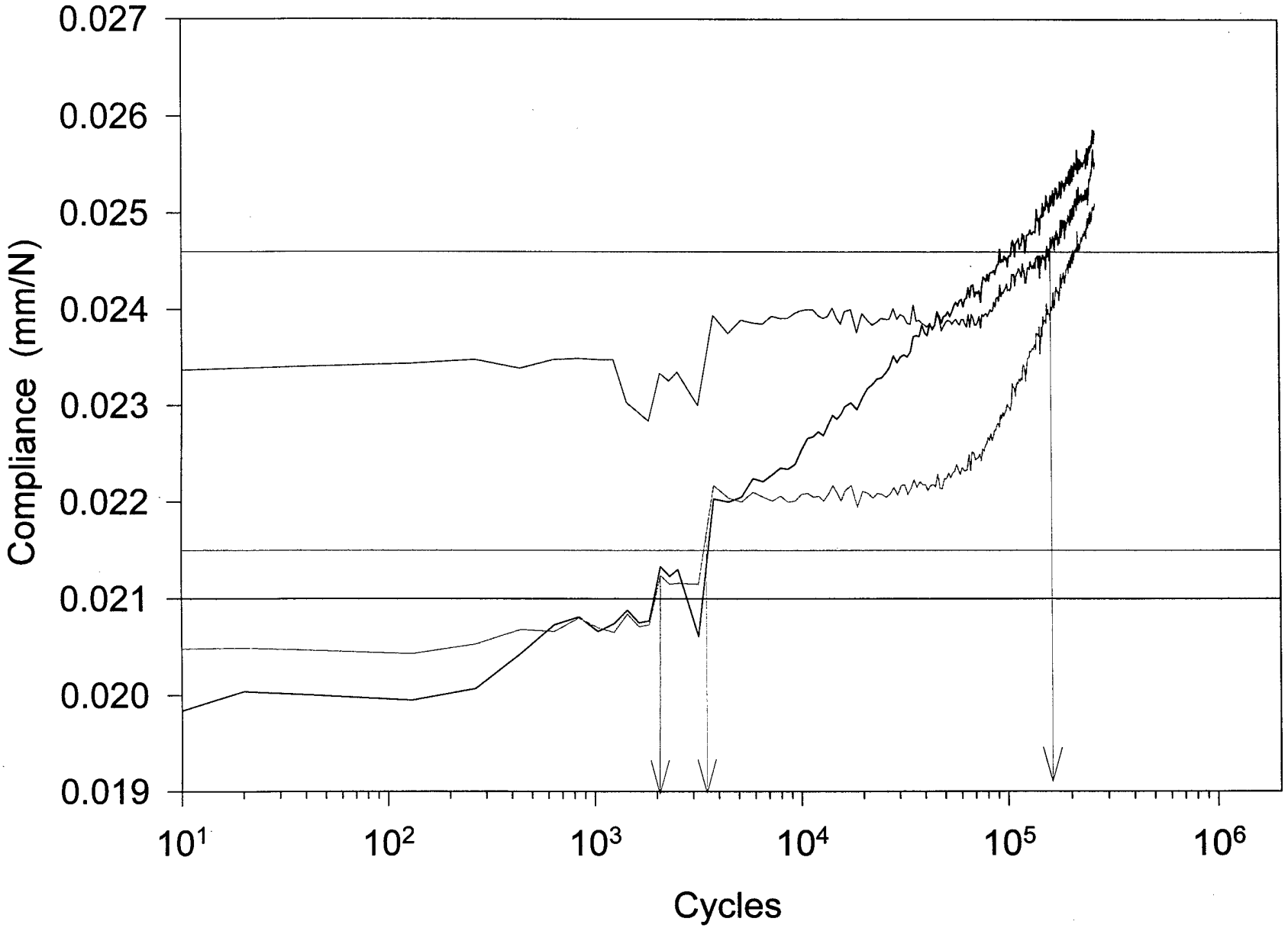
S2/8552 δmax =1.8mm f=20Hz
0.027
0.026
0.025
0.024
0.023
0.022
0.021
0.020
0.019
Compliance (mm/N)
10^1
10^2
10^3
10^4
10^5
10^6
Cycles

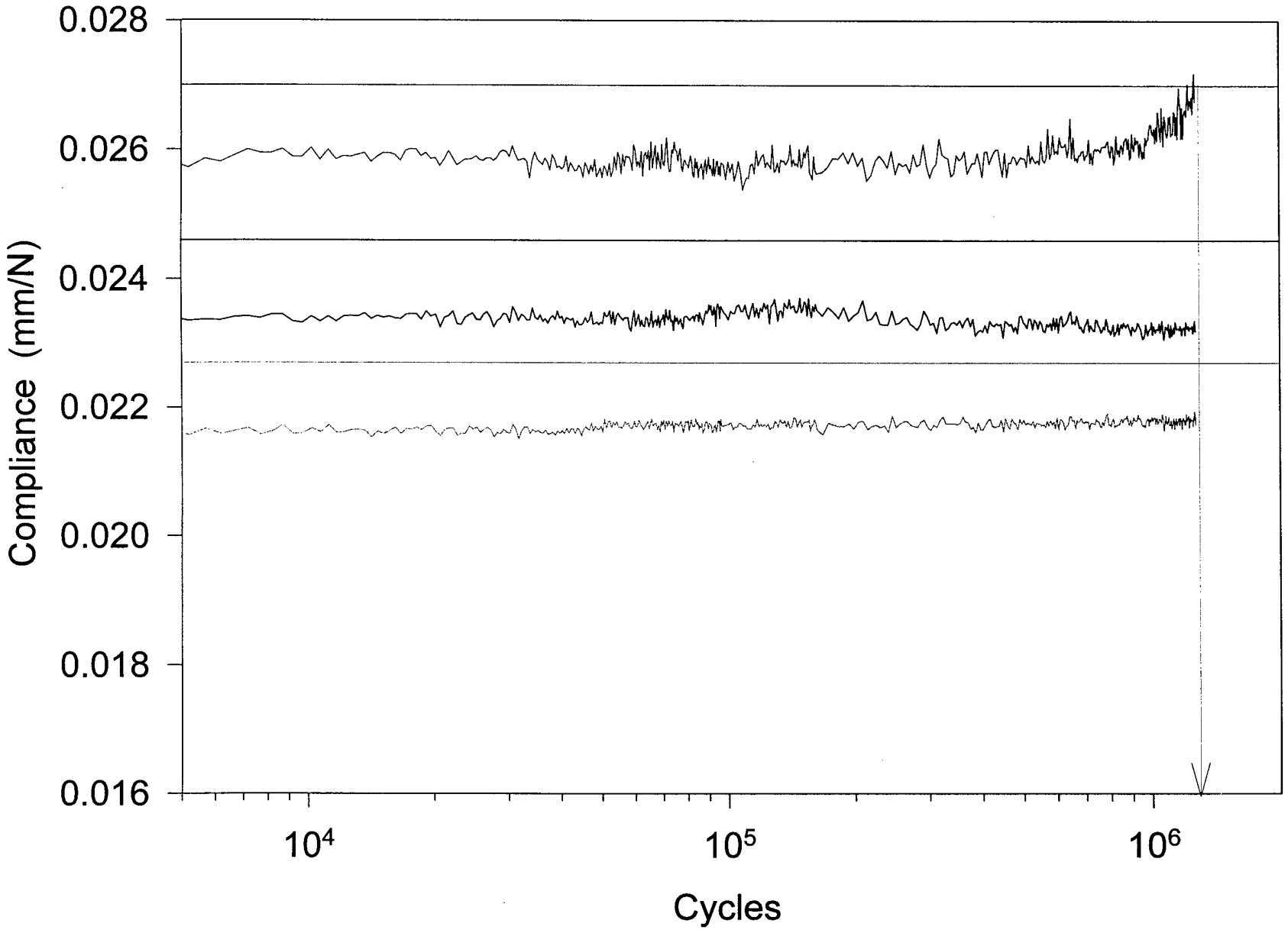
S2/8552 δ_{max} =1.5mm f=20Hz
0.028
0.026
0.024
0.022
0.020
0.018
0.016
Compliance (mm/N)
10^4
10^5
10^6
Cycles